A Study of Active Species and Stereo-, Regio-, and Substrate-Selectivity in Olefin Polymerization Mediated by Bis(salicylaldiminato) Group 4 Transition Metal Catalysts

HARUYUKI MAKIO

2011

Table of Contents

General Introduction

1. Historical Implications of Ziegler-Natta Catalysts

Ziegler-Natta catalysis operates in an interdisciplinary region between macromolecular chemistry and organometallic chemistry, and has created an intimate link between academia and industry. Because this thesis is concerned with an olefin polymerization catalyst that is one of the youngest descendants of the Ziegler-Natta catalyst, and also because the author was educated and trained as a polymer chemist as well as organometallic chemist and who is now working in industry, it seems appropriate to briefly review the history of Ziegler-Natta catalysts and its mutual interactions with other fields of chemistry, which has eventually resulted in the development of bis(salicylaldiminato) group 4 transition metal catalysts (FI catalysts), the topic of this thesis.

1.1. Macromolecular chemistry and Ziegler-Natta catalysts

A number of polymeric substances that occur naturally in nature like silk, wool, cotton, starch, proteins, and others have been known and used by man for many centuries. In the 19th century, some natural polymers were chemically modified (on an empirical basis) and used as, for example, vulcanized rubber, rayon, celluloid, etc., and the first synthetic polymer, Bakelite, was produced on a commercial scale in 1907. However, the chemical structures of these polymers was virtually unknown until Hermann Staudinger proposed the Macromolecule Hypothesis, that is, polymers are long chain molecules consisting of covalently connected atoms with almost arbitrarily large molecular weights.[1] The counterproposal made by the leading organic chemists at that time was the Association Theory, that is, the polymers are a cluster of small molecules held together by an unknown force, and the properties of what are now recognized as polymers are derived from their colloidal nature. The Macromolecule Hypothesis by Staudinger gradually gained acceptance within the scientific community as new evidence for the high molecular weight of the polymeric materials was obtained by membrane osmometry, viscosity, and X-ray diffraction.[2] Staudinger received the Chemistry Nobel Prize in 1953 for his discoveries in the field of macromolecular chemistry.

Since many of the macromolecules appeared to have a recurring structural unit, and if each structural unit is covalently bonded together in the same way as found in small molecules, then another way to prove the existence of macromolecules is to construct a "polymer" having a recurring structural unit from the corresponding "monomer" by means of well-understood covalent bond forming reactions. In 1929, Carothers and coworkers at DuPont started an investigation into the synthesis of polyesters and polyamides,[3] and by recognizing addition polymerization (A polymers) and condensation polymerization (C polymers) they were able to discover the first synthetic fiber called Nylon. Since then, many polymerization reactions have been developed for various monomers using a number of known bond-forming reactions (**Table 1**), which made the 20th century truly the age of plastics (synthetic polymers).

Table 1. Commercialization of selected synthetic polymers[a]

Year	Polymer	Producer
1909	Poly(phenol–co–formaldehyde)	General Bakelite Corporation
1927	Poly(vinyl chloride)	B.F. Goodrich
1929	Poly(styrene–co–butadiene)	I.G. Farben
1930	Polystyrene	I.G. Farben/Dow
1936	Poly(methyl methacrylate)	Rohm and Haas
1936	Nylon 66 (polyamide 66)	DuPont
1936	Neoprene (poly(chloroprene))	DuPont
1939	Polyethylene	ICI
1943	Poly(dimethylsiloxane)	Dow Corning
1954	Poly(ethylene terephthalate)	ICI
1957	Isotactic polypropylene	Montecatini
1960	Poly(p-phenylene terephthalamide)	DuPont
1982	Polyetherimide	GEC

[a]Excerpted and modified from "Sperling, L. H. *Introduction to Physical Polymer Science*, John Wiley & Sons, Inc. 2006"

Although ethylene was known to be extremely difficult to polymerize, scientists at Imperial Chemical Industries (ICI) managed to produce polyethylene (rather accidentally) and brought it to commercial production in the 1930s. The polymerization was mediated via a radical species and extremely harsh conditions were required to obtain polyethylene, that is, pressures of 1,000–2,000 atm and temperatures around 200 °C were applied. Polyethylene produced by this high pressure process possesses short and long branches and thus has low crystallinity and density, and so is known as low density polyethylene (LDPE). Due to the weak allylic carbon–hydrogen bonds in the methyl group of propylene, the radical process cannot polymerize propylene into high molecular weight polymers.

In 1951, Banks and Hogan at Phillips Petroleum discovered that chromium catalysts could polymerize ethylene into crystalline polyethylene at much lower pressures and temperatures than the radical process. They also found that the Cr catalyst afforded crystalline polymers even from propylene.[4] Independently, Ziegler and coworkers at Max-Plank Institute investigated the reaction of ethylene with triethylaluminum, and found that ethylene molecules inserted into Al–C bonds (Aufbaureaktion), resulting in higher aluminum alkyls (Eq. 1, 'al' stands for 1/3Al)

$$\text{R-al} + i\ \text{CH}_2{=}\text{CH}_2 \longrightarrow \text{R}(\text{CH}_2\text{CH}_2)_i\text{-al} \qquad (1)$$

In 1953, they found (in a serendipitous way) that an addition of a small amount of transition metal salts to the said Aufbaureaktion caused a drastic change in the product molecular weights, which eventually led to the discovery of Ziegler catalysts.[5,6] Ziegler catalysts are formed by the reaction of a transition metal compound and an organometallic compound of main group metals, the representative example of which is a combination of $TiCl_4$ and Et_3Al. Ziegler catalysts can polymerize ethylene into high molecular weight polyethylene at high activity even under the atmospheric pressure of ethylene. The polyethylenes produced

with the Cr (Phillips) and the Ti (Ziegler) catalysts were revealed to have a linear structure with a few branches, and therefore they possess high crystallinity and density (high density polyethylene, HDPE). Soon after the discovery of Ziegler catalysts, Natta and coworkers at the Milan Polytechnic observed that a modified Ziegler catalyst polymerized propylene into crystalline polymers. By X-ray investigations, the crystalline polypropylene was revealed to have the exact arrangement of chains in the crystal lattice, which led Natta to the discovery of stereospecific polymerization.[7,8] The obtained polypropylene had the same stereochemical configuration (*R* or *S*) at the methine carbons along the main chain (assuming that initiating and terminating chain ends are distinguishable), named isotactic polypropylene (**Chart 1a**). When the stereochemistry at the methine carbons is arranged in an alternating manner (–*RSRSRS*–), the polymers have syndiotactic stereochemistry (**Chart 1b**). If there is no apparent stereoregularity, the polymers are atactic. For these achievements, Ziegler and Natta shared the 1963 Nobel Prize in Chemistry.

a) Isotactic polypropylene

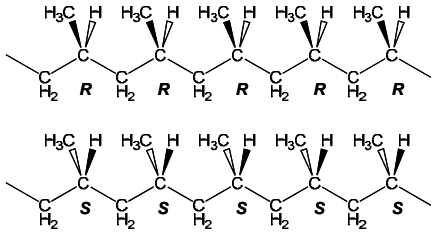

b) Syndiotactic polypropylene

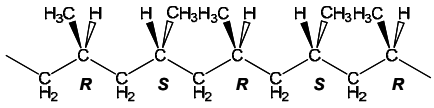

Chart 1

1.2. Petrochemical industry and Ziegler-Natta catalysts

The petroleum industry began in the middle of the 19th century when the Standard Oil Company founded by John D. Rockefeller supplied people with kerosene (mostly C_9–C_{16} hydrocarbons) from his oil refineries for cooking and heating. The low boiler byproducts (naphtha, largely C_5–C_9 hydrocarbons) from the refineries were considered useless at the time. At the start of the 20th century, large scale manufacturing of modern automobiles began and gasoline obtained by the catalytic cracking of petroleum was found to efficiently power the internal-combustion engines of automobiles and other means of transportation. Proliferation of electricity and two World Wars further expanded the use of petroleum as an energy source.

Another way to use petroleum was initiated by the discovery of steam radical cracking, which provided an efficient way to convert naphtha into basic petrochemicals, ethylene, propylene, butenes, butadiene, and aromatics. These chemicals served as the basic building blocks for many chemical products and form the foundation of the petrochemical industries that produce textiles, plastics, pharmaceuticals, rubber, coatings, and adhesives, etc. The petrochemical industry thus began in the 1920s and steadily expanded. The

discovery of Ziegler-Natta catalysts in the 1950s further launched the petrochemical industry into a period of unprecedented growth. The new plastics called polyolefins were found to be the most versatile of polymers in that they possess a lot of suitable properties, that is, superior mechanical and physical properties, excellent chemical inertness, good processability, and easy recyclability. Another and yet the most significant reason behind this outstanding expansion of polyolefin manufacturing lies with the technological advances in polymerization catalysis which steadily broadened the scope of available polyolefin products and also made the production processes extremely efficient (*vide infra*). The polyolefin industry became the largest sector in the petrochemical industry so that polyolefinic materials are now the most used synthetic plastics today and the worldwide consumption of these materials was more than 100 million tons in 2005.

However, the initial Ziegler-Natta catalysts required a process to extract the catalyst residue from the polymers using alcohol (de-ashing process). Concerning the production of isotactic polypropylene, amorphous atactic polypropylene concomitantly formed as a byproduct must be removed. The purification process caused operational complexity and significant economic disadvantage to the manufacturing plants. The oil embargo by petroleum exporting nations in the 1970s demanded streamlining of the manufacturing processes in order to cope realistically with the soaring oil price. Since Ziegler-Natta catalysts are a solid catalyst, efforts to enlarge the specific surface areas were made in order to increase the activity. In fact, investigation on the number of active sites revealed that only a fraction of the titanium species on the surface (< 1 %) served as an effective polymerization catalyst. These efforts were eventually rewarded with the discovery of the $MgCl_2$-supported titanium catalysts by Mitsui Petrochemical Industry (now Mitsui Chemicals, Inc.) in Japan[9] and Montedison in Italy[10] in 1968.

The reaction rate of Ziegler-Natta polymerizations (R_p) can be expressed by the equation,

$$R_p = k_p \times [C^*] \times [\text{olefin}]^n$$

where k_p and [C*] represents the reaction rate constant of olefin insertion and the concentration of effective active sites, respectively. Introduction of $MgCl_2$ to Ziegler-Natta catalysts resulted in a 20–60 % increase in the concentration of effective active sites ([C*]) as expected. In addition, rather unexpectedly, it was found that the $MgCl_2$ was even more effective in accelerating the rate of the olefin insertion reaction (k_p) by about two orders of magnitude, on average.[11] The combined activity enhancement dispensed with the de-ashing process from polyethylene production because the content of the catalyst residues is satisfactorily low enough not to affect the quality of polymer products. The $MgCl_2$-supported titanium catalysts also significantly increased the activity of the propylene polymerization. However, a large amount of atactic polypropylene was coproduced with the isotactic polypropylene. A solution to this problem was found again at Mitsui and Montedison in 1974. The formation of atactic polypropylene was considerably reduced by adding ethyl benzoate to the catalyst without a significant reduction in activity. In 1975, the two companies started a joint collaboration on $MgCl_2$-supported titanium catalysts including electron donors, which resulted in the creation of highly sophisticated industrial catalysts. It was later found that the activity and

isospecificity of the isotactic portions were significantly enhanced by the addition of electron donors (**Table 2**).

The role of electron donors has been the subject of intensive research in academia and industry but this has not been clearly demonstrated yet. After further development in preparation methods and electron donors, the latest $MgCl_2$-supported titanium catalysts show ~10^3× higher activity than the original Ziegler-Natta catalyst, yielding highly isotactic polypropylene in > 98 % selectivity, and are still the most widely employed catalyst for the production of polyolefins worldwide.

Table 2. Effects of $MgCl_2$ and ethyl benzoate in propylene polymerization with Ziegler-Natta catalysts[a]

Catalyst	I.I.[c] (wt%)	Relative efficiency	Fraction of active Ti (mol%)	k_p[d] (L/mol/s)
$TiCl_3$-Et_2AlCl	90	1	0.2–0.63	2.5
$TiCl_4/MgCl_2$-Et_3Al	30	250	20–60	240–730
$TiCl_4/MgCl_2$/EB-Et_3Al/EB[b]	94	140	2.8	2,700

[a]See ref. 011; [b]EB = ethyl benzoate as an electron donor; [c]Isotactic index measured as boiling heptane insoluble fractions; [d]Chain propagation rate constant.

1.3. Organometallic chemistry and Ziegler-Natta catalysts

Ziegler-Natta catalysts helped establish a new polymerization method in polymer chemistry, which is significantly different from traditional radical, cationic, anionic polymerizations based on organic chemistry, that is Ziegler-Natta catalysts have their base in organometallic chemistry and that the transition metal species having a metal–carbon bond and ancillary ligands determine the reactivity and selectivities of the polymerizations. Thus, Ziegler-Natta catalysts prompted intense research into organometallic chemistry, which originally arose at the interface of classic organic and inorganic chemistry. Because the progress of the transition-metal catalyzed olefin polymerization and organometallic chemistry have had reciprocal and mutually beneficial interaction with each other, it would be worthwhile to briefly review the historical background of organometallic chemistry.

Organometallic chemistry deals with the chemical compounds containing bonds between the carbon and a metal in contrast to coordination compounds that have bonds between a metal and the organic ligands through heteroatoms such as oxygen or nitrogen, represented by the octahedral Werner complexes. The first organometallic compound known as Zeise's salt was synthesized back in 1827 (**Chart 2**).[12] As Zeise believed that his salt was a derivative of ethylene combined with platinum despite the long controversy, the composition was confirmed in 1861, and the structure was identified by X-ray analysis in 1969 as we know it now. It is interesting to know that the first organometallic compound was a transition metal olefin π-complex rather than main group metal σ-bonded alkyls that followed in succession, that is, organozinc (1849), organoaluminum (1859), organoborane (1860), organosilane (1863), organomagnesium (1900), and organolithium (1917). These main group metal alkyls found extensive use applications in organic and inorganic synthesis.

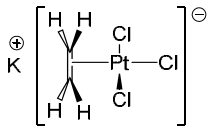

Zeise's salt

Chart 2

However, it was in the 1950s that organometallic chemistry was truly established as an important branch of chemistry. This is because around that time, important discoveries on the synthesis and the catalysis of organotransition metal compounds were made in rapid succession and organometallic species derived from transition metal complexes were conceived as important intermediates in industrially important catalytic reactions. The earliest examples of transition metal catalysis were invented in the late 1930s to 1940s, which are the Reppe reaction (**Scheme 1**), the production of acrylic acid from acetylene and carbon monoxide using $Ni(CO)_4$, and hydroformylation by Roelen (**Scheme 2**), the production of propionaldehyde from ethylene, carbon monoxide and hydrogen using $Co_2(CO)_8$. Both processes are believed to involve: 1) formation of a metal hydride, M–H; 2) insertion of acetylene or ethylene to the M–H species, resulting in M–C bond; 3) insertion of a CO ligand into the M–C bond; and 4) release of the products via hydrolysis or hydrogenation. Thus, the M–H and M–C are the key species to turn the catalytic cycles. The Wacker reaction, which was industrially scaled in the late 1950s, is based on a palladium catalyst combined with a cupric salt and also involves formation of the Pd–C bond and β-elimination as a key step to forming acetaldehyde from ethylene and water.

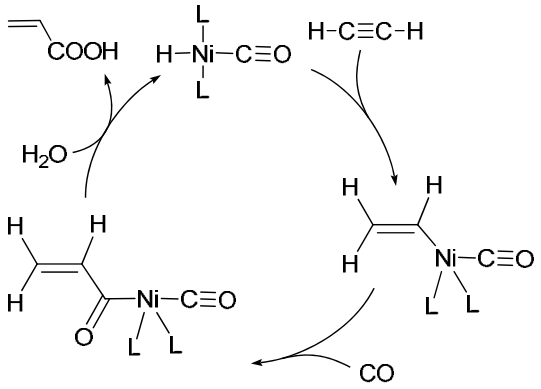

Scheme 1 Reppe Process

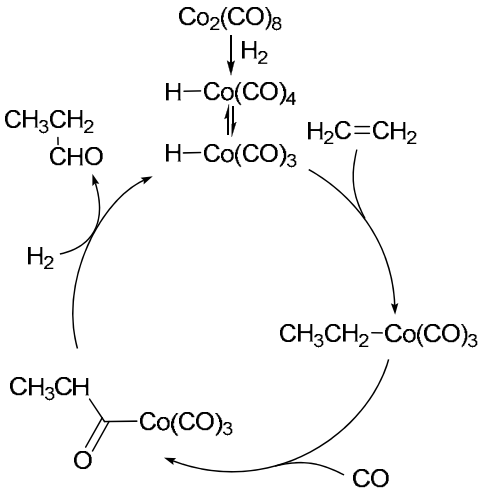

Scheme 2 Hydroformylation

With regard to the synthesis of organometallic complexes, the discovery (Pauson)[13] and identification (Wilkinson, Woodward, Fischer)[14,15] of ferrocene (**Chart 3**) in 1951 and 1952 marked the beginning of the synthesis of a vast family of cyclopentadienyl complexes (metallocenes) with various transition metals and the extensive research into their chemistry and catalysis. Wilkinson and Fischer received the Nobel Prize in

Chemistry in 1973 for their contributions to organometallic compounds. And last but not least, the olefin polymerization by Ziegler-Natta catalysts mentioned above also created a momentum for the research for organotransition metal chemistry.

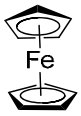

Ferrocene

Chart 3

All these examples listed above demonstrate and determine the significance of organometallic chemistry based on transition metals, and have set off a flood of research activities on organotransition metal complexes and their reactions. Chemistry of metal carbene species (M=C) and olefin metathesis reactions with them, which is closely related to M–C species and σ-bond metathesis in olefin polymerization, is another recent triumph of organometallic chemistry that won the Nobel Prize in Chemistry in 2005 for Chauvin, Grubbs, and Schrock.[16]

2. Paradigm Shift in Ziegler-Natta Catalysts

Progress in organometallic chemistry caused a paradigm shift in olefin polymerization with the Ziegler-Natta catalysts, a shift from ill-defined multi-sited catalysts to well-defined single-site catalysts, which allows for the rational understanding of polymerization reactions with meticulously designed molecular catalysts. With the discovery in the 1980s of metallocene catalysts, single-site molecular catalysts have become an industrial reality, not a mere academic interest.

2.1. Discovery of metallocene catalysts

Ziegler-Natta catalysts are complex mixtures that are generated on the solid surface and they are chemically inhomogeneous (the term "Ziegler-Natta catalysts" is used in a narrow sense in this context, only standing for Ti-based catalysts). Nevertheless, the olefin polymerization mechanism is fairly well understood in general mainly through the extensive analysis of polymer products. Regarding the reaction mechanism of olefin polymerization, the Cossee-Arlman mechanism[17,18] is generally accepted, that is, 1) the reaction of a titanium compound and alkylaluminums forms coordinatively unsaturated Ti–C species; 2) to the Ti–C species, an olefin molecule coordinates via a π-bond; 3) the coordinated olefin inserts into the Ti–C bond in *cis*-fashion via a four-membered metallacyclic transition state, and 4) the insertion regenerates a new Ti–C bond and a vacant site, and the repetitive cycles of 2) to 4) furnish linear polyolefins (**Scheme 3**).

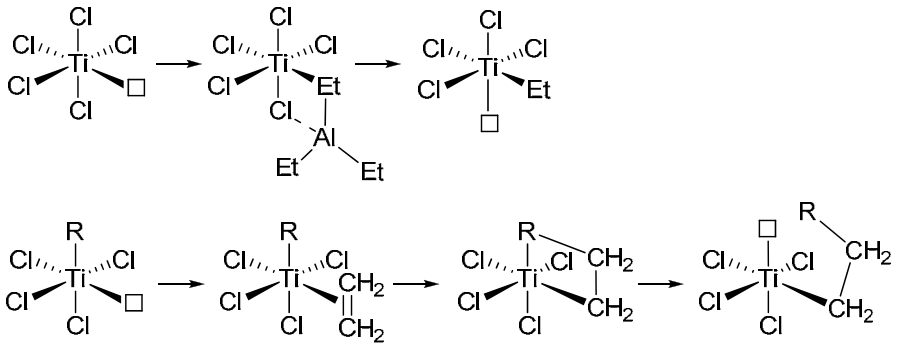

Scheme 3. Cossee mechanism of activation (above) and propagation (below)

However, little means were available to directly observe and identify the active species for heterogeneous Ziegler-Natta catalysts and the structure of the active species is still a scientific debate. Thus, studies to elucidate the active species and the precise reaction mechanisms of Ziegler-Natta catalysis using soluble well-defined organometallic complexes were initiated by several groups soon after the discoveries of Ziegler-Natta catalysts and metallocene complexes in the early 1950s. These cross-disciplinary research efforts in polymer chemistry and organometallic chemistry turned out to be fruitful and later resulted in the discovery of metallocene and subsequent post-metallocene chemistry.

2.1.1. Activation and active species

In the late 1950s, investigation of $(C_5H_5)_2TiCl_2$ in combination with alkylaluminum compounds was initiated by Natta and Breslow and their coworkers as a soluble model for the Ziegler-Natta catalysts. Natta and coworkers isolated a blue crystalline complex from a homogeneous solution of $(C_5H_5)_2TiCl_2/AlEt_3$ and crystallographically determined the structure as $(C_5H_5)_2Ti(\mu\text{-}Cl)_2AlEt_2$, where both the metals had a tetrahedral geometry and two bridging chlorines.[19–21] The complex showed only low activities in ethylene polymerization. Breslow and Newburg also investigated the reaction between $(C_5H_5)_2TiCl_2$ and alkylaluminum compounds and isolated a similar crystalline complex. They demonstrated that the titanium complex, which exhibited low ethylene polymerization activity consistent with the observations by Natta, was a trivalent Ti^{III} complex. However, ethylene polymerization with the complex in the presence of a small amount of oxygen resulted in an activity as high as typical heterogeneous Ziegler-Natta catalysts, $TiCl_4/Et_2AlCl$.[22,23] They concluded that the active species responsible for the high activity was a tetravalent Ti(IV) species oxidized by oxygen, and proposed a partially ionized species of the type, $[(C_5H_5)_2Ti^{IV}\text{–}Et]^{\delta+}[(\mu\text{-}Cl)AlEtCl_2]^{\delta-}$ (**1**) for these polymerizations. UV-visible spectroscopic study further reinforced the hypothesis that species **1** could be responsible for ethylene polymerization.[24] It is known that these early studies led Cossee to propose the coordination-insertion mechanism mentioned above. Subsequently, studies of titanocene/alkylaluminum systems with various alkyl groups were carried out.[25–27] Since multiple equilibria between several species and aluminum alkyls and rapid deactivation processes were involved in these systems, true identity of the active species was inconclusive.

In the 1970s, Reichert and Meyer found that addition of water to the soluble catalyst, $(C_5H_5)_2TiEtCl$-$EtAlCl_2$ (Al/H_2O = 20, 100), caused increased activity in ethylene polymerizations.[28] Similarly, Long and Breslow observed activity increase for the catalyst, $(C_5H_5)_2TiCl_2$-Me_2AlCl, upon addition of water (Al/H_2O = 3), suggesting formation of a dimeric alumoxane such as ClMeAl–O–AlClMe.[29] Sinn, Kaminsky and coworkers reported that a maximum activity was observed at the Al/H_2O molar ratios between 2 to 5 for $(C_5H_5)_2ZrMe_2$-AlR_3 (R = Me, Et) catalysts. Later, methylalumoxane (MAO) separately prepared by a reaction of Me_3Al and water (conventionally described as a structure having recurring units $(–AlMe–O–)_n$) was found to serve as an excellent activator for metallocene compounds, reaching ethylene polymerization activity at 10^2 kg/mmol-Zr h bar, and affording polymers having narrower molecular weight distributions than traditional Ziegler-Natta catalysts (single-site catalysts).[30,31] This discovery made metallocene catalysts industrially feasible in terms of activity and also rejuvenated the studies on the active species involved in Ziegler-Natta catalysis using soluble well-defined complexes.

Eisch and coworkers isolated and characterized a cationic species (**2**) from the reaction between a mixture of $(C_5H_5)_2TiCl_2/MeAlCl_2$ and $Ph\text{-}C{\equiv}CSiMe_3$.[32] This finding strongly suggested formation of the species, $[(C_5H_5)_2Ti–Me]^{\delta+}[AlCl_4]^{\delta-}$, and *cis*-insertion between the titanium–carbon bond.

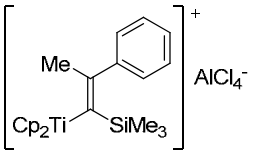

2

Watson, Bercaw, and Marks demonstrated that organolanthanide complexes, $(Me_5C_5)_2MR$ (M = Lu, Sc) and $[(Me_5C_5)_2MH]_2$ (M = La, Nd, Lu), which in their monomeric forms are isoelectronic to the cationic species of group 4 metallocene ($[Cp'_2M–R]^+$: Cp' represents a generic form of a cyclopentadienyl ligand), exhibited olefin insertion and ethylene polymerization activities.[33–35] These results also provided support for the hypothesis that 14e cationic species, $[Cp'_2M–R]^+$, mediate olefin polymerization. Jordan and coworkers synthesized and crystallographically characterized a cationic zirconocene complex, $[(C_5H_5)_2ZrMe(thf)][BPh_4]$ (**3**), from $(C_5H_5)_2ZrMe_2$ and $Ag[BPh_4]$. Cationic complex **3** did show ethylene polymerization activity.[36,37] In the early 1990s, Marks and Ewen independently discovered that perfluoroarylborane ($B(C_6F_5)_3$) can activate group 4 metallocene alkyls into highly active olefin polymerization catalysts. Furthermore, $B(C_6F_5)_3$ allowed for isolation of base-free cationic complexes such as $[Cp'_2M–Me][MeB(C_6F_5)_3]$. Chien, Rausch,[38] Ewen,[39] Turner,[40] and Marks[41] developed trityl or ammonium salts of perfluoroarylborate, $([A]^+[B(C_6F_5)_4]^–$, A: Ph_3C; $HNRR'_2$) as highly efficient cocatalysts for activating metallocene alkys. In these examples, activation takes place by heterolytic cleavage of M–R bonds via alkide (alkyl anion)/hydride abstraction or protonolysis (Eqs. 2–4), providing compelling evidence that the active species are alkyl metal cations of the type $[Cp'_2M–R]^+$ that are attended by weakly-coordinating counteranions ($Y^–$).

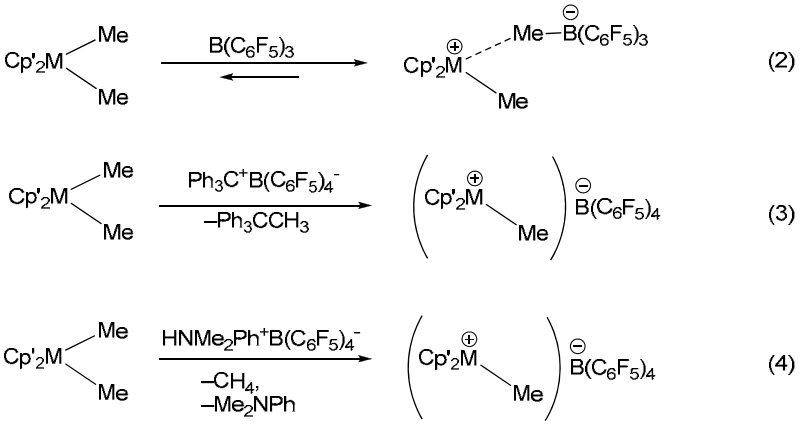

According to this activation principle, many new activators were designed and developed based on B, Al, and other metals.[42] In association with these well-defined catalyst–activator systems, activation with MAO is also considered to form a cationic species by extracting an alkyl anion from metallocene alkyls presumably at strongly Lewis acidic three-coordinated Al sites, forming a stable counteranion.

2.1.2. Regio- and stereochemistry

The well-defined single-site nature of metallocene catalysts has promoted an understanding of the relationship between the electronic and structural features of the metallocene catalysts and their reactivity and selectivity. One of the most significant achievements with this regard is the clarification of the stereoregulating mechanism of propylene polymerization and by extension the substantiation of highly isotactic and also highly syndiotactic polypropylene by rational catalyst design using stereo-rigid *ansa*-metallocene by Brintzinger, Ewen, and their coworkers.[43–45]

According to the Cossee-Arlman mechanism, one can notice that there can be four orientations for an α-olefin monomer to coordinate to a metal and insert into a M–C bond (**Figure 1**). The orientation determines the regio- and stereochemistry of the monomer insertion. When α-olefin monomers (CH_2=CHR) coordinate and insert so that the newly formed metal-bound carbon is primary (M–CH_2CHR–), it is called primary insertion or 1,2-insertion. Insertion in the opposite manner to form M–CHRCH_2– is therefore secondary insertion or 2,1-insertion. This is about regiochemistry of monomer insertion and the Ti-based Ziegler-Natta catalysts are known to be strictly regioselective to primary insertion, while soluble vanadium Ziegler-Natta catalysts prefer secondary insertion.

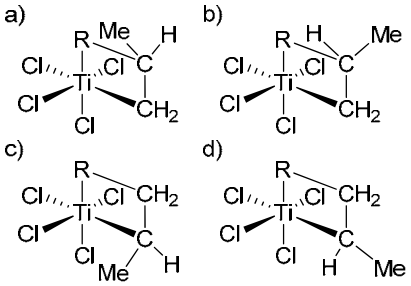

Figure 1. Stereo- and regioselectivity of propylene insertion. a) Primary insertion at *si*-face, b) primary insertion at *re*-face, c) secondary insertion at *re*-face, d) secondary insertion at *si*-face.

Stereochemistry is concerned with the selectivity between *re*- and *si*-face of prochiral α-olefin monomers (**Figure 1**). If coordination and insertion take place selectively at a particular prochiral face (*-re-re-re-re-re-re- or -si-si-si-si-si-si-*), the result is isotactic polymers. Alternating selection of prochiral face (*-re-si-re-si-re-si-*) leads to syndiotactic polymers. There can be two chiral elements to determine the face selectivity during polymerization. One is the asymmetric carbon of the last inserted monomer unit of a growing polymer chain (chain-end control). The other is chirality elements existing at the metal center generated by the surrounding ligands (enantiomorphic site control). The two origins of stereospecificity can be easily distinguished by examining the stereo-defects of polypropylene by ^{13}C NMR spectroscopy.[46] When the former chirality dictates the stereochemistry of each monomer enchainment, a misinsertion reverses the stereochemistry of the following insertions, resulting in an isolated *m* or *r* diad defect. When the latter chirality exercises site control, a misinsertion with incorrect stereochemistry is immediately corrected, causing a successive *mm* or *rr* triad defect (**Figure 2**). In general, the selectivity of chain-end control largely depends on monomer structures, and usually low polymerization temperature is required to achieve even moderate stereoregularity. The site control is unique to transition metal catalyzed polymerization, and can reach a high regularity at higher polymerization temperature.

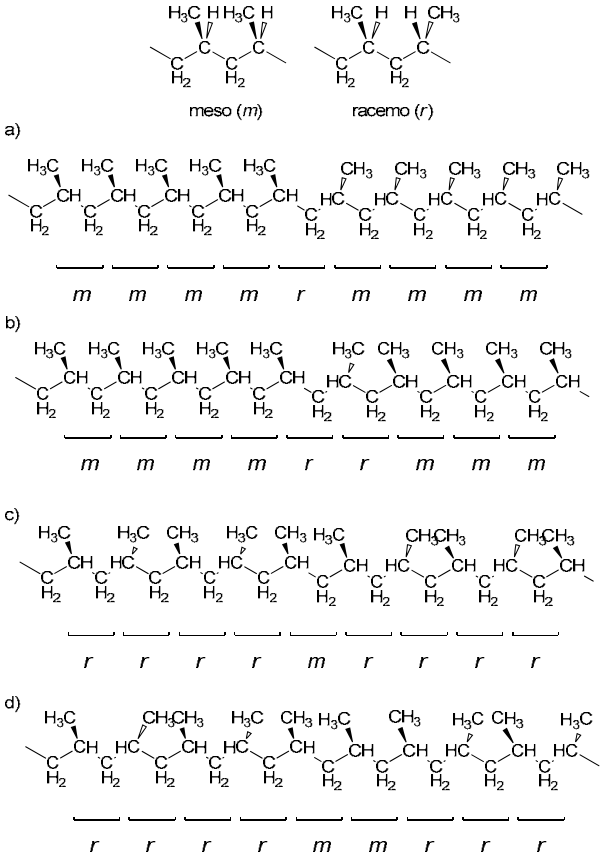

Figure 2. Stereo-sequence of polypropylene: a) isotactic via chain-end control, b) isotactic via site control, c) syndiotactic via chain-end control, d) syndiotactic via site control.

In the tetrahedral framework of group 4 metallocenes (Cp'_2MX_2), non-spectator ligands X are always located *cis* to one another, and then form polymerization sites upon activation as mentioned above. Spectator Cp' ligands can form a chiral environment typically when they are bound together through a bridge structure (*ansa*-metallocene), which makes the *cis*-bound polymerization sites either homotopic, enantiotopic, or diastereotopic. The C_α–C_β bond of a metal bound alkyl group can be oriented to a less crowded quadrant to avoid steric congestion with the Cp' ligands. To the species, propylene monomer coordinates in primary fashion and inserts to the M–C_α bond via the four center metallacyclic transition state. The face selection of the prochiral propylene monomer is made by the steric non-bonding interaction between the methyl group of the propylene monomer and the β-carbon of the metal-bound alkyl in the four center metallacyclic transition state so that the methyl group and the β-carbon are always *anti* across the plane of the metallacycle. According to this mechanism, C_2 symmetric complexes that have homotopic reaction sites yield isotactic polypropylenes, while complexes with C_s symmetry whose active sites are enantiotopic afford syndiotactic polypropylenes when assuming regular alternating chain migratory insertions (**Figure 3**). The mechanism coincides with the proposed model for heterogeneous Ziegler-Natta catalysts, in which chiral surface sites were assumed to play the role for determining the orientation of the growing polymer chains.

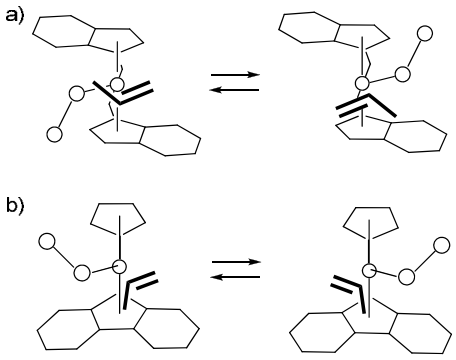

Figure 3. Face selectivity during chain migratory insertion. Due to repulsive interaction between the C_β of propagating chain and the methyl group of propylene; a) C_2-symmetric metallocene favors *re*-coordination in this instance, b) C_s-symmetric metallocene alternates *re*- and *si*-coordination in each migratory insertion.

2.2. Post-metallocene and FI catalysts

With advanced understanding of olefin polymerization catalysis with transition metal complexes, metallocene catalysts expanded the scope of research into neighboring group 3 metallocenes (including rare earth metals, *vide supra*) or group 5 Cp'/diene complexes that were isoelectronic to 14e cationic group 4 metallocene alkyls[47,48] and into other Cp-related ligands such as carborane derivatives.[49,50] Bercaw,[51] Okuda,[52,53] Stevens,[54] and Canich[55] developed complexes bearing linked amido-cyclopentadienyl ligands, represented by $Me_2Si(Me_4C_5)(^tBuN)MX_2$ (**Chart 4**). These linked Cp'-amido complexes are not isoelectronic

to group 4 metallocenes anymore but they are electronically more unsaturated and sterically more accessible than bis(cyclopentadienyl) analogues, exhibiting much higher activities toward α-olefins.

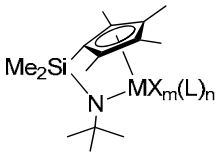

Chart 4

Also developed since the early 1990s were a number of catalysts that have non-Cp ligands based on nitrogen, oxygen, sulfur, phosphorus and the combinations of these as coordinating atoms in combination with group 3–6, 8–10, and 13 metals.[56,57] Particularly successful among these early examples were diamido complexes based on group 4 metals (**4**),[58,59] aminopyridinato tantalum(V) complexes (**5**),[60] pyridyl-diimine iron complexes (**6**),[61–63] and nickel diimine complexes (**7**),[64] all of which demonstrated ethylene polymerization activities higher than 1 kg/mmol-M h bar.

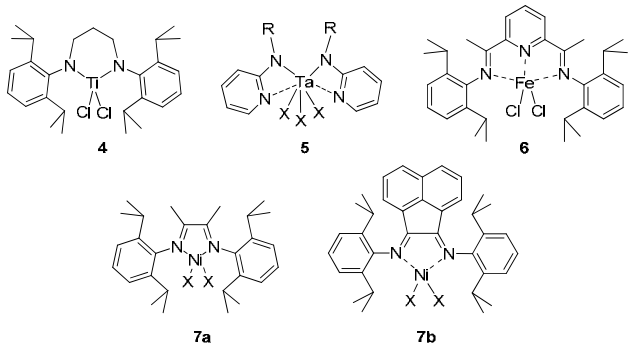

Amidst this period, post-metallocene research at Mitsui Chemicals has yielded several families of group 4 metal olefin polymerization catalysts bearing two non-symmetric heteroatom chelate ligands such as [N, N¯], [O, O¯], and [N, O¯] (**Chart 5**).[65] The most successful class of catalysts are group 4 bis(phenoxy–imine) complexes (now known as FI catalysts).[66] Phenoxy–imine represents substituted salicylaldiminato ligands (phenolates). Although it is not a general term, it is widely used in the scientific community and is therefore used throughout this thesis.

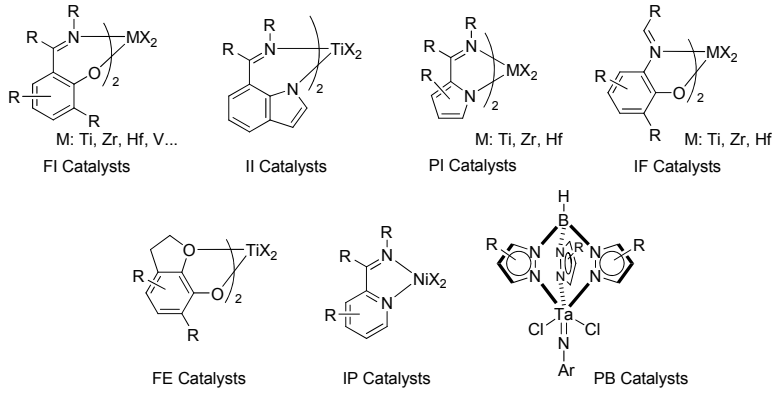

Chart 5

FI catalysts display extremely high activities in ethylene polymerization > 10^3 kg/mmol-Zr h bar, which eclipses the metallocenes as the newest and highest activity catalyst for olefin polymerization to date. Incidentally, the same ligand motif was reported around the same time as Ni complexes, which also exhibited high olefin polymerization activities for late metal catalysts (**Chart 6**).[67–69]

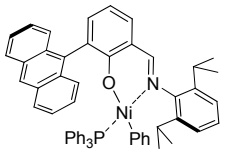

Chart 6

2.2.1. Discovery of FI catalysts

Conventional bridged quadridentate phenoxy–imine ligands represented by salen, salphen and their analogs were examined for their coordination chemistry with transition and/or main group metals and the chemical reactivity of the resulting complexes. Particularly remarkable is their use as an asymmetric catalyst for oxidation reaction by introducing chirality at their bridging backbones.[70–72] However, phenoxy–imine complexes were barely examined as olefin polymerization catalysts before the "metallocene revolution" in the 1980s. Nevertheless, the first work on olefin polymerization catalysts related to phenoxy–imine ligands was carried out about the same time when metallocene/alkylaluminum systems were examined as a soluble model of Ziegler-Natta catalysts by Natta and Breslow (*vide supra*). In 1964, Taylor screened several phenoxy–azo and phenoxy–imine chelating compounds (L: bridged and non-bridged) in combination with $TiCl_4$ in search for another soluble version of the Ziegler catalysts.[73] He found that some chelating agents simply deactivated active heterogeneous $TiCl_4/Et_2AlCl$ catalysts at higher molar ratios of L to Ti, whereas some non-bridged chelating agents caused an initial drop in activity followed by an increase at a particular L/Ti ratio, implying that chelated Ti complexes may serve as a soluble Ziegler catalyst (**Scheme 4**).

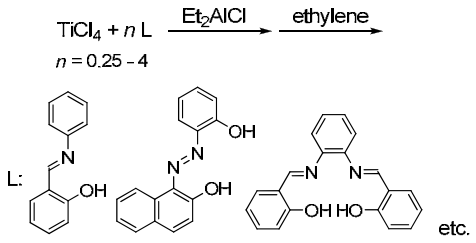

Scheme 4

The advent of metallocene catalysts promoted a search for ancillary ligands other than the cyclopentadienyl groups that can support metal–carbon bonds. Floriani and coworkers successfully prepared and characterized Ti(salen)Me_2 (**8**) by alkylation of Ti(salen)Cl_2 (**9**) with MeLi under carefully controlled conditions (**Scheme 5**).[74,75] In contrast to tetrahedral metallocene complexes, complex **8** adopts an octahedral geometry with a *trans* arrangement of the two methyl groups. Dimethyl complex **8** was

unstable and decomposed via intramolecular methyl migration to the imine. Other attempted alkylations with various alkylating agents were accompanied by side reactions such as the alkylation of the imines either directly by the alkylating agents or by the M–R migration, resulting in monoalkyl Ti complex **10**, and also the reduction to Ti(III) to form Ti(salen)R(thf) (**11**) in the reactions in THF. As such, the outcomes of the reactions were found to be extremely sensitive to the nature of solvents and alkylating agents.

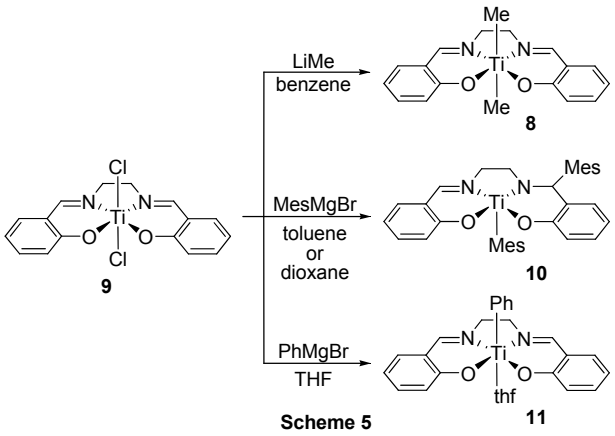

Scheme 5

These examples explicitly raised two important issues involved in phenoxy–imine ligated early metal complexes, that is 1) an octahedral complex can adopt either *cis*- or *trans*-arrangement of the reactive X ligands and salen or related quadridentate [O⁻NNO⁻] ligand motifs are prone to adopt *trans*-X geometry (X: reactive non-spectator ligands), which is not adequate for efficient reactions between reagent and substrate ligands such as olefin insertion and σ-bond metathesis, and 2) an electrophilic nature particularly when coordinated to early metals makes the imine units extremely susceptible to nucleophilic metal alkyls or any other nucleophiles in the reactions.

Issue 2) will be dealt with later in this General Introduction and Part I when discussing activation and synthesis of alkyl complexes of FI catalysts. With regard to issue 1), a lot of research focused on the X–M–X angles has revealed that a certain type of bridged tetradentate phenoxy–imine [O⁻NNO⁻] ligand can afford *cis*-X-like geometry (**Chart 7**). Floriani and coworkers synthesized Zr and Hf complexes bearing acen (*N*,*N'*-ethylenebis(acetylacetoneiminate)), whose Cl–M–Cl angles were 87.2(1)° for Zr and 87.4(1)° for Hf (**12**), although they were not used for any reactions.[76] Subsequently, Jordan and coworkers prepared alkylzirconium complexes supported by substituted acen ligands (**13**), which had the C–Zr–C angles between *cis* and *trans* geometry (129.9(2)°).[77] Moore and coworkers reported that bis(phenoxy–ketimine) ligands having *trans*-1,2-cyclohexylene bridge afforded complex **14** with *cis*-N/*cis*-O/*cis*-Cl geometry with titanium center (Cl–Ti–Cl angle is 86.9(1)°).[78] In a series of studies, Scott and coworkers demonstrated that tetradentate bis(phenoxy–imine) ligands possessing 2,2'-biaryl bridge gave a C_2-symmetric *cis*-N/*trans*-O/*cis*-X complex (for example, Cl–Zr–Cl angle is 103.56° for **15**).[79–84] However, these complexes only exhibited little to low activities for ethylene polymerization despite their *cis*-X arrangements,

suggesting that the *cis*-X arrangement is a necessary requirement but not a sole condition that must be met for highly efficient olefin insertion catalysts.

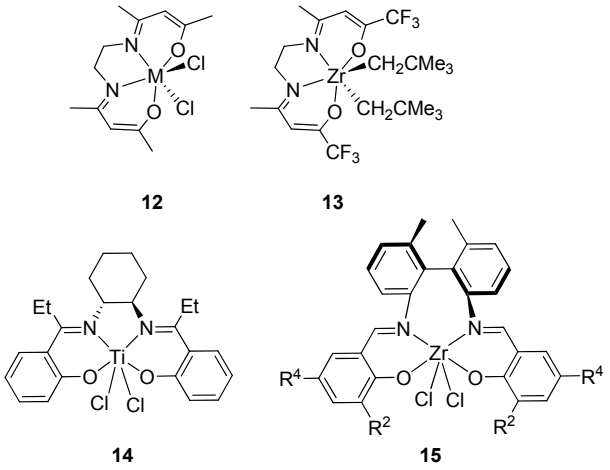

12 **13** **14** **15**

Chart 7

Floriani,[76,85,86] Jordan,[87] and scientists at Mitsui[66] employed two bidentate [NO$^-$] ligands with group 4 metals instead of one quadridentate [O$^-$NNO$^-$] ligand. X-ray crystallographic studies revealed that these complexes possessed in common a *cis*-N/*trans*-O/*cis*-X geometry around the metal center (**16**: Cl–Zr–Cl = 96.9(1)°;[76] **17**: C–Zr–C = 96.8(2)°;[86] **18**: C–Zr–C = 91.0(2)°;[87] **20**: Cl–Ti–Cl = 103.10(8)°;[88] **21**: Cl–Zr–Cl = 100.38(5)°[89]), probably because the substituents on the imine nitrogens (even small methyl groups) discouraged two nitrogens and two oxygens to make a coplanar configuration around the metal and also the shortest M–O bonds tend to favor a *trans* arrangement (**Chart 8**). Subsequent research into FI catalysts ($(L^{FI})_2MX_2$, L^{FI} represents a generic form of the phenoxy–imine ligand) proved the generality of this C_2 symmetric *cis*-N/*trans*-O/*cis*-X geometry in the solid state with a few exceptions.[90,91]

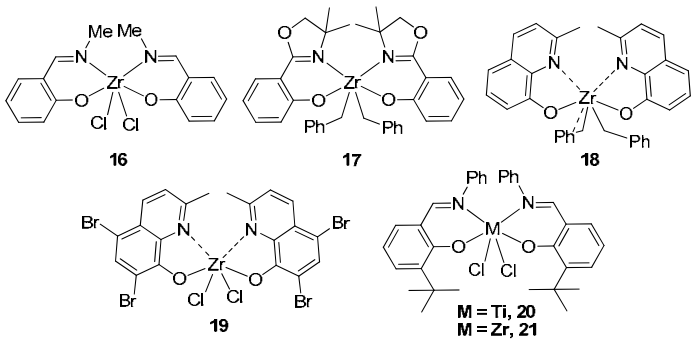

16 **17** **18** **19** **M = Ti, 20** **M = Zr, 21**

Chart 8

Despite apparent similarity of these complexes in configuration, FI catalysts having relatively large substituents at *ortho* to the phenolic oxygen (R^2 substituent) exhibited far higher activities for ethylene polymerization than complexes **16**–**19** (**Table 3**). In fact, the activity of the Zr-FI catalyst was one of the highest among all the olefin polymerization catalysts including metallocenes.[89,92] An FI complex without R^2

substituents prepared by Floriani and coworkers was not examined for olefin polymerizations. However, later studies indicated that lack of R^2 substituents was fatal in order to serve as a good catalyst (*vide infra*).[90,91]

Table 3. Ethylene polymerization activity of group 4 complexes bearing bis[N,O] ligands

Complex	T_p (°C)	Ethylene (atm)	Cocatalyst	Activity (kg-polymer/mmol-M h atm)	Reference
16	–	–	–	n/e[a]	76
17	r.t.	1	$HNEt_3BPh_4$	< 0.01	86
18	23	2	$HNMe_3B(C_6F_5)_4$	0	87
19	30	8	$^iBu_3Al/HNMe_3B(C_6F_5)_4$	0.041	87
20	25	1	MAO	3.4	88
21	25	1	MAO	519	89

[a] Not examined for polymerization

Despite an apparent similarity between **21** and **15** in their chemical functionalities and overall C_2-symmetric *cis*-X configuration, the difference in polymerization activity was striking. The low activities observed for the bridged complexes in general can stem from the significant constraints imposed by the rigid structures due to the relatively short bridging backbones. In fact, the significant differences in structural parameters such as N–M–N, O–M–O angles within the same general *cis*-N/*trans*-O/*cis*-X geometry were observed between a bridged and non-bridged complexes.[84,93]

Consistent with this hypothesis, complexes **22**, **23** having long and flexible bridging structures (C_6-linkage) exhibited high activity (**22**: 9.1 kg-polyethylene/mmol-M h atm; **23**: 2.6 kg-polyethylene/mmol-M h atm) that were much higher than for the complexes having shorter bridging groups (**Chart 9**).[94,95]

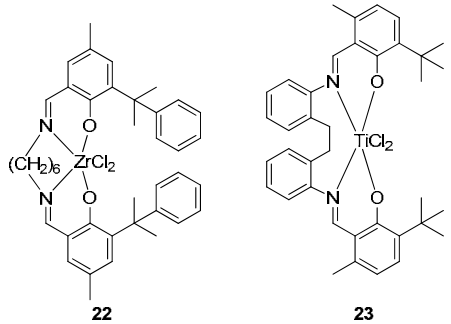

22 **23**

Chart 9

Due to the straightforward synthesis, phenoxy–imine compounds possess a large diversity from the electronic and steric point of view, offering a high degree of freedom for catalyst design. Out of the theoretical five structural isomers for the octahedron furnished with two imine nitrogens, two phenolic oxygens, and two X ligands, FI catalysts seem to have an intrinsic tendency to take those *cis*-X geometries as mentioned above (**Chart 10**). It is important to note here that, within this common *cis*-N/*trans*-O/*cis*-X framework, the R^2 substituents are placed above and below the latent reaction sites, the X–M–X moiety,

and the substituents on the imine nitrogens (R^1 substituents) are situated at the skewed backside of the X–M–X moiety (**Figure 4**). Subsequent research into FI catalysts has revealed that these two substituents (R^1 and R^2) located at specific positions near the reaction sites have a tremendous influence on the polymerization characteristics of FI catalysts, providing effective and specific means to control the reactivity and selectivity of the polymerizations as described below.

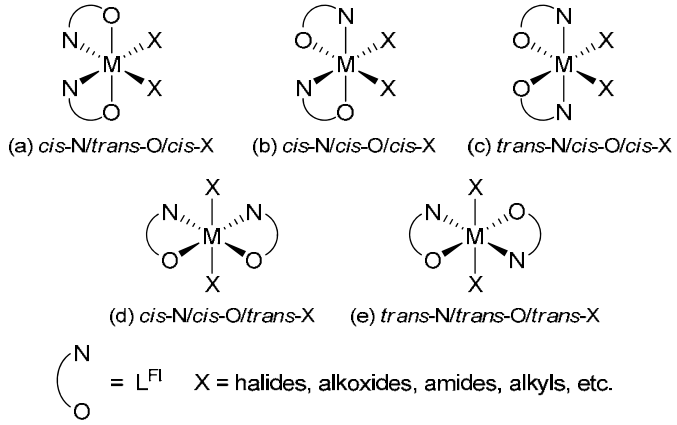

Chart 10

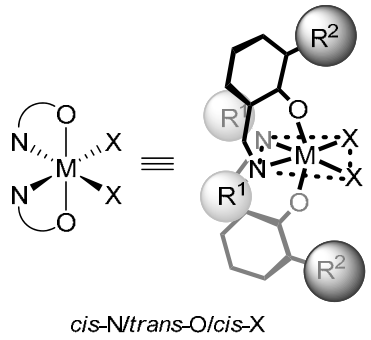

Figure 4. Spatial arrangement of R^1 and R^2 substituents of FI catalyst in the ordinary *cis*-N/*trans*-O/*cis*-X octahedral geometry.

2.2.2. Substituents on the imine nitrogen (R^1)

The steric and electronic nature of R^1 substituents shows significant impact on polymerization characteristics with FI catalysts. For example, the polymerization activity can be electronically manipulated by electron-withdrawing aryl R^1 substituents (**Chart 11**). The activity increase from 3.58 kg-polymer/(mmol-M h) for the prototypical Ti-FI catalyst **20** to 34.8 kg-polymer/(mmol-M h) for **24** (R^1 = 3,5-$F_2C_6H_3$) has been demonstrated. Likewise, activity values of 43.3 kg-polymer/(mmol-M h) for **25** (R^1 = 3,4,5-$F_3C_6H_2$) and 40.3 kg-PE/mmol-Ti h for **26** (R^1 = 3,5-$(CF_3)_2C_6H_3$) are typical examples.[90,91,96] This electronic effect presumably stems from an increased propagation rate due to the enhanced electrophilicity of the metal center, which decreases the insertion barrier.

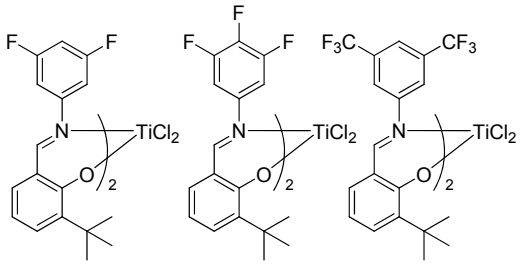

24 **25** **26**

Chart 11

R^1 substituents are also known to exhibit a significant influence on the molecular weight of the obtained polymers, in other words, on the chain transfer processes. Bulky R^1 substituents generally increase the polymer molecular weight. By increasing the size of *ortho*-substituents of the *N*-aryl groups, the molecular weights of polyethylene increase in the order of H < *o*-Me < *o*-*i*Pr < *o*-*t*Bu at the expense of activity, which decreases progressively in the opposite order.[90,92,97] In a series of cycloalkyl groups as R^1, a similar trend was observed also toward the lower molecular weight region in the order of 2-methylcyclohexyl > cyclohexyl > cyclopentyl > cyclobutyl > cyclopropyl. The polyethylene molecular weights obtained with Zr-FI catalysts bearing cyclopentyl, cyclobutyl, cyclopropyl R^1 groups reach the order of 10^3, and the polyethylenes have very high vinyl chain-end contents (**Table 4**).[90,91,98,99] Further studies have shown that the molecular weights were apparently independent of the monomer concentration, while the activities increased linearly at higher monomer concentration, showing that both propagation and β-H transfer are first order in monomer concentration. Therefore, the chain transfer involved in these polymerizations is the β-H transfer to a coordinating ethylene. In fact, DFT calculations have revealed that these complexes favor the β-H transfer reaction via a bimolecular path over a unimolecular transfer to the Zr center by $\Delta\Delta E$ = 48 to 58 kJ/mol mainly due to the extremely unstable nature of the $(L^{FI})_2$Zr-H species. Because R^1 substituents on the imine nitrogens are located at the backside of the X–M–X reaction sites, it is quite possible that the R^1 substituents have a non-bonding interaction with the X ligands. This was confirmed by the X-ray structures of Zr-FI catalysts, which demonstrated that the Cl–Zr–Cl bond angles were narrowed as R^1 substituents became larger (R^1 = cyclobutyl (**27**: 100.64(3)º), cyclohexyl (**29**: 99.8(2)º), 2-Me-cyclohexyl (**30**: 98.00(6)º)). The narrower bond angles observed for the bulkier R^1 groups will cause destabilization of the six-centered transition state of the chain transfer more than the four-centered transition state of the propagation, and the higher rate of the propagation relative to the chain transfer results in higher molecular weight polymers, which was indeed confirmed by DFT calculations.

Table 4. Effects of the R^1 substituents of Zr-FI complexes on ethylene polymerization.[a]

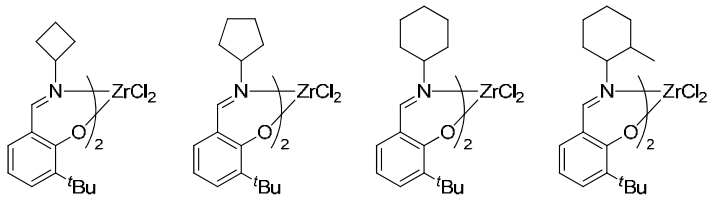

27 **28** **29** **30**

Complex	Activity (kg-polymer/mmol-M h)	M_w (g/mol)	M_w/M_n	Vinyl terminated chain end (mol%)
27	31.6	2,000	2.0	91
28	67.2	3,600	2.1	95
29	87.7	14,000	1.7	96
30	93.0	290,000	4.9	71

[a]Polymerization conditions: toluene 250 mL, complex 0.5 μmol, dried MAO 0.625 mmol, ethylene feed 100 L/h, 25 °C, 5 min.

An ultimate goal of controlling the chain transfer reactions is a living polymerization which has no chain transfer or chain termination reactions by definition. Interestingly, R^1 substituents were again a key to achieving the robust living polymerization with Ti-FI catalysts. Scientists at Mitsui discovered that Ti-FI complexes having *ortho*-fluorinated phenyl groups as R^1 exhibited typical living polymerization characteristics for ethylene and propylene at ambient temperature or higher despite the large excess of MAO that is a potential chain transfer agent.[90,91,100–103] The PDI (polydispersity index defined by M_w/M_n) values are extremely narrow and the molecular weights proportionally increase with polymerization time. On the other hand, the *meta*- or *para*-fluorinated complexes demonstrate ordinary non-living polymerizations (PDI ~2).

As mentioned above, *ortho*-substitution at the *N*-aryl groups (R^1 substituents) causes the increase of polymer molecular weights and the decrease of polymerization activity. When compared between *o*-F-C_6H_4 and *o*-Me-C_6H_4 as R^1 (R^2 = ^{t}Bu) for Ti-FI complexes, the ethylene polymerization activity of the *o*-F complex drops (60 g-polymer/mmol-Ti h) more than the *o*-Me complex (300 g-polymer/mmol-Ti h) relative to a control (R^1 = C_6H_5, 3,240 g-polymer/mmol-Ti h) (at 25 °C). Considering the van der Waals radii of the *ortho*-substituents (H: 1.20 Å; F: 1.47 Å; Me: 3.947 Å), it is rational to assume that this activity difference cannot be argued by simple steric effects. The ethylene polymerization data for a series of *N*-fluorinated-aryl Ti-FI complexes are shown in **Figure 5**. It is evident that the activity depression is commonly observed for the *ortho*-F substituted living complexes when compared with the *meta*- or *para*-fluorinated non-living complexes having the same numbers of fluorine(s). As indicated by the PDI values in parentheses, all the *ortho*-F complexes perform living polymerization, whereas the other complexes without the *ortho*-F demonstrate non-living polymerization. For both series of *ortho*- and *meta*/*para*-fluorinated complexes, the activities increase as the number of fluorines increases, and the activity of complex **31** bearing a perfluorophenyl group as R^1 far exceeds that of the non-fluorinated control

(activity: 4.15 kg-polymer/mmol-M h atm), while keeping a narrow molecular weight distribution close to unity, meaning that complex **31** is a highly active and robust living ethylene polymerization catalyst.[101] These and related Ti-FI complexes polymerize propylene into moderately to highly syndiotactic polymers again in a robust living manner for the *ortho*-F complexes.[90,91,102–109]

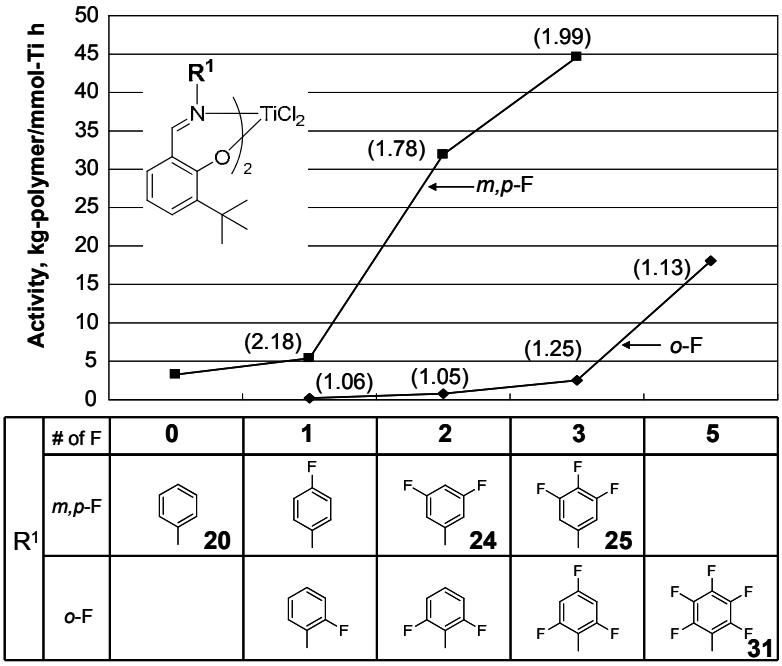

Figure 5. Ethylene polymerization with *N*-fluorinated-aryl Ti-FI complexes. Polymerization conditions: toluene 250 mL, MAO 1.25 mmol, complex 0.4–5.0 μmol, ethylene 0.1 MPa, 100 L/h, 1–5 min, 50 °C. The numbers in parenthesis are Mw/Mn determined by GPC (polyethylene calibration).

Living olefin polymerization catalysts have been available in the past.[109] However, when considering the limitations they imposed for their livingness (low polymerization temperatures to suppress side reactions and thereby low TOF, limitation of applicable monomers and achievable molecular weight of polymers, etc.), the living nature of these Ti-FI complexes at temperatures much higher than room temperature for both ethylene and propylene (with high syndiospecificity for propylene) is truly remarkable. In particular, the living polymerizations with **31** is extraordinary in that it exhibits very high TOF comparable to non-living Cp_2ZrCl_2, and the living propagating species is stable at least 1 h at ambient temperature in the absence of monomers.[91]

One rationale for the robust livingness brought by the *ortho*-F was proposed based on DFT calculations on the cationic species bearing an *n*-propyl group as a model of a propagating alkyl group.[90,101–103] In the calculated structure of the propagating model, one of the *ortho*-F(s) was observed in proximity to the β-hydrogen atoms (~2.3 Å) of the growing chain (van der Waals radii of H and F are 1.20 and 1.47 Å, respectively) and weak attractive and electrostatic interactions between the *ortho*-F and β-H were expected (the electrostatic energy ~30 kJ/mol), which can stabilize the chain-transfer-prone β-agostic state of the cationic polymeryl-titanium and avert unwanted β-H transfer reactions (**Figure 6**). Such

hypothetical C–F···H–C interactions were experimentally observed by Chan and coworkers for some phenoxy–pyridine Zr complexes (for example, **32**) bearing a cyclometalated aryl group by NMR spectroscopy and X-ray and neutron crystallography.[110–112]

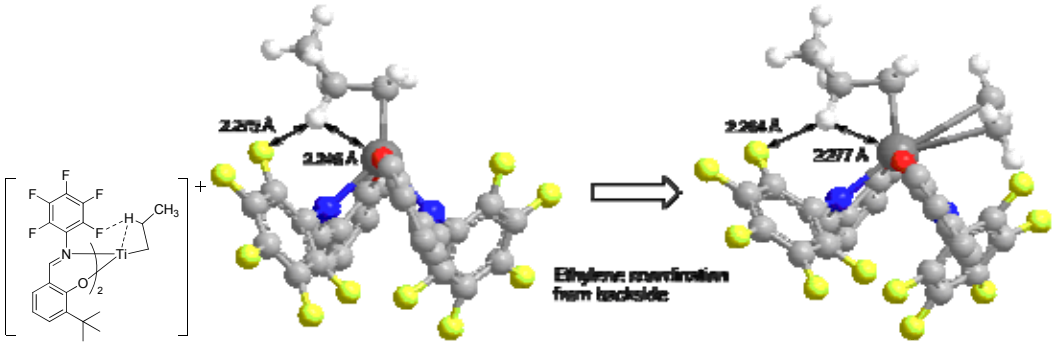

Figure 6. DFT-optimized structure of a cationic *n*-propyl species derived from **31**; a β-agostic state (left) and a π-complex via ethylene backside attack[113] (right). Phenolic aryl groups are simplified for clarity.

Mecking and co-workers revealed that a structurally related Ti enolatoimine complex bearing an *ortho*-F(s) *N*-aryl group (**33**) was an excellent ethylene living polymerization catalyst, whereas the corresponding complexes having *ortho*-methyl substituted (**34**) or non-substituted *N*-aryl groups (**35**) were not.[114] Recently, the *ortho*-F···Ti interaction was suggested as a rationale for the observed living polymerization for these complexes.[115]

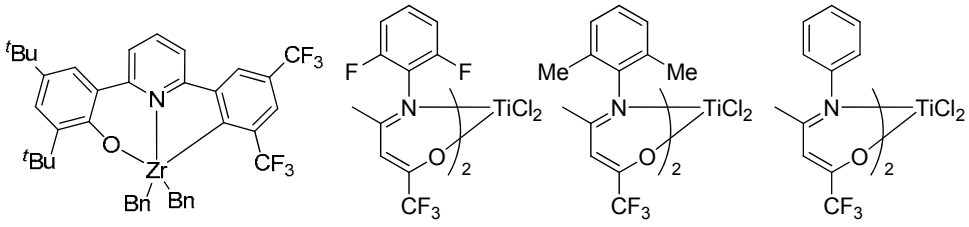

32 **33** **34** **35**

2.2.3. Substituents adjacent to the phenolic oxygen (R^2)

Systematic studies on catalyst efficiency revealed a keen relationship between the ethylene polymerization activity and the steric bulkiness of the R^2 substituents for a series of Zr-FI catalysts **21**, **36**–**44** (**Table 5**).[90–92,97] When a particularly bulky tertiary R^2 group, CPh_2Me, is introduced, the activity of complex **44** reaches an unprecedented level, 6,550 kg-polymer/(mmol-M h). This activity corresponds to a TOF of 64,900 $s^{-1}atm^{-1}$, standing as one of the most efficient catalysts not only for olefin polymerization but also for any catalytic reaction.

Table 5. Effects of the substituents of FI-Zr complexes on ethylene polymerization activity[a]

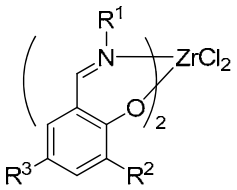

Complex	R^1	R^2	R^3	Activity (kg-polymer/mmol-M h)
36	Phenyl	Me	H	0.4
37	Phenyl	^{i}Pr	H	0.9
21	Phenyl	^{t}Bu	H	519
38	Phenyl	^{t}Bu	Me	331
39	Phenyl	1-Adamantyl	Me	714
40	Phenyl	Cumyl	Me	2,096
41	Cyclohexyl	^{t}Bu	Me	82
42	Cyclohexyl	1-Adamantyl	Me	434
43	Cyclohexyl	Cumyl	Me	4,315
44	Cyclohexyl	CPh_2Me	H	6,552

[a]Polymerization conditions: toluene 250 mL, MAO 1.25 mmol, Al/Zr = 250–625,000, ethylene 0.1 MPa, 25 °C, 5 or 10 min. [b]Polymerization conditions: ^{n}heptane 500 mL, complex 0.005 μmol, MAO 1.25 mmol, ethylene pressure 0.9 MPa, 75 °C, 15 min.

The R^2 substituents are also relevant to the above-mentioned syndiospecificity of Ti-FI catalysts, that is, the syndioselectivity is linearly correlated with the volume of R^2 substituents, meaning higher selectivity for larger R^2. To this end, Ti-FI catalyst **48**, which possesses a trimethylsilyl group as an R^2 substituent, was found to produce a highly syndiotactic PP (*rr* 93 %, 25 °C polymerization) with a very high T_m of 152 °C, representing one of the highest melting temperature (T_m) for syndiotactic polypropylene ever synthesized.[107,108]

Table 6. Effects of the R^2 substituents of FI-Ti complexes on propylene polymerization behavior[a]

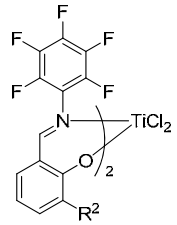

Complex	R^2	Activity (g-polymer/mmol-M h)	M_n[b] (kg/mol)	M_w/M_n[b]	T_m[c] (°C)	[*rr*] (%)
45	H	30.7	189.0	1.51	n. d.[d]	43
46	Me	68.8	260.2	1.22	n. d.[d]	50
47	^{i}Pr	31.1	153.7	1.16	n. d.[d]	75
31	^{t}Bu	3.7	28.5	1.11	137	87
48	Me_3Si	5.9	47.0	1.08	152	93

[a]Polymerization conditions: toluene 250 mL, complex 10 μmol, MAO 2.5 mmol, propylene 0.1 MPa, 25 °C, 5 h. [b]Determined by GPC (PP calibration). [c]Determined by DSC. [d]Not detected.

The obtained syndiotactic polypropylenes were revealed to possess the *rrrm* and *rrmr* pentad sequences as the main source of stereo-errors, indicating that the polymerization apparently followed a chain-end-control mechanism despite apparent C_2-symmetry of these Ti-FI catalysts. Research on the chain-end structures of living and non-living polymers, sequence distributions of propylene polymers with a small amount of (^{13}C-labeled) ethylene units, and cyclopolymerization of 1,6-heptadiene established the peculiar regiochemistry involved in propylene polymerization mediated by Ti-FI catalysts activated with MAO.[116–118] This can be summarized as: 1) exclusive 1,2-insertion to Ti–H (assumed after the β-H transfer) and to Ti–Me species; 2) preferential 1,2-insertion to Ti–CH_2CH_2–R; 3) regio-random insertion to Ti–CH_2CH–RR'; and 4) highly regulated 2,1-insertion to Ti–CH(R')CH_2–R. In fact, this selectivity is consistent with the observed regio-block structures obtained by this class of catalyst.[108,119]

In line with these experimental results on the Ti-FI complexes, Cavallo and coworkers proposed based on the combined QM/MM calculations that the observed chain-end controlled syndiospecificity could be explained by postulating fluxional interconversion between Δ and Λ isomers of the octahedral Ti-FI complexes.[120,121] Such fluxional isomerization was observed for several FI and related complexes.[87,122–124] In the model shown in **Figure 7**, *re*-chain/Λ isomer A is more stable than *re*-chain/Δ isomer D and isomer A favors propylene coordination at *si*-face, where the chirality of a polymer chain end (α-carbon) is transferred to the coordinating face of a propylene monomer (chain-end control) via migratory insertion. The resulting *si*-chain/Λ isomer B isomerizes into more stable *si*-chain/Δ isomer C, which favors propylene coordination at *re*-face, generating *re*-chain/Δ isomer D, which again isomerizes into more stable *re*-chain/Λ isomer A, coming back right where the whole series of events started. The repetitive cycle of isomerization/insertion

certainly affords the syndiotactic sequences of polypropylene. Note that the face selection in this model is made by steric repulsion between the methyl group of the propylene monomer and the R^2 substituents, which is in accord with the R^2-dependent syndioselectivity observed experimentally. Thus, R^2 substituents located above and below the reaction sites can make a face selection of prochiral propylene monomer.

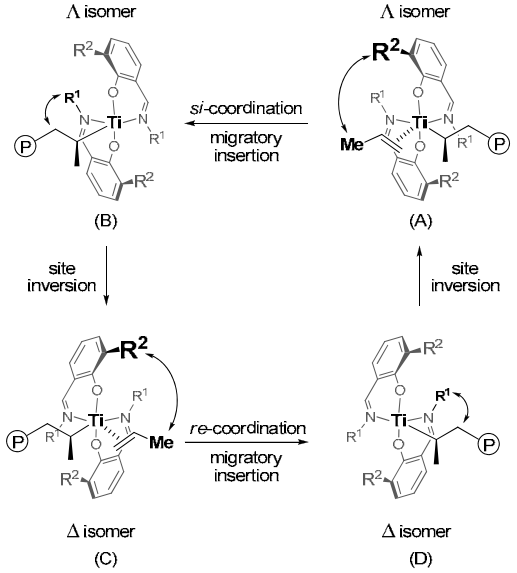

Figure 7. A proposed site-inversion mechanism for syndioselective propylene polymerization promoted by phenoxy–imine Ti catalysts.

Similarly, R^2 substituents are conveniently located to control comonomer incorporations in copolymerization, which is a selectivity between monomer substrates.[125,126] In the living polymerization with *N*-perfluorinated aryl Ti complexes (**31**, **45**–**47**, **49**), complex **31** (R^2 = ^{t}Bu) exhibited far higher activity (6–13×) than the others (R^2 = cyclohexyl, ^{i}Pr, Me, H) in ethylene homopolymerization. However, in the copolymerization of ethylene with 1-hexene, the activities became much lower and similar to each other (0.8 – 1.8 g-polymer/(mmol-Ti h)) but all the (co)polymerizations exhibited a typical living behavior as exemplified by very small PDI values (< 1.2). Under the conditions examined, the comonomer uptake follows the order of the size of R^2 (H > Me > ^{i}Pr ~ cyclohexyl >> ^{t}Bu). The same trend was observed for 1-octene and 1-decene copolymerizations, although the comonomer uptakes were slightly reduced from C_6 to C_8 to C_{10} olefins. Clearly, steric effects between R^2 and the comonomers are at work in these examples, which is logical because the R^2 substituents are situated above and below the reaction sites.

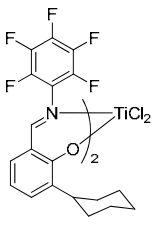

49

2.2.4. Activation of FI catalysts

As mentioned above, the catalytically active species of group 4 metallocene catalysts is a 14e cationic alkyl metal species, $[Cp'_2M–R]^+$, which can be generated from neutral catalyst precursors (Cp'_2MX_2) by activation with MAO or boron-based cocatalysts (*vide supra*). The activation process is thus considered to involve one or both of the following: 1) alkylation of M–X bonds in the precursor, making at least one M–R bond, and 2) developing coordinative and electronic unsaturation at the metal center. Therefore, in order to use the boron-based cocatalysts, an alkylated catalyst precursor, Cp'_2MR_2, must be employed because those boron-based cocatalysts have no capability for alkylation unlike MAO. Alternatively, activation of metallocene (Cp'_2MX_2) having non-alkyl X ligands can be performed by a combination of trialkylaluminums (e.g., ^{i}Bu$_3$Al) and perfluoroaryl borate salts (e.g., $[Ph_3C][B(C_6F_5)_4]$), where the alkylaluminums play the role of alkylation for the Cp'_2MX_2 at least partially, and the resulting alkyl complex can generate a cationic alkyl species with the borates simultaneously. Thus, for metallocene catalysts, this activation method has been generally considered to be chemically equivalent to the activation with MAO or with boron-based cocatalysts with metallocene dialkyls.

However, when this activation method (^{i}Bu$_3$Al/$[Ph_3C][B(C_6F_5)_4]$) is applied to FI catalysts, the polymerization results were strikingly different from those with MAO activation. This is because a reaction of FI catalyst precursors ($(L^{FI})_2MX_2$) and ^{i}Bu$_3$Al causes the *in situ* generation of a new species (**50**), where the imine is reduced to an amine by ^{i}Bu$_3$Al or its contaminant ^{i}Bu$_2$AlH (**Scheme 6**, in these experiments, FI complexes and ^{i}Bu$_3$Al are mixed for 10 min before polymerization).[90–92] The resulting phenoxy–amine complexes exhibited a number of interesting polymerization characteristics owing to their unusual N donors, ^{i}Bu$_2$Al-N, being bulkier and weaker donors than the imine-nitrogen. In general, phenoxy–amine species are lower in polymerization activity than the corresponding phenoxy–imine species, but they tend to polymerize olefinic monomers into extremely high molecular weight polymers.

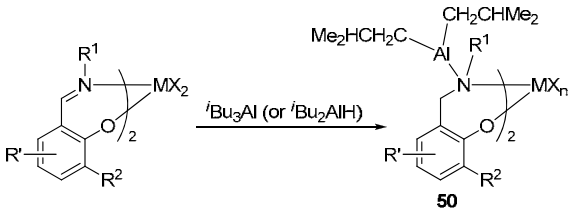

Scheme 6

With regard to polymerization of propylene and α-olefins, Ti-FI catalysts bearing reduced phenoxy–amine ligands afford high molecular weight polymers, whose regio- and stereo-insertion chemistry is nearly completely irregular.[127] For polymerization of higher alpha-olefins, the activity became higher in the order of 4-methyl-1-pentene > 1-decene > 1-octene > 1-hexene, which is completely opposite to the ordinary order obtained with a typical *ansa*-metallocene, *rac*-(C_2H_4)(1-indenyl)$_2ZrCl_2$.[128] In addition, the polymerization exhibits a zeroth order dependence on the concentration of 1-hexene, which is also unusual for an early metal catalyst. These peculiar polymerization characteristics suggest, combined with

the results of DFT calculations, that the amine donors ($^{i}Bu_2Al$-N) are extremely labile and that one of them is detached from the Ti metal during monomer coordination and insertion. Therefore, the probable scenario is that the larger monomer and the growing polymer chain derived thereof enhance the dissociation of the N donor, which makes the active species sterically more open and more electrophilic and thus accelerates the polymerizations.

When Zr- or Hf-FI complexes are activated with $^{i}Bu_3Al/[Ph_3C][B(C_6F_5)_4]$, these catalysts polymerize propylene into high molecular weight polypropylenes with moderate isotacticity (Zr: *mmmm* 35.9 %, T_m 103.5 °C; Hf: *mmmm* 55.7 %, T_m 123.8 °C).[129] Similar reduced phenoxy–amine active species are assumed for these polymerizations, too.

3. Summary and Outline of This Thesis

As described above, transition metal olefin insertion polymerization catalysts have evolved dynamically over the past 60 years, and they have been the main driver behind the development of the polyolefin industry and the petrochemical industry. While the majority of commercially available polyolefins are still produced with the heterogeneous, multi-sited Ziegler–Natta catalysts (as represented by $MgCl_2$-supported $TiCl_4$ catalysts), single-site metallocene catalysts have become more prevalent in recent years. Well-defined discrete molecular catalysts equipped with appropriately designed cyclopentadienyl-based organic π-ligands have allowed scientists to understand and even control the reactivity and the selectivity of olefin polymerizations in a rational manner, which was impossible with the traditional Ziegler–Natta catalysts supported on the ill-defined inorganic surfaces that served as a part of their ligands.

Post-metallocene catalysts that followed metallocene catalysts have offered further diversity and opportunities for the development of olefin polymerization catalysis in that they have sterically and electronically offered a much higher degree of freedom for catalyst design than metallocene catalysts. Among the post-metallocene catalysts developed, FI catalysts possess an especially large diversity of structures sterically and electronically thanks to their straightforward synthesis and modular properties. This is one of the most desired and suitable features for a polymerization catalyst in order to respond to market demands that are also diversified over a wide range. Another distinctive feature of FI catalysts is that they are octahedral complexes, thus are rather similar to heterogeneous Ziegler-Natta catalysts consisting of hexagonal crystals, but are quite different from tetrahedral metallocene catalysts. In addition, coordination of two bidentate ligands around a metal makes FI catalysts possess *cis*-oriented X ligands, which is considered to be indispensable for efficient olefin polymerization. Furthermore, the bis-ligation also gives a structural flexibility to FI catalysts in sharp contrast to classic quadridentate [O^-NNO^-] ligands like salen and salphen. Several experimental and theoretical studies point to dynamic fluxional structures for the octahedral framework, which is considered to be responsible for some of the unique polymerization characteristics of FI catalysts.

It should also be noted that within the thermodynamically most stable *cis*-N/*trans*-O/*cis*-X geometry of

FI catalysts, R^1 and R^2 substituents are situated at suitable positions for strategically controlling the polymerization reactions. As typical examples, the relationship between R^1 substituents and polymer molecular weights including the living polymerization (in other words, chain transfer reactions) and also the relationships between R^2 substituents and catalytic activity, stereospecificity, and comonomer incorporation are highlighted.

The last issue raised in this General Introduction is susceptibility of the imine function to nucleophiles, which causes the unique olefin polymerizations with the phenoxy–amine species generated *in situ* by $^{i}Bu_3Al$. However, the vulnerability of the imine also makes it extremely difficult to prepare alkyl complexes of FI catalysts (**Scheme 5**). Many attempts to synthesize an alkyl complex based on Schiff base ligands have failed due to electrophilic attack of alkylating agents or intramolecular migratory insertion of a M–C bond to the imine, particularly when combined with group 4 metals that make the imine even more electrophilic. These situations have hampered FI catalysts to be activated with boron-based activators without being reduced at the imine moiety. Moreover, despite these interesting polymerization characteristics, the true identity of the active species of FI catalysts remained unknown before this study.

In view of this background, Part I of this thesis will focus on observation, identification, and characterization of the active species involved in olefin polymerization with FI catalysts. Chapter 1 deals with the activation of Ti- and Zr-FI catalysts activated with MAO, which was observed by ^1H NMR spectroscopy. From a reaction of a living Ti-FI complex, $(L^{FI})_2TiCl_2$ (**31**) with MAO in toluene-d_8, formation of a cationic monomethyl species, $[(L^{FI})_2Ti–Me]^+$ was identified for the first time. The species has a C_2 symmetry similar to its precursor on the NMR time scale and indeed polymerizes ethylene or propylene into living propagating species. The methyl cationic species was irreversibly transformed into inactive species via a ligand transfer reaction to Me_3Al, which turns out to constitute a major deactivation path for this class of complex.

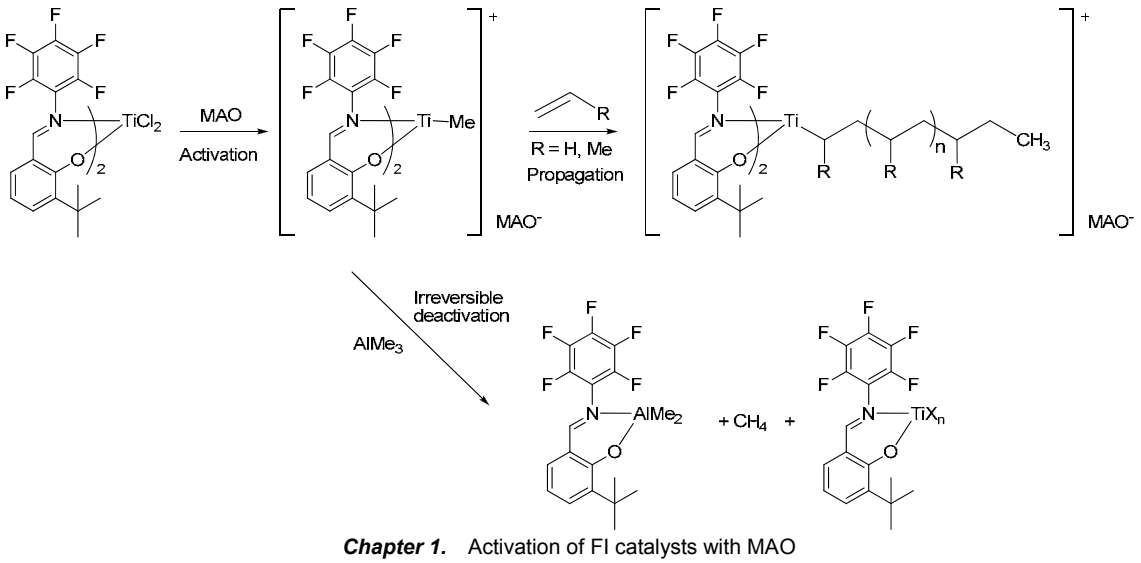

Chapter 1. Activation of FI catalysts with MAO

Chapter 2 concerns synthesis of alkylated FI complexes. It was demonstrated that the dimethyl or monomethyl halide group 4 complexes, $(L^{FI})_2TiMe_2$ (**51**) or $(L^{FI})_2TiMeBr$ (**52**), are achievable via salt metathesis reactions between X_nMR_{4-n} (R: Me; X: Br, Cl; n = 2, 3) and sodium salts of the phenoxy–imine ligands (L^{FI}-Na). The obtained dimethyl complex can be activated with $B(C_6F_5)_3$ and $[Ph_3C][B(C_6F_5)_4]$ in well defined manners into monomethyl cationic species, $[(L^{FI})_2Ti–Me][Me_nB(C_6F_5)_{4-n}]$ (n = 0, 1), which are similar to the MAO-activated species mentioned above. The methyl species was grown into a propagating species by adding a small amount of ethylene, in which the Ti-bound methylene protons were identified by ^{1}H NMR spectroscopy. Nature of the ion-pairs and the reaction mechanisms are discussed based on the spectroscopic results.

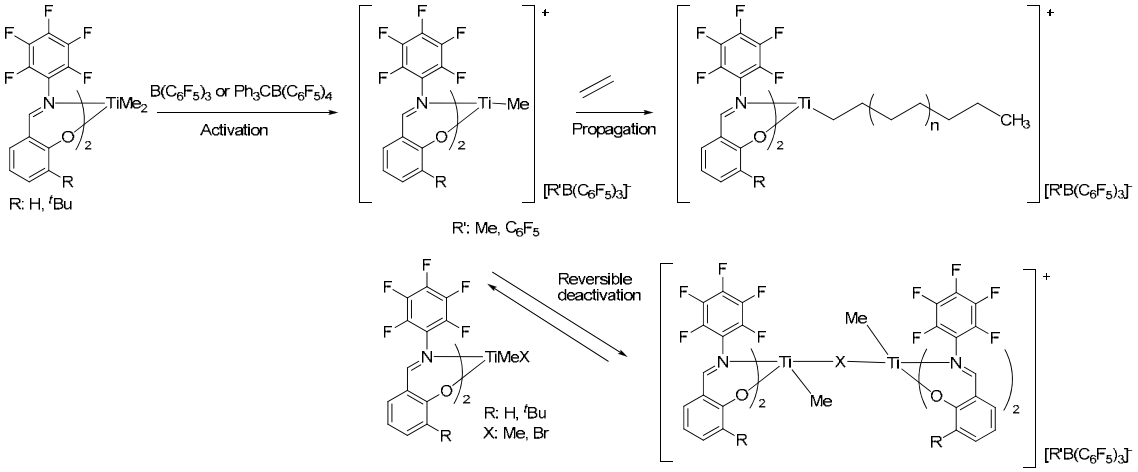

Chapter 2. Synthesis and characterization of alkylated FI complexes and their activation with boron-based activators

Having gained insight into the active species, Part II of this thesis will discuss selectivities involved in olefin polymerizations mediated by FI catalysts. Chapter 3 reports on isoselective propylene polymerization with Zr- and Hf-FI catalysts activated with ^{i}Bu$_3$Al/$[Ph_3C][B(C_6F_5)_4]$. Microstructural analyses of the isotactic polymers suggest that the polymerization probably proceeds via a site-control mechanism with a 1,2-insertion of propylene. Among the complexes examined, a Hf complex produced polypropylene with very high isotacticity ([*mmmm*] 96.8 %, T_m 165.1 ºC) that is comparable to that made by the best heterogeneous Ziegler–Natta catalysts.

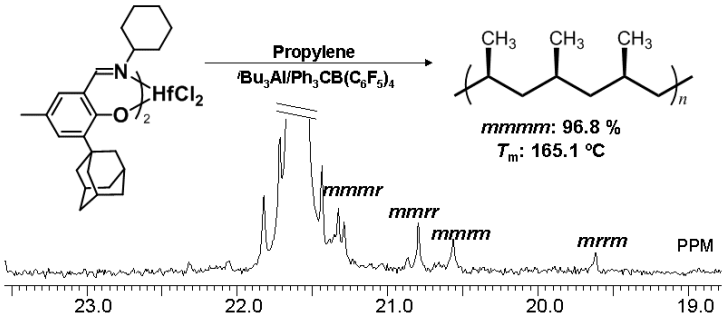

Chapter 3. Isoselective propylene polymerization with FI catalysts

Chapter 4 presents the investigation into the stereo- and regioselectivities in propylene polymerization mediated by Zr- and Hf-FI complexes with MAO. ^{13}CNMR analyses of the resultant polymers clarified that propylene monomers are enchained prevailingly in a 1,2-fashion and in a virtually nonstereoselective manner. These polymerization characteristics make a sharp contrast to those of Ti congeners, where 2,1-insertion is the main propagation mode, and moderately to highly syndiotactic polypropylenes can be obtained.

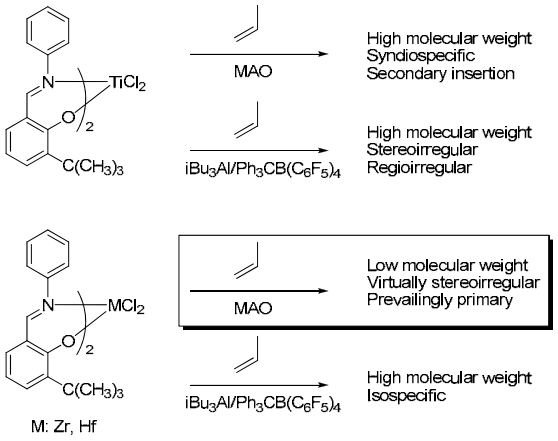

Chapter 4. Stereo- and regioselectivity of zirconium and hafnium FI complexes activated with MAO

In Chapter 5, substrate selectivity in ethylene/propylene copolymerization with a series of Zr-FI catalysts were investigated. One of the Zr-FI catalysts investigated in this study can discern ethylene from a mixture of ethylene and propylene with more than 99 % selectivity. Density functional theory (DFT) calculations have revealed a spatially confined reaction site in the transition states of the migratory insertion which is just the right size for an ethylene molecule but too small for a propylene one. The substituents adjacent to the phenolic oxygens are of crucial importance in developing the size/shape-selectivity.

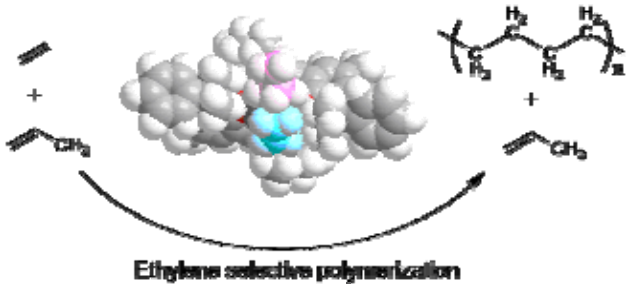

Chapter 5. Substrate selective polymerization using zirconium FI catalysts

Part III of this thesis will describe the synthesis of chain-end functionalized polyolefins using FI catalysts and metallocene catalysts. Chapter 6 reports on chain-end functionalized polyethylene and polypropylene including a telechelic polypropylene by means of a living polymerization mediated with a Ti-FI catalyst. Functionalized initiators can be generated from a stoichiometric reaction of the active

$[(L^{FI})_2Ti–Me]^+$ species and ω-functionalized-α-olefins, which is designed on the basis of understanding the activation process, and the differences between the first and second monomer insertions in the regio-chemistry and the reactivity. Chain-end capping can also be accomplished using ω-functionalized-α-olefins in a quantitative manner.

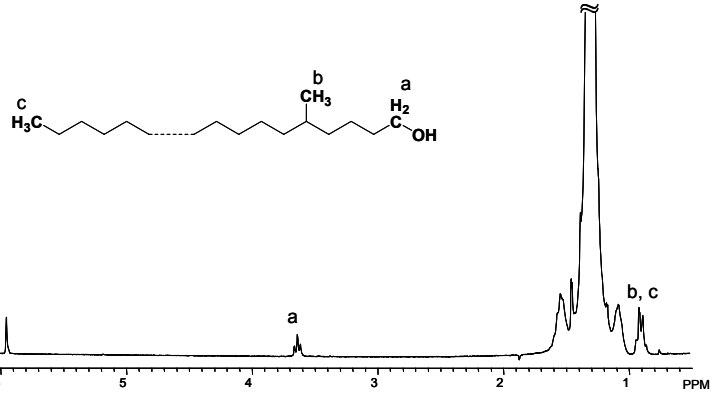

Chapter 6. Chain-end functionalized polyolefins using a living titanium FI catalyst

In Chapter 7, chain-end functionalities are introduced at the terminating chain ends using chain transfer reaction. Silanolytic chain transfer is well known as a versatile way to introduce organosilane functions at chain termini, simultaneously achieving molecular weight control. The scope of silanolytic chain transfer can be extended to SiO_2-supported heterogeneous Zr olefin polymerization catalysts. While the breadth of applicability appears to be somewhat narrower than the case of homogeneous single-site catalysts, the first group 4 systems capable of functioning in the slurry mode and of producing functionalized ethylene homopolymers have been developed.

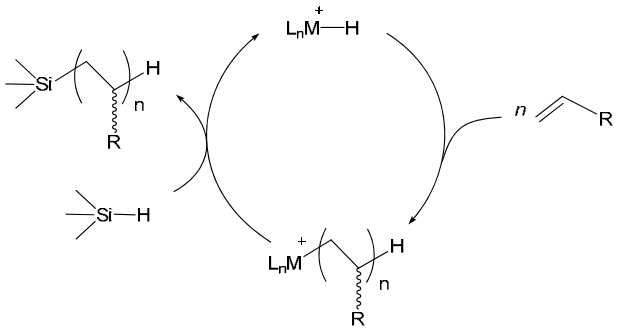

Chapter 7. Silanolytic chain transfer for end-functionalization of polyolefins

References

(1) Staudinger, H.; Lüthy, M. *Helv. Chim. Acta* **1925**, *8*, 41–64.

(2) Mülhaupt, R. *Angew. Chem. Int. Ed.* **2004**, *43*, 1054–1063.

(3) Carothers, W. H. *J. Am. Chem. Soc.* **1929**, *51*, 2548–2559.

(4) MacDermott, K. *Chem. Eng. News* **1999**, *77*, 49–50.

(5) Ziegler, K.; Holzkamp, E.; Breil H.; Martin, H. *Angew. Chem.* **1955**, *67*, 541–547.

(6) Wilke, G. Karl Ziegler, in Memoriam. In *Coordination Polymerization*; Chen, J. C. W., Ed.; Academic Press, Inc., New York, 1975, pp 1–13.

(7) Natta, G.; Pino, P.; Corradini, P.; Danusso, F.; Mantica, E.; Mazzanti, G.; Moraglio, G. *J. Am. Chem. Soc.* **1955**, *77*, 1708–1710.

(8) Porri, L. Giulio Natta–His Life and Scientific Achievements. In *Macromolecular Symposia*; Giarrusso, A.; Ricci, G.; Tritto, I., Eds.; Wiley-VCH, Weinheim, 2004, pp 1–5.

(9) Mitsui Petrochemical U.S. Patent 3642746; Ger. Patent 1939074 1968.

(10) Montedison Ger. Patent 2000586 1968.

(11) Masuda, T.; Makio, H.; Miyashita, A. In *Catalysis in Precision Polymerization*; Kobayashi, S., Ed.; John Wiley & Sons, Chichester, 1997, pp 18–54.

(12) Hunt, L. B. *Platinum Metals Rev.* **1984**, *28*, 76–83.

(13) Kealy, T. J.; Pauson, P. L. *Nature* **1951**, *168*, 1039–1040.

(14) Wilkinson, G.; Rosenblum, M.; Whiting, M. C.; Woodward, R. B. *J. Am. Chem. Soc.* **1952**, *74*, 2125–2126.

(15) Fischer, E. O.; Pfab, W. Z. *Naturforsch. B: Chem. Sci.* **1952**, *7*, 377–379.

(16) Astruc, D. *New J. Chem.* **2005**, *29*, 42–56.

(17) Cossee, P. *J. Catal.* **1964**, *3*, 80–88.

(18) Arlman, E. J.; Cossee, P. *J. Catal.* **1964**, *3*, 99–104.

(19) Natta. G.; Pino, P.; Mazzanti, G.; Giannini, U. *J. Am. Chem. Soc.* **1957**, *79*, 2975–2976.

(20) Natta. G.; Pino, P.; Mazzanti, G.; Giannini, U.; Mantica, E.; Peraldo, M. *J. Polym. Sci.* **1957**, *26*, 120.

(21) Natta, G.; Corradini, P.; Bassi, I. W. *J. Am. Chem. Soc.* **1958**, *80*, 755–756.

(22) Breslow, D. S.; Newburg, N. R. *J. Am. Chem. Soc.* **1957**, *79*, 5072–5073.

(23) Breslow, D. S.; Newburg, N. R. *J. Am. Chem. Soc.* **1959**, *81*, 81–86.

(24) Long, W. P.; Breslow, D. S. *J. Am. Chem. Soc.* **1960**, *82*, 1953–1957.

(25) Chien, J. C. W. *J. Am. Chem. Soc.* **1959**, *81*, 86–92.

(26) Skupinska, *J. Chem. Rev.* **1991**, *91*, 613–648.

(27) Dyachkovskii, F. S.; Shilova, A. K.; Shilov, A. E. *J. Polym. Sci., Part C* **1967**, *16*, 2333–2339.

(28) Reichert, K. H.; Meyer, K. R. *Makromol. Chem.* **1973**, *169*, 163–176.

(29) Longo, W. P.; Breslow, D. S. *Justus Liebigs Ann. Chem.* **1975**, 463–469.

(30) Sinn, H.; Kaminsky, W. *Adv. Organomet. Chem.* **1980**, *18*, 99–149.

(31) Sinn, H.; Kaminsky, W.; Vollmer, H.-J.; Woldt, R. *Angew. Chem.,Int. Ed. Engl.* **1980**, *19*, 390–392.

(32) Eisch, J. J.; Piotrowski, A. M.; Brownstein, S. K.; Gabe, E. J.; Lee, F. L. *J. Am. Chem. Soc.* **1985**, *107*, 7219–7221.

(33) Watson, P. L.; Parshall, G. W. *Acc. Chem. Res.* **1985**, *18*, 51–56.

(34) Thompson, M. E.; Bercaw, J. E. *Pure & Appi. Chem.* **1984**, *56*, 1–11.

(35) Jeske, G.; Lauke, H.; Mauermann, H.; Swepston, P. N.; Schumann, H.; Marks, T. J. *J. Am. Chem. Soc.* **1985**, *107*, 8091–8103.

(36) Jordan, R. F.; Dasher, W. E.; Echols, S. F. *J. Am. Chem. Soc.* **1986**, *108*, 1718–1719.

(37) Jordan, R. F.; Bajgur, C. S.; Willett, R.; Scott, B. *J. Am. Chem. Soc.* **1986**, *108*, 7410–7411.

(38) Chien, J. C. W.; Tsai, W. M.; Rausch, M. D. *J. Am. Chem. Soc.* **1991**, *113*, 8570–8571.

(39) Ewen, J. A.; Elder, M. J. Eur. Pat. Appl. EP 0426637 1991.

(40) Turner, H. W. Eur Pat. Appl. EP 0 277 004 A1 1988.

(41) Yang, X.; Stern, S.; Marks, T. J. *Organometallics* **1991**, *10*, 840–842.

(42) Chen, E.-X.; Marks, T. J. *Chem. Rev.* **2000**, *100*, 1391–1434.

(43) Brintzinger, H. H.; Fischer, D.; Muelhaupt, R.; Waymouth, R. M. *Angew. Chem., Int. Ed. Engl.* **1995**, *34*, 1143–1170.

(44) Ewen, J. A. *J. Am. Chem. Soc.* **1984**, *106*, 6355–6364.

(45) Kaminsky, W.; Külper, K.; Brintzinger, H.; Wild, F. *Angew. Chem., Int. Ed. Engl.* **1985**, *24*, 507–508.

(46) For example, Busico, V.; Cipullo, R. *Prog. Polym. Sci.* **2001**, *26*, 443–533.

(47) Mashima, K.; Fujikawa, S.; Nakamura, A. *J. Am. Chem. Soc.* **1993**, *115*, 10990–10991.

(48) Mashima, K.; Fujikawa, S.; Tanaka, Y.; Urata, H.; Oshiki, T.; Tanaka, E.; Nakamura, A. *Organometallics* **1995**, *14*, 2633–2640.

(49) Crowther, D. J.; Borkowsky, S. L.; Swenson, D.; Meyer, T. Y.; Jordan, R. F. *Organometallics* **1993**, *12*, 2897–2903.

(50) Kreuder, C.; Jordan, R. F.; Zhang, H. *Organometallics* **1995**, *14*, 2993–3001.

(51) Shapiro, P. J.; Schaefer, W. P.; Labinger, J. A.; Bercaw, J. E.; Cotter, W. D. *J. Am. Chem. Soc.* **1994**, *116*, 4623–4640.

(52) Okuda, J. *Chem. Ber.* **1990**, *123*, 1649–1651.

(53) Okuda, J. *Dalton Trans.* **2003**, *12*, 2367–2378.

(54) Stevens, J. C.; Timmers, F. J.; Rosen, G. W.; Knight, G. W.; Lai, S. Y. Eur. Pat. Appl., EP 0 416 815 A2 1991.

(55) Canich, J. A. Eur. Pat. Appl., EP 0 420 436 A1 1991.

(56) Britovsek, G. J. P.; Gibson, V. C.; Wass, D. F. *Angew. Chem. Int. Ed.* **1999**, *38*, 428–447.

(57) Gibson, V. C.; Spitzmesser, S. K. *Chem. Rev.* **2003**, *103*, 283–316.

(58) Scollard, J. D.; D. H.; McConville, D. H.; Payne, N. C.; Vittal, J. J. *Macromolecules* **1996**, *29*, 5241–5243.

(59) Scollard, J. D.; McConville, D. H. *J. Am. Chem. Soc.* **1996**, *118*, 10008–10009.

(60) Hakala, K.; Löfgren, B.; Polamo, M.; Leskelä, M. *Macromol. Rapid Commun.* **1997**, *18*, 635–638.

(61) Britovsek, G. J. P.; Gibson, V. C.; Kimberley, B. S.; Maddox, P. J.; McTavish, S. J.; Solan, G. A.; White, A. J. P.; Williams, D. J. *Chem. Commun.* **1998**, 849–850.

(62) Small, B. L.; Brookhart, M.; Bennett, A. M. A. *J. Am. Chem. Soc.* **1998**, *120*, 4049–4050.

(63) Gibson, V. C.; Redshaw, C.; Solan, G. A. *Chem. Rev.* **2007**, *107*, 1745–1776.

(64) Johnson, L. K.; Killian, C. M.; Brookhart, M. *J. Am. Chem. Soc.* **1995**, *117*, 6414–6415.

(65) Matsugi, T.; Fujita, T. *Chem. Soc. Rev.* **2008**, *37*, 1264–1277.

(66) Saitoh, J.; Mitani, M.; Matsui, S.; Sugi, M.; Tohi, Y.; Tsutsui, T.; Fujita, T.; Nitabaru, M.; Makio, H. EP-0874005, Apr. 26, 1997.

(67) Johnson, L. K.; Bennett, A. M.; Ittel, S. D.; Wang, L.; Parthasarathy, A.; Hauptman, E.; Simpson, R. D.;

Feldman, J.; Coughlin, E. B. WO Pantent 9830609, 1998.

(68) Bansleben, D. A.; Friedriich, S. K.; Younkin, T. D.; Grubbs, R. H.; Wang, C.; Li, R. T. WO Pantent 9842664, 1998.

(69) Wang, C.; Friedrich, S.; Younkin, T. R.; Li, R. T.; Grubbs, R. H.; Bansleben, D. A.; Day, M. W. *Organometallics* **1998**, *17*, 3149–3151.

(70) Matsumoto, K.; Saito, B.; Katsuki, T. *Chem. Commun.* **2007**, 3619–3627.

(71) Hobday, M. D.; Smith, T. D. *Coord. Chem. Rev.* **1973**, *9*, 311–337.

(72) Cozzi, P. G. *Chem. Soc. Rev.* **2004**, *33*, 410–421.

(73) Taylor, K. J. *Polymer* **1964**, *5*, 207–211.

(74) Floriani, C.; Solari, E.; Corazza, F.; Chiesi-Villa, A.; Guastini, C. *Angew. Chem., Int. Ed. Engl.* **1989**, *28*, 64–66.

(75) Solari, E.; Floriani, C.; Chiesi-Villa, A.; Rizzoli, C. *J. Chem. Soc., Dalton Trans.* **1992**, 367–371.

(76) Corazza, F.; Solari, E.; Floriani, C.; Chiesi-Villa, A.; Guastini, C. *J. Chem. Soc., Dalton Trans.* **1990**, 1335–1344.

(77) Tjaden, E. B.; Swenson, D. C.; Jordan, R. F.; Petersen, J. L. *Organometallics* **1995**, *14*, 371–386.

(78) Corden, J. P.; Errington, W.; Moore, P.; Wallbridge, M. G. H. *Chem. Commun.* **1999**, 323–324.

(79) Woodman, P.; Hitchcock, P. B.; Scott, P. *Chem. Commun.* **1996**, 2735–2736.

(80) Woodman, P. R.; Munslow, I. J.; Hitchcock, P. B.; Scott, P. *J. Chem. Soc., Dalton Trans.* **1999**, 4069–4076.

(81) Woodman, P. R.; Alcock, N. W.; Munslow, I. J.; Sanders, C. J.; Scott, P. *J. Chem. Soc., Dalton Trans.* **2000**, 3340–3346.

(82) Knight, P. D.; Clarke, A. J.; Kimberley, B. S.; Jackson, R. A.; Scott, P. *Chem. Commun.* **2002**, 352–353.

(83) Knight, P.D.; O'Shaughnessy, P. N.; Munslow, I. J.; Kimberley, B. S.; Scott, P. *J. Organomet. Chem.* **2003**, *683*, 103–113.

(84) Knight, P. D.; Clarkson, G.; Hammond, M. L.; Kimberley, B. S.; Scott, P. *J. Organomet. Chem.* **2005**, *690*, 5125–5144.

(85) Cozzi, P. G.; Floriani, C. *Inorg. Chem.* **1995**, *34*, 2921–2930.

(86) Cozzi, P. G.; Gallo, E.; Floriani, C.; Chiesi-Villa, A.; Rizzoli, C. *Organometallics* **1995**, *14*, 4994–4996.

(87) Bei, X.; Swenson, D. C.; Jordan, R. F. *Organometallics* **1997**, *16*, 3282–3302.

(88) Matsui, S.; Tohi, Y.; Mitani, M.; Saito, J.; Makio, H.; Tanaka, H.; Nitabaru, M.; Nakano, T.; Fujita, T. *Chem. Lett.* **1999**, 1065–1066.

(89) Matsui, S.; Mitani, M.; Saito, J.; Tohi, Y.; Makio, H.; Tanaka, H.; Fujita, T. *Chem. Lett.* **1999**, 1263–1264.

(90) Makio, H.; Kashiwa, N.; Fujita, T. *Adv. Synth. Catal.* **2002**, *344*, 477–493.

(91) Makio, H.; Fujita, T. *Acc. Chem. Res.* **2009**, *42*, 1532–1544.

(92) Matsui, S.; Mitani, M.; Saito, J.; Tohi, Y.; Makio, H.; Matsukawa, N.; Takagi, Y.; Tsuru, K.; Nitabaru, M.; Nakano, T.; Tanaka, H.; Kashiwa, N.; Fujita, T. *J. Am. Chem. Soc.* **2001**, *123*, 6847–6856.

(93) Cuomo, C.; Strianese, M.; Cuenca, T.; Sanz, M.; Grassi, A. *Macromolecules* **2004**, *37*, 7469–7476.

(94) Ishii, S.; Mitani, M.; Saito, J.; Matsuura, S.; Furuyama, R.; Fujita, T. *Stud. Surf. Sci. Catal.* **2003**, *145*, 49–54.

(95) Clarkson, G. J.; Gibson, V. C.; Goh, P. K. Y.; Hammond, M. L.; Knight, P. D.; Scott, P.; Smit, T. M.; White, A. J. P.; Williams, D. J. *Dalton Trans.* **2006**, 5484–5491.

(96) Ishii, S.-i.; Saito, J.; Mitani, M.; Mohri, J.-i.; Matsukawa, N.; Tohi, Y.; Matsui, S.; Kashiwa, N.; Fujita, T. *J.*

Mol. Catal. A **2002**, *179*, 11–16.

(97) Matsui, S.; Mitani, M.;Saito, J.; Matsukawa, N.;Tanaka, H.; Nakano, T.; Fujita, T. *Chem. Lett.* **2000**, 554–555.

(98) Ishii, S.; Mitani, M.; Saito, J.; Matsuura, S.; Kojoh, S.-i.; Kashiwa, N.; Fujita, T. *Chem. Lett.* **2002**, 740–741.

(99) Terao, H.; Ishii, S.; Saito, J.; Matsuura, S.; Mitani, M.; Nagai, N.; Tanaka, H.; Fujita, T. *Macromolecules* **2006**, *39*, 8584–8593.

(100) Saito, J.; Mitani, M.; Mohri, J.-i.; Yoshida, Y.; Matsui, S.; Ishii, S.-i.; Kojoh, S.-i.; Kashiwa, N.; Fujita, T. *Angew. Chem., Int. Ed.* **2001**, *40*, 2918–2920.

(101) Mitani, M.; Mohri, J.-i.; Yoshida, Y.; Saito, J.; Ishii, S.; Tsuru, K.; Matsui, S.; Furuyama, R.; Nakano, T.; Tanaka, H.; Kojoh, S.-i.; Matsugi, T.; Kashiwa, N.; Fujita, T. *J. Am. Chem. Soc.* **2002**, *124*, 3327–3336.

(102) Mitani, M.; Nakano, T.; Fujita, T. *Chem. –Eur. J.* **2003**, *9*, 2396–2403.

(103) Furuyama, R.; Saito, J.; Ishii, S.; Makio, H.; Mitani, M.; Tanaka, H.; Fujita, T. *J. Organomet. Chem.* **2005**, *690*, 4398–4413.

(104) Mason, A. F.; Tian, J.; Hustad, P. D.; Lobkovsky, E. B.; Coates, G. W. *Isr. J. Chem.* **2002**, *42*, 301–306.

(105) Saito, J.; Mitani, M.; Mohri, J.-i. Ishii, S.-i.; Yoshida, Y.; Matsugi, T.; Kojoh, S.-i.; Kashiwa, N.; Fujita, T. *Chem. Lett.* **2001**, 576–577.

(106) Tian, J.; Hustad, P. D.; Coates, G. W. *J. Am. Chem. Soc.* **2001**, *123*, 5134–5135.

(107) Mitani, M.; Furuyama, R.; Mohri, J.-i.; Saito, J.; Ishii, S.-i.; Terao, H.; Kashiwa, N.; Fujita, T. *J. Am. Chem. Soc.* **2002**, *124*, 7888–7889.

(108) Mitani, M.; Furuyama, R.; Mohri, J.; Saito, J.; Ishii, S.; Terao, H.; Nakano, T.; Tanaka, H.; Fujita, T. *J. Am. Chem. Soc.* **2003**, *125*, 4293–4305.

(109) Coates, G. W.; Hustad, P. D.; Reinartz, S. *Angew. Chem., Int. Ed.* **2002**, *41*, 2236–2257.

(110) Kui, S. C. F.; Zhu, N.; Chan, M. C. W. *Angew. Chem., Int. Ed.* **2003**, *42*, 1628–1632.

(111) Chan, M. C. W.; Kui, S. C. F.; Cole, J. M.; McIntyre, G. J.; Matsui, S.; Zhu, N.; Tam, K.-H. *Chem. –Eur. J.* **2006**, *12*, 2607–2619.

(112) Chan, M. C. W. *Macromol. Chem. Phys.* **2007**, *208*, 1845–1852.

(113) Nakano, T. Unpublished data.

(114) Yu, S.-M.; Mecking, S. *J. Am. Chem. Soc.* **2008**, *130*, 13204–13205.

(115) Bryliakov, K. P.; Talsi, E. P.; Mller, H. M.; Baier, M. C.; Mecking, S. *Organometallics* **2010**, 29, 4428–4430.

(116) Saito, J.; Mitani, M.; Onda, M.; Mohri, J.-I.; Ishii, S.- I.; Yoshida, Y.; Nakano, T.; Tanaka, H.; Matsugi, T.; Kojoh, S.-I.; Kashiwa, N.; Fujita, T. *Macromol. Rapid Commun.* **2001**, *22*, 1072–1075.

(117) Lamberti, M.; Pappalardo, D.; Zambelli, A.; Pellecchia, C. *Macromolecules* **2002**, *35*, 658–663.

(118) Hustad, P. D.; Tian, J.; Coates, G. W. *J. Am. Chem. Soc.* **2002**, *124*, 3614–3621.

(119) Mazzeo, M.; Strianese, M.; Lamberti, M.; Santoriello, I.; Pellecchia, C. *Macromolecules* **2006**, *39*, 7812–7820.

(120) Milano, G.; Cavallo, L.; Guerra, G. *J. Am. Chem. Soc.* **2002**, *124*, 13368–13369.

(121) Corradini, P.; Guerra, G.; Cavallo, L. *Acc. Chem. Res.* **2004**, *37*, 231–241.

(122) Niemeyer, J.; Kehr, G.; Fröhlich, R.; Erker, G. *Dalton Trans.* **2009**, 3731–3741.

(123) Axenov, K. V.; Klinga, M.; Lehtonen, O.; Koskela, H. T.; Leskelae, M.; Repo, T. *Organometallics* **2007**, *26*, 1444–1460.

(124) Tohi, Y.; Makio, H.; Matsui, S.; Onda, M.; Fujita, T. *Macromolecules* **2003**, *36*, 523–525.

(125) Furuyama, R.; Mitani, M.; Mohri, J.; Mori, R.; Tanaka, H.; Fujita, T. *Macromolecules* **2005**, *38*, 1546–1552.

(126) Sakuma, A.; Weiser, M.-S.; Fujita, T. *Polym. J.* **2007**, *39*, 193–207.

(127) Saito, J.; Mitani, M.; Matsui, S.; Kashiwa, N.; Fujita, T. *Macromol. Rapid Commun.* **2000**, *21*, 1333–1336.

(128) Saito, J.; Suzuki, Y.; Makio, H.; Tanaka, H.; Onda, M.; Fujita, T. *Macromolecules* **2006**, *39*, 4023–4031.

(129) Saito, J.; Onda, M.; Matsui, S.; Mitani, M.; Furuyama, R.; Tanaka, H.; Fujita, T. Macromol. *Rapid Commun.* **2002**, *23*, 1118–1123.

Part I. Active Species in Olefin Polymerization with FI Catalysts

Chapter 1. Activation of FI catalysts with MAO

Abstract

Solution structures of bis(phenoxy–imine) group 4 transition metal complexes (FI catalysts) were investigated using ^{1}H NMR spectroscopy. At least two isomers exist in equilibrium for FI catalyst precursors, bis[*N*-(3-*tert*-butylsalicylidene)anilinato]zirconium(IV) dichloride (**21**), and bis[*N*-(3,5-dicumylsalicylidene)anilinato]zirconium(IV) dichloride (**53**), while bis[*N*-(3-*tert*-butylsalicylidene)-2,3,4,5,6-pentafluoroanilinato]titanium(IV) dichloride (**31**) exhibits only one isomer under the conditions examined. Upon activation with MAO, all precursors (**21,53,31**) generate two species at ambient temperature judging from some key signals in the ^{1}H NMR. When temperature is raised (up to 75 °C), one species (**21a**,**53a**,**31a**) converts irreversibly to the other species (**21b**,**53b**,**31b**) with concurrent formation of methane. Investigation into the species derived from **31**, which is known to be a robust living polymerization catalyst, revealed that this transformation was a decomposition process of a cationic monomethyl species $[(L^{FI})_2M–Me]^+[MAO]^–$ (**21a**,**53a**,**31a**) into $(L^{FI})AlMe_2$ (**21b**,**53b**,**31b**), methane, and unidentified transition metal complexes via a ligand transfer reaction. The living cationic monomethyl species $[(L^{FI})_2Ti–Me]^+[MAO]^–$ (**31a**) can be grown into a propagating species by adding ethylene (**31c**) and propylene (**31d**). Living propagating species **31d** was robust toward the ligand transfer reaction and stable even at 60 °C. Activation and deactivation of FI catalysts are discussed based on these observations.

Introduction

As mentioned in the General Introduction, the catalytically active species in metallocene-mediated olefin polymerization was identified as a cationic alkyl–metal species $[Cp'_2Zr–R]^+$ and the activation processes and polymerization mechanisms were extensively investigated in relation to the structures of ancillary ligands, counteranions derived from the activators, and the structures of the resulting polyolefins. In the olefin polymerization catalyzed by the metallocenes, of particular interest is that dynamic and reversible structural change of the active species within a time scale of chain propagation results in unique polymerization processes and polymers. For example, Waymouth and coworkers developed a polymerization process where a non-bridged bis(2-arylindenyl)zirconocene, whose structure reversibly changes from chiral to achiral at the rate similar to the propagation, produces stereoblock polymers (**Scheme 1**).[1]

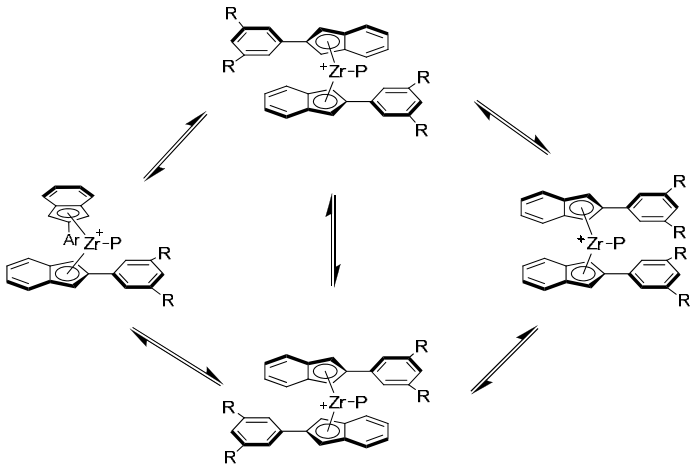

Scheme 1

Another example includes ansa-metallocene compounds bearing a dialkylaminoethyl group on the cyclopentadienyl ligands, which produces polyethylenes having bimodal molar mass distributions upon activation with MAO, presumably because of an association/dissociation equilibrium between Lewis acidic MAO and the amino groups (**Scheme 2**).[2]

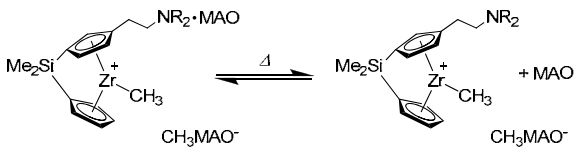

Scheme 2

Some research into FI catalyst precursors or related complexes has suggested that dynamic equilibria among isomers were possible[3,4] and that this configurational fluxionality was a key to understanding some of the unique polymerization characteristics of FI catalysts. For example, Zr-FI complex bis[*N*-(3,5-dicumylsalicylidene)anilinato]zirconium(IV) dichloride (**53**) yielded polyethylenes having uni-, to

bi-, to tri-modal molecular weight distributions depending on the polymerization temperatures (0–75 °C), while bis[*N*-(3-*tert*-butylsalicylidene)anilinato]zirconium(IV) dichloride (**21**) yielded unimodal polyethylenes in the same temperature range (**Figure 1**).[5] Solution structures of these catalyst precursors were investigated using ^{15}N NMR spectroscopy of ^{15}N-enriched complexes **21*** and **53***, demonstrating that complex **53** (**53***) adopted a C_1-symmetric *cis*-N/*cis*-O/*cis*-Cl geometry as a major isomer (isomer b) and the ordinary C_2-symmetric *cis*-N/*trans*-O/*cis*-Cl geometry as a minor isomer (isomer a) in the molar ratio at a/b = 12/88. Regarding complex **21** (**21***), the a/b ratio is 84/16. Moreover, the signals for the nonequivalent imine nitrogen atoms (isomer b) were coalesced into one peak above room temperature, meaning that the isomer was racemized on the NMR timescale (**Figure 2**). This configurational fluxionality of the FI catalysts possibly forms three distinctive active species, producing polyethylene having trimodal molecular weight distributions.

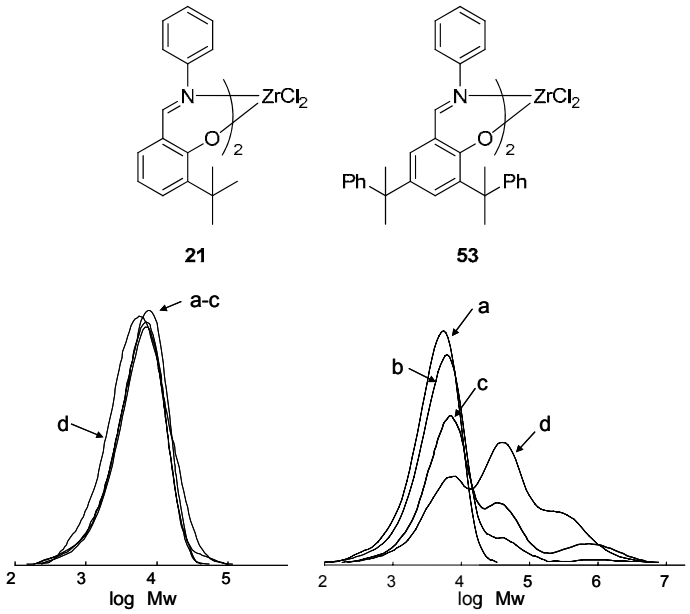

Figure 1. GPC elution curves of the polyethylenes produced with complexes **21** (left) and **53** (right) at a) 0 °C; b) 25 °C; c) 40 °C; d) 75 °C. Polymerization conditions: 100 L/h of ethylene, 250 mL of toluene, 0.02 mmol of precatalyst, 62,500 equiv of MAO, polymerization time 5 min.

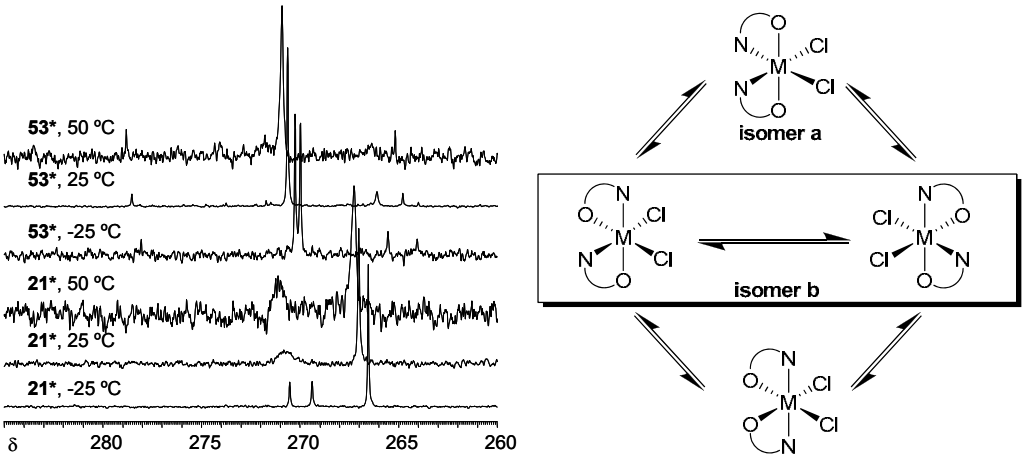

Figure 2. ^{15}N NMR of complexes **21*** and **53*** in $C_2D_2Cl_4$ recorded on a JEOL ECP 500 (FT, 500 MHz, 50.7 MHz, ^{15}N) spectrometer. Chemical shifts for ^{15}N spectra were referenced based on the absolute frequency of the spectrometer and are reported relative to $Me_4N^+X^-$.

The syndiospecific propylene polymerization with Ti-FI catalysts such as bis[*N*-(3-*tert*-butylsalicylidene)-2,3,4,5,6-pentafluoroanilinato]titanium(IV) dichloride (**31**) is also assumed to involve isomerization of Δ and Λ isomers during polymerization (**Figure 7** in General Introduction). In addition, the intriguing C–F···H–C attractive interaction proposed for the *ortho*-fluoroaryl Ti-FI catalysts as a rationale for the robust living polymerization (**Figure 6** in General Introduction) is subject to proof by an investigation into solution structures of the active species of the FI catalysts.

Despite these interesting observations and proposals, identities and properties of the catalytically active species for the bis(phenoxy–imine) group 4 complexes (FI catalysts) remained virtually unknown before this author's endeavor as reported in this chapter, although a cationic active species was postulated via an analogy to the metallocene catalysts and other post-metallocene catalysts.

In view of this situation, the author reports herein on an investigation aimed at observation and identification of the catalytically active species of bis(phenoxy-imine) group 4 transition metal complexes using ^{1}H NMR spectroscopy for FI catalyst precursors, bis[*N*-(3-*tert*-butylsalicylidene)anilinato]zirconium(IV) dichloride (**21**), and bis[*N*-(3,5-dicumylsalicylidene)anilinato]zirconium(IV) dichloride (**53**), and bis[*N*-(3-*tert*-butylsalicylidene)-2,3,4,5,6-pentafluoroanilinato]titanium(IV) dichloride (**31**).

Results and Discussion

Upon activation of **21** with DMAO (Dried MAO, see Experimentals) at Al/Zr = 110 ([Zr] = 7.0 μmol) at ambient temperature in toluene-d_8, two new imine signals appear at 7.81 and 7.51 ppm distinct from the peak at 7.54 ppm for **21** (**Figure 3A**).

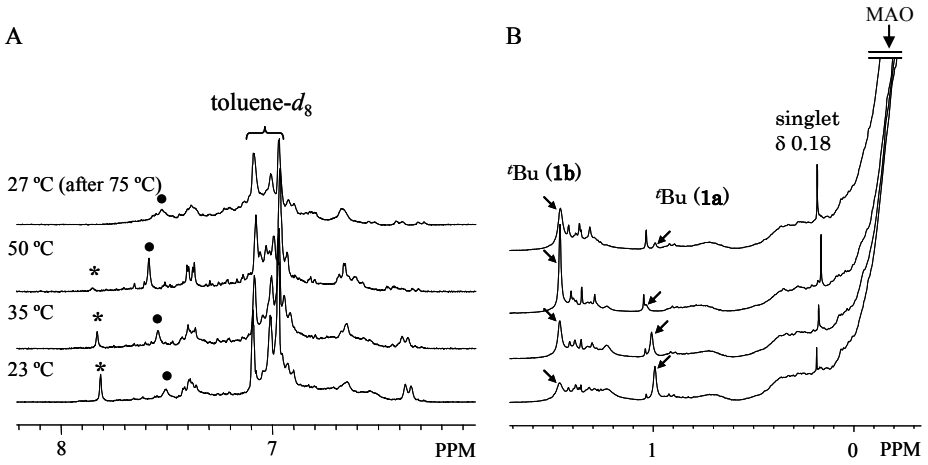

Figure 3. Variable temperature (VT) ^{1}H NMR spectra of aromatic (A) and aliphatic region (B) of **21**/DMAO. The imine signals for species **21a** and **21b** are marked with * and •, respectively.

With increased temperature, the imine peak at 7.81 ppm decreases in intensity and shifts downfield slightly (7.85 ppm at 50 °C). The imine peak around 7.81ppm disappears at about 50 °C, while the peak at 7.51 ppm increases in intensity and shifts downfield significantly (7.60 ppm at 50 °C and 7.65 ppm at 75 °C). This indicates that two species are generated and that one species (**21a**, **Figure 3**) is transformed into the other (**21b**, **Figure 3**). After cooling to room temperature, the signals for **21b** remain but those for **21a** do not reappear, which suggests that the transformation of **21a** to **21b** is irreversible. With all temperatures examined, judging by the single imine in the ^{1}H NMR spectra, species **21a** and **21b** seem to have one set of ligand signals. Another feature is the appearance and growth of a sharp singlet at 0.18 ppm during the transformation of **21a** to **21b** (**Figure 3B**), which turns out to be assignable to methane by comparison with an authentic sample.

Precatalyst **53** was activated with DMAO (Al/Zr = 224, [Zr] = 6.3 μmol) in a similar manner to precatalyst **21** at ambient temperature in toluene-d_8. The ^{1}H NMR spectra of **53**/DMAO are more complicated than those of **21**/DMAO. However, as the temperature increases, broad signals at 7.95 ppm decrease in intensity and disappear around 75 °C (denoted as * in **Figure 4A**), while a new signal similar in chemical shift to that of **21b** (~7.5 ppm, denoted as • in **Figure 4**) as well as another signal at 7.7 ppm appear (denoted as × in **Figure 4**). This irreversible increase and decrease of these and other signals, although they are poorly resolved and unassignable, suggests that a irreversible transformation from **53a** to **53b** is taking place in a similar manner to the **21**/DMAO system.

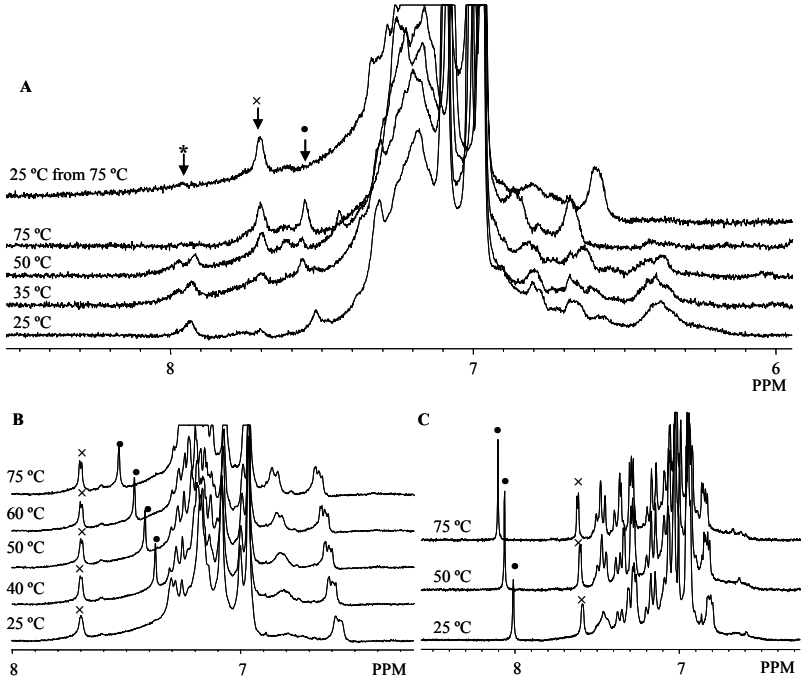

Figure 4. VT-^{1}H NMR spectra of **53**/DMAO: A) the first heating in toluene-d_8; B) the second heating in toluene-d_8; C) the third heating in $C_2D_2Cl_4$.

After complete formation of species **53b** the spectra are less complicated. The second heating of the reaction mixture clearly demonstrates that the signal at 7.4–7.5 ppm (• in **Figure 4B**) is a singlet and the signal around 7.7 ppm is a doublet (J = 2.31 Hz). These two signals are almost equal in intensity at all temperatures examined and the integration approximates one proton for each signal. Therefore, the singlet and the doublet can be assigned to the imine proton and one of the aromatic protons, respectively. When all volatiles were removed from the NMR tube *in vacuo* and deuterated tetrachloroethane ($C_2D_2Cl_4$) was added (**Figure 4C**), resolution was significantly improved. The signal for the imine proton significantly shifts downfield to 8.1 ppm ($\Delta \sim 0.7$ ppm at 25 °C, • in **Figure 4C**), showing sensitivity to solvent polarity as well as the temperature, while the chemical shift of the doublet around 7.6 ppm (× in **Figure 4C**) does not shift significantly in $C_2D_2Cl_4$ or varying temperatures, which confirms the assignments. A sharp singlet at 0.18 ppm (methane) appeared in a similar manner to the reaction of **21**/DMAO.

Therefore, the activation processes for these Zr-FI catalyst precursors (dichlorides, **21** and **53**) are initially transformed into the species (**21a** and **53a**), and then irreversibly into the other species (**21b** and **53b**) with the concurrent generation of methane upon heating (Eq. 1).

$$(L^{FI})_2ZrCl_2\ (\mathbf{21}, \mathbf{53}) + \text{DMAO} \longrightarrow \mathbf{21a}, \mathbf{53a} \xrightarrow[\Delta]{} \mathbf{21b}, \mathbf{53b} + CH_4 \qquad (1)$$

To further examine the generality of the observations made with precursors **21** and **53**, bis[*N*-(3-*tert*-butylsalicylidene)-2,3,4,5,6-pentafluoroanilinato]titanium(IV) dichloride (**31**) was chosen as a precursor as the next experiment. There are several advantages of investigating this complex: i) the

perfluorinated phenyl ring simplifies the aromatic region of the spectra; ii) greater solubility improves resolution even at room temperature; and iii) the living nature of this catalyst may allow *in situ* observation of subsequent reactions with olefins.[6–9] In $CDCl_3$ or toluene-d_8 at room temperature, **31** shows only a single set of ligand signals in contrast to **21** and **53** under the same conditions. This indicates that **31** exists as a single isomer possessing C_2 symmetry.

Activation of **31** with DMAO at room temperature in toluene-d_8 leads to the formation of two species (**Figure 5**). With the perfluorinated ligand, each species is fairly well separated from each other and from the solvent signals, which allowed us to determine that both species have only one set of ligand signals. Thus, as shown in **Figure 5**, each species gives rise to five signals (i.e., imine (s, 1H), phenol (dd, dd, t, 3H) and *tert*-butyl (s, 9H) signals) though one triplet overlaps with the solvent signals. In addition to these signals assignable to the ligands, another broad singlet appears at 1.97 ppm. Upon increasing the temperature, the signals of the dominant species at room temperature (**31a**) decrease in intensity and the signals for the other minor species (**31b**) increase. The singlet at 1.97 ppm decreases in intensity in accordance with the decrease in intensity of the signals derived from **31a**. The conversion of **31a** to **31b** is irreversible and the imine signal for **31b** shifts downfield with increased temperature in contrast to the other temperature independent signals. In addition, the formation of methane is again observed. These observations are similar to those seen in the previously described reactions involving precursors **21** and **53**, demonstrating that these characteristics have generality in the activation processes of FI catalysts with MAO irrespective of Zr or Ti as a metal center. Since MAO does not produce methane upon heating, the transition metal species is involved in the methane formation.

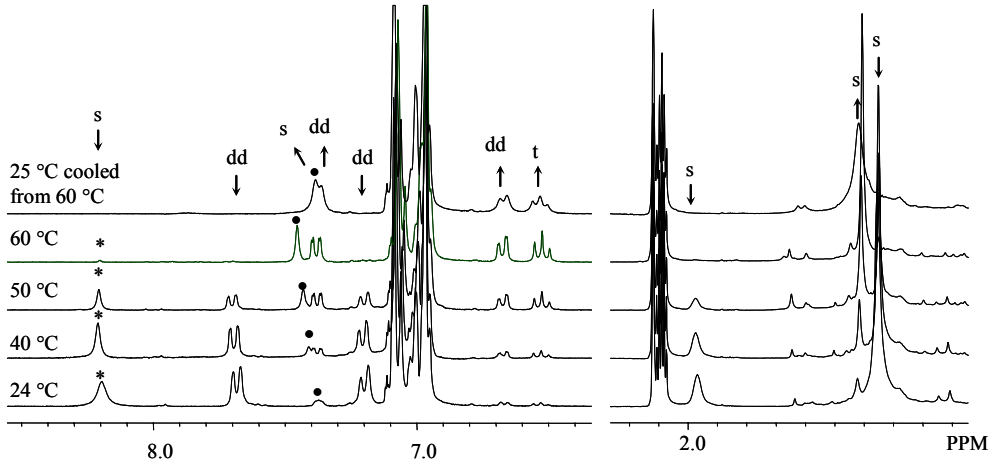

Figure 5. VT-^{1}H NMR spectra of **31**/DMAO in toluene-d_8 (Al/Ti = 108, [Ti] = 14.0 mmol). Symbols denote the imine protons of **31a** (*) and **31b** (•).

To identify species **31b**, various olefins were added to investigate whether or not olefin insertion would occur. Introduction of ethylene to **31b** (Al/Ti = 53; ethylene/Ti ~ 2, **Figure 6B**) leads to the formation of solid polyethylene despite the small amount of ethylene added in the tube. The ^{1}H NMR spectra of the reaction mixture shows that large signals of **31b** remain unchanged in the mixture and additional small broad signals in conjunction with broad polyethylene signals exist (**Figure 6C**). It is therefore likely that only a fraction of Ti

species (probably **31a**) act as a polymerization catalyst and that **31b** has no ability for ethylene polymerization. To further confirm the reactivity of **31b**, reactions with bulkier olefins were examined. Styrene did not react with **31b** even at 75 ºC. With regard to the reaction of **31b** with 1-hexene, only isomerization to internal olefins was observed. The low reactivity toward α-olefin insertion concludes that species **31b** (and probably **21b** and **53b**) is not the active species for olefin polymerization.

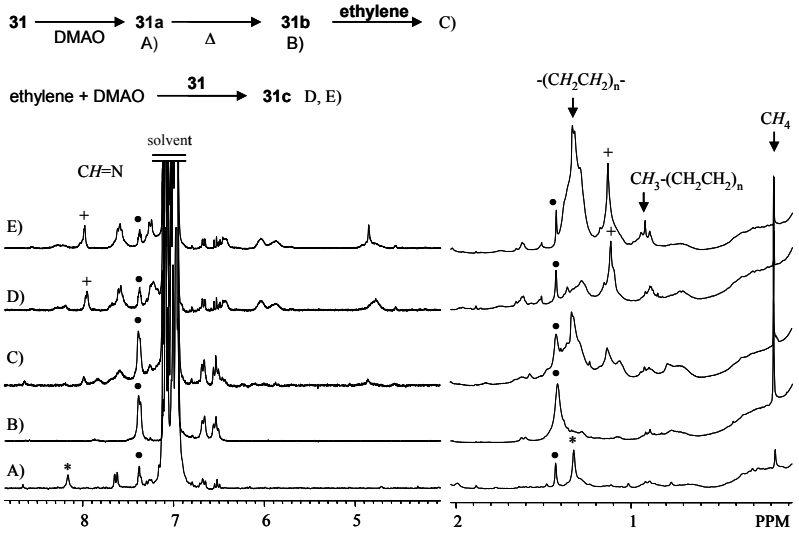

Figure 6. ^{1}H NMR spectra of **31**/DMAO in toluene-d_8. A) **31**/DMAO (1/108) at 24 °C; B) **31**/DMAO (1/108) after reaction at 60 °C; C) **31**/DMAO (1/53) after reaction at 60 °C for 5 min, ethylene (2 equiv to Ti) was added; D) activation in the presence of ethylene, DMAO/ethylene/**31** (67/1.4/1); E) activation in the presence of ethylene, DMAO/ethylene/**31** (71/7/1). Characteristic imine and ^{t}Bu signals are marked with * for **31a**, • for **31b**, and + for **31c**.

Polymerization with FI catalysts usually starts without an induction period even below room temperature indicating the extremely rapid formation of the active species. Therefore, it is pertinent to assume that immediately formed active species **31a** turns gradually into inactive species **31b** in the absence of a reacting monomer. Since the singlet at 1.97 ppm of **31a** integrates to 3H when the imine proton at 8.20 ppm is integrated to 2H, the singlet can be assigned to the Ti-bound methyl group. Considering also the significant downfield shift of the imine proton from **31**, species **31a** can be identified as the cationic methyl species, $[(L^{FI})_2Ti–CH_3]^+$ as seen in the activation of metallocene catalysts. However, it is extremely difficult to observe ethylene polymerization with **31a** in an NMR tube, because of inefficient mixing, the relatively high concentration of **31a** employed for NMR experiments, and the high activity of **31a** easily causing inhomogeneity of the polymerization reaction. Lowering the temperature to slow the reaction is also difficult because the oligomeric MAO tends to solidify the reaction mixture especially at low temperatures.

Because **31a**/DMAO forms an extremely robust living polymerization catalyst and the living species stays alive at least one hour in the absence of monomer,[6–9] it may be possible to prepare a living propagating species in a Schlenk tube under diluted conditions, and then to concentrate and transfer it alive into an NMR tube. Thus, activation in the presence of ethylene was carried out in a Schlenk tube by

injecting a toluene solution of **31** into a toluene solution of DMAO (~70 equiv to Ti) and ethylene (1.4 or 7 equiv to Ti) at 0 ºC under vigorous stirring. After removing all volatiles *in vacuo*, the residue was dissolved again in toluene-d_8 and given NMR observation. A new set of signals (species **31c**) was observed in addition to those of **31b** and the growing polyethylene signals, of which intensity depends on the amounts of ethylene added to the reactions. The peaks corresponding to **31c** are similar to those of **31a** except for the imine chemical shift, which appears slightly upfield (7.9 – 8.0 ppm) in comparison to the imine signal of **31a** (8.19 ppm) but much further downfield than the signal of **31b** (7.37 ppm). It should also be noted that a triplet at ~0.9 ppm assignable to a methyl group at polyethylene termini arises in these spectra. Therefore, **31c** can be attributed to a living propagating species $[(L^{FI})_2Ti–(CH_2CH_2)_nCH_3]^+$. The signals of **31c** also appear in the spectrum in **Figure 6C** albeit small in intensity.

The less reactive species **31b** with a diminished cationic character may be assigned to i) a heterobinuclear complex with alkylaluminum compounds, $[(L^{FI})_2Ti\text{-}\mu_2\text{-}(CH_3)(X)\text{-}Al(CH_3)(X)]^+$ (X: $-CH_3$ or -Cl) or ii) a $(L^{FI})_nAlMe_{3-n}$ (n = 1 or 2) complex where $(L^{FI})^-$ is transferred from the Ti center (**Chart 1**). There are examples of the formation of similar complexes in metallocenes and other early transition metal complexes.[10,4] The reaction between (L^{FI})–H and $AlMe_3$ (~0.5 equiv) in toluene-d_8 at room temperature monitored by ^{1}H NMR indicates the formation of a compound similar to **31b** as a major product (**Figure 7A**). The imine proton of the major product shows similar temperature dependence to that of **31b**. From the integration, the major product is assignable to $(L^{FI})AlMe_2$ (^{1}H NMR (δ, C_7D_8): 7.39-7.36 (m, 3H), 6.60 (dd, 1H), 6.51 (t, 1H), 1.43 (s, 9H), -0.35 (t, 6H)) which coexists with unreacted (L^{FI})–H, suggesting that **31b** is an aluminum FI complex $(L^{FI})AlMe_2$.

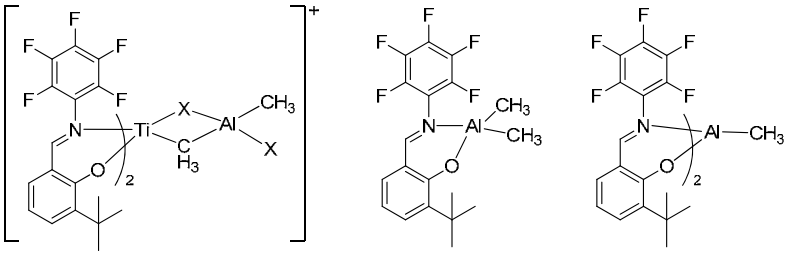

Chart 1

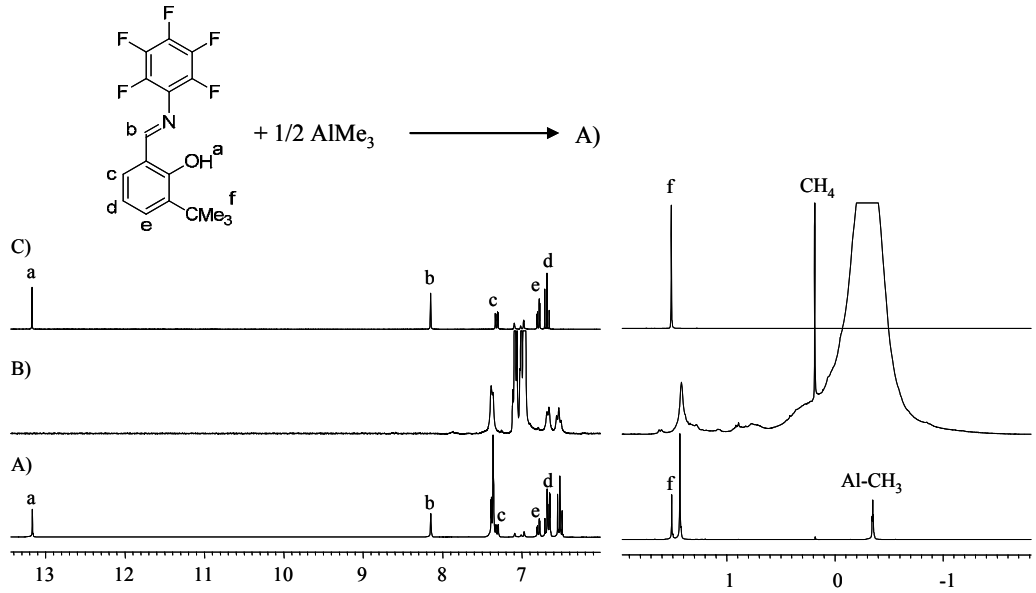

Figure 7. ^{1}H NMR spectra of A) a free ligand and 0.5 equiv. of $AlMe_3$ (see the inset figure); B) **31**/DMAO (1/108) after reaction at 60 °C; C) a free ligand (270 MHz, room temperature, in toluene-d_8).

Similar species were observed through the reaction of **31**, $AlMe_3$, and $Ph_3CB(C_6F_5)_4$. Two species very similar to **31a**, and almost identical to **31b**, are observed in the ^{1}H NMR spectrum (**Figure 8**). The signal of $Ph_3CC\mathit{H_3}$ is clearly seen at 2.0 ppm, indicating methide abstraction from titanium,[11] which in turn suggests the generation of a cationic titanium species. These observations are in agreement with the generation of $[(L^{FI})_2Ti–CH_3]^{+}[B(C_6F_5)_4]^{-}$ similar to **31a** with concomitant formation of **31b**.

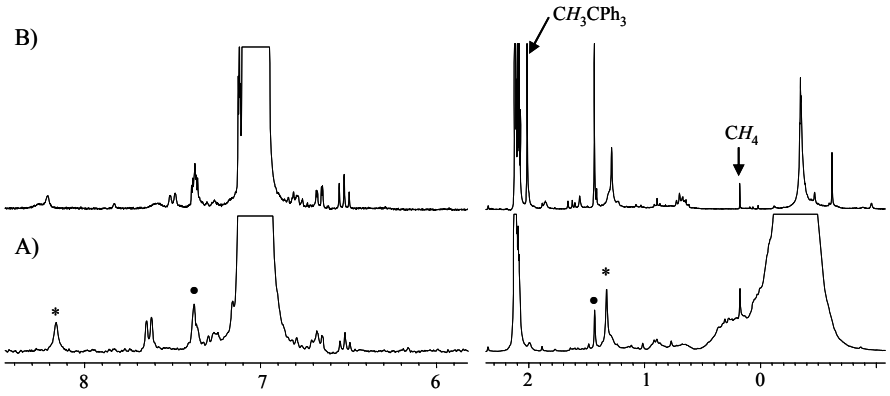

Figure 8. ^{1}H NMR spectra of A) **31**/DMAO (1/108) at 24 °C; B) **31**/$AlMe_3$/$Ph_3CB(C_6F_5)_4$ (1.0/2.8/1.04) in toluene-d_8.

The activation of **31** was attempted in the presence of propylene by the same method used to activate **31** in the presence of ethylene. As observed with the ethylene system, species **31b** (the imine protons are marked with • in Figure 6) and **31d** (supposedly the living propagating species bearing a polypropylene chain, the imine proton is marked with ▲ in **Figure 9**) were observed . As temperature increases, **31d** is slowly transformed into **31b** but a significant amount of **31d** remains even at 75 ºC for more than 15 min.

Considering the fact that species **31a** turned to **31b** completely at 60 ºC, the thermal stability of **31d** toward formation of **31b** probably stems from a bulkier growing chain of propylene, which discourages the formation of **31b**, and is consistent with the robust living nature of this catalyst.

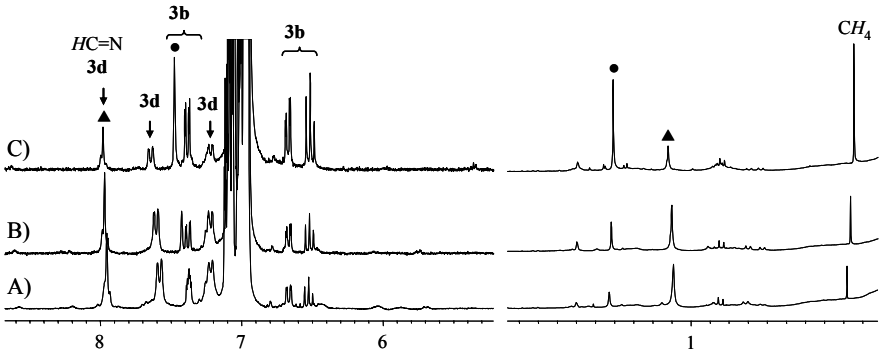

Figure 9. VT-^{1}H NMR spectra of **31** activated with DMAO in the presence of propylene (Al/Ti/propylene = 72/1/1.4), A) at 26 °C; B) at 50 °C; C) at 75 °C after being kept for 15 min. The imine and ^{t}Bu protons of **31b** and **31d** are marked with • and ▲, respectively.

Active species **31a**, **31c**, **31d** exhibit only a set of ligand signals similar to C_2-symmetric precatalyst **31**, suggesting that these species also have a C_2 symmetry. Combined with the results of DFT calculations,[7,8] these species most likely have a *cis*-N/*trans*-O configuration leaving the reaction sites in *cis*-disposition. While **31a** is decomposed at a higher temperature range into an Al-FI complex, (L^{FI})$AlMe_2$, methane, and an unidentified Ti complex (paramagnetic), propagating species **31d** exhibits higher tolerance toward the decomposition. This ligand transfer deactivation path probably occurs via C–H bond activation by the M–CH_3 species at one of the methyl groups of $AlMe_3$, which appears to be general for FI catalysts when activated with MAO (**Scheme 3**).

These results qualitatively explain many general characteristics of olefin polymerizations mediated by FI catalysts, e.g., i) a bulky substituent next to the phenolic oxygen (R^2 substituent) increase catalytic activity;[12] ii) DMAO exhibits higher activity than commercially available MAO (regular MAO) that contains a larger amount of $AlMe_3$ than DMAO;[13] and iii) reaction of FI catalysts with a cocatalyst in the absence of a monomer lowers catalytic activity compared to activation in the presence of a monomer. These observations can be rationalized in terms of discouraging the formation of inactive species with $AlMe_3$ by i) steric hindrance of substituents close to reaction center, ii) lower $AlMe_3$ content in DMAO, and iii) steric protection by a bulkier growing polymer chain.

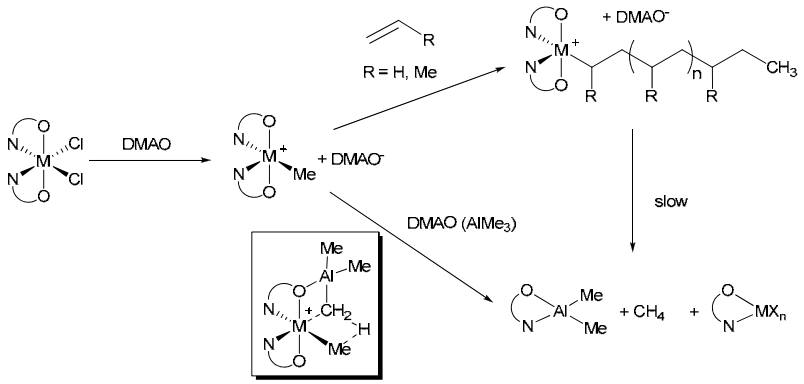

Scheme 3

Conclusion

Reaction NMR experiments were conducted for the activation of three FI catalyst precursors with DMAO. The chemical shifts of imine protons are well-separated at lower field and are sensitive to the structure and cationic character of the generated species to serve as a good probe for the identification of the catalytically active species. The results suggest that for all three precursors the active cationic methyl species are generated immediately and slowly transformed into inactive aluminum complexes bearing a phenoxy-imine ligand. Activation of living precatalyst **31** in the presence of ethylene or propylene leads to the formation of a cationic propagating species, which is thermally more robust than the corresponding methyl species toward transformation to the aluminum species. These results qualitatively explain general polymerization characteristics observed with FI catalysts. Expected fluxionality between configurational isomers could not be examined in detail because the systems suffer from heterogeneity due to solidified MAO at lower temperatures and the formation of the aluminum complex at higher temperatures.

Experimentals

Materials and Methods.

All manipulations of air-sensitive materials were performed in Schlenk-type glassware on a dual-manifold Schlenk line or in a nitrogen-filled glove box with a high capacity recirculator (< 1 ppm O_2). Deuterated solvents were obtained from Cambridge Isotope Laboratories (all ≥ 99 atom %D), freeze-pump-thaw degassed, dried over activated molecular sieves, and stored in resealable flasks. Precatalysts **21**, **31**, **53** were prepared as described in previous papers.[5–7,14] Commercially available MAO (Albemarle, 1.2 M in toluene) was dried under vacuum to obtain a white powder, dissolved in deuterated toluene, and dried again to remove a trace amount of residual non-deuterated toluene. This dried MAO (DMAO) was added as a powder whose molecular weight is 58 based on -Al(CH_3)O- unit.

Physical and Analytical Measurements.

NMR spectra were recorded on JEOL GSX 270 spectrometer (FT, 270 MHz, ^{1}H). Chemical shifts were

referenced using internal solvent resonances and are reported relative to tetramethylsilane. NMR experiments on air-sensitive samples were conducted in Teflon valve-sealed sample tubes (J. Young). In VT-NMR experiments, each temperature transition was conducted at intervals around 5–10 min including temperature equilibration and data collection.

References and Notes

(1) Coates, G. W.; Waymouth, R. M. *Science* **1995**, *267*, 217–219.

(2) Muller, C.; Lilge, D.; Kristen, M. O.; Jutzi, P. *Angew. Chem. Int. Ed. Engl.* **2000**, *39*, 789–792.

(3) Strauch, J.; Warren, T. H.; Erker, G.; Fröhlich R.; Saarenketo, P *Inorg. Chim. Acta* **2000**, *300–302*, 810–821.

(4) Bei, X.; Swenson, D. C.; Jordan, R. F. *Organometallics* **1997**, *16*, 3282–3302.

(5) Tohi, Y.; Makio, H.; Matsui, S.; Onda, M.; Fujita, T. *Macromolecules* **2003**, *36*, 523–525.

(6) Saito, J.; Mitani, M.; Mohri, J.-i.; Yoshida, Y.; Matsui, S.; Ishii, S.-i.; Kojoh, S.-i.; Kashiwa, N.; Fujita, T. *Angew. Chem., Int. Ed.* **2001**, *40*, 2918–2920.

(7) Mitani, M.; Mohri, J.-i.; Yoshida, Y.; Saito, J.; Ishii, S.; Tsuru, K.; Matsui, S.; Furuyama, R.; Nakano, T.; Tanaka, H.; Kojoh, S.-i.; Matsugi, T.; Kashiwa, N.; Fujita, T. *J. Am. Chem. Soc.* **2002**, *124*, 3327–3336.

(8) Mitani, M.; Nakano, T.; Fujita, T. *Chem. –Eur. J.* **2003**, *9*, 2396–2403.

(9) Furuyama, R.; Saito, J.; Ishii, S.; Makio, H.; Mitani, M.; Tanaka, H.; Fujita, T. *J. Organomet. Chem.* **2005**, *690*, 4398–4413.

(10) For example, Bochmann, M.; Lancaster, S. J. *Angew. Chem. Int. Ed. Engl.* **1994**, *33*, 1634–1637.

(11) No reactions were observed between $AlMe_3$ and $Ph_3CB(C_6F_5)_4$.

(12) See General Introduction of this thesis.

(13) Furuyama, R.; Saito, J.; Ishii, S.; Mitani, M.; Matsui, S.; Tohi, Y.; Makio, H.; Matsukawa, N.; Tanaka, H.; Fujita, T. *J. Mol. Catal. A* **2003**, *200*, 31–42.

(14) Matsui, S.; Mitani, M.; Saito, J.; Tohi, Y.; Makio, H.; Matsukawa, N.; Takagi, Y.; Tsuru, K.; Nitabaru, M.; Nakano, T.; Tanaka, H.; Kashiwa, N.; Fujita, T. *J. Am. Chem. Soc.* **2001**, *123*, 6847–6856.

Chapter 2. Synthesis and characterization of alkylated FI complexes and their activation with boron-based activators

Abstract

Synthesis of $[C_6F_5N{=}CH(2\text{-}O\text{-}C_6H_3\text{-}3\text{-}R)]_2TiMeX$ (R: ^{t}Bu; X: Br (**52**), R: ^{t}Bu; X: Me (**51**), R: H; X: Me (**54**)) was achieved by the reaction of methylated titanium halides, $Me_{2-m}TiX_{2+m}(DME)_n$ (DME: 1,2-dimethoxyethane; *m* = 1, X = Br, *n* = 0 (**55**) or *m* = 0, X = Cl, *n* = 1 (**56**)) with sodium salts of phenoxy-imine ligands. X-ray analysis revealed that complex **51** adopts a distorted octahedral structure having a *trans*-O, *cis*-N, *cis*-Me disposition as is commonly observed for FI dichloride complexes, which is consistent with the observed NMR spectra. These complexes can be activated with equimolar amounts of $B(C_6F_5)_3$ or $Ph_3CB(C_6F_5)_4$ to form monomethyl cationic species, which upon addition of a small amount of ethylene monomer allows room temperature observation of cationic polymeryl species, including the diastereotopic Ti-bound α-methylene protons.

Introduction

In Chapter 1 of this thesis, the active species of a living Ti-FI catalyst (**31**) activated with MAO was identified as a cationic monoalkyl species $[(L^{FI})_2Ti–R]^+[MAO]^–$ (**Scheme 1**), and the species was found to be deactivated via a ligand transfer reaction to trimethylaluminum, resulting in $(L^{FI})AlMe_2$, methane, and unidentified metal species that presumably have a phenoxy–imine ligand remaining. However, there are several problems associated with MAO, that is, its ill-defined structure and reaction profile, large signals appearing in NMR, the viscosity or solidification at lower temperature that makes NMR resolution poor, and side reactions caused by alkylaluminums such as the ligand transfer reaction mentioned above.

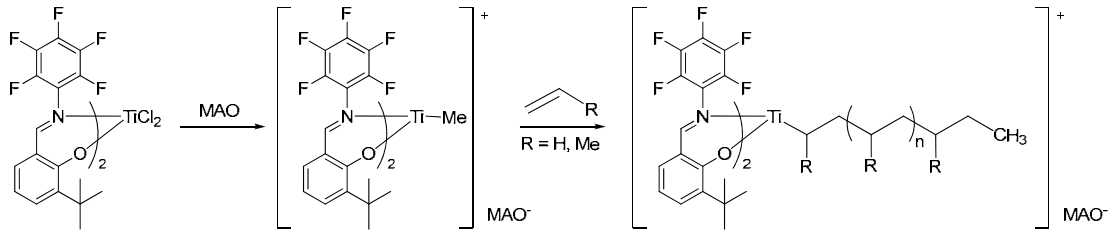

Scheme 1

To circumvent these problems, synthesis of alkyl complexes is of great value since such complexes can be activated in a well-defined manner using an equimolar amount of perfluoroaryl boranes or borate salts without the need for alkylaluminums (See Eqs. 2–4 in General Introduction). Direct observations of these alkyl cationic species have contributed to a fundamental understanding of active species and olefin polymerization mechanisms with metallocenes and related complexes.

However, alkylation of $(L^{FI})_2MX_2$ to prepare dialkyl precursors, $(L^{FI})_2MR_2$ (Eq. 1), is not straightforward due to the reactive imine groups in the ligands. The alkylating agents, M'–R (M': Li, Mg, Al, Zn, etc.) are nucleophiles, which of course react with electrophiles, in this case, either the metal center (M) or comparably electrophilic imine carbons (*C*H=NR). In addition, even though once the alkylated M–R bond is formed, it can subsequently migrate to the imine via intramolecular insertion to form an M–N–CH–R moiety, which is common chemistry for early metals. This tendency is especially salient when M is a highly electrophilic early transition metal in a high oxidation state, which makes the imine even more electrophilic.[1–3]

In addition to alkylation of metal chloride complexes (Eq. 1), an alkane elimination reaction using metal precursor MR_4 (M: group 4 metal; R: CH_2Ph, CH_2CMe_3, CH_2SiMe_3, etc.) and ligands having acidic protons (Eq. 2) was often successful for the synthesis of alkyl complexes.[4–10] Drawbacks of this method include limited alkyl groups available as metal precursors, which often show different reactivity from ordinary alkyls used in olefin polymerization reaction, and 1,2-migratory insertion of the M–R to the imine, which is still ostensible for group 4 complexes.

$L_2MX_2 + 2\ R–M' \longrightarrow L_2MR_2 + 2\ M'X$ (1)

$(L–H)_2 + MR_4 \longrightarrow L_2MR_2 + 2\ R–H$ (2)

(L: ancillary ligand; RM': alkylating agent)

Alkylation of **31** is even more challenging because electron-withdrawing perfluorophenyl groups make the imines more electrophilic. Nevertheless, alkyl complexes of **31** are highly desired because when activated with MAO, **31** catalyzes highly robust living ethylene and living syndiospecific propylene polymerizations even above room temperature, which may allow us to capture the active species alive by spectroscopic means. Moreover, these solution structures may shed light on the issues involving dynamic processes proposed for this catalyst such as the fluxional inversion among stereoisomers and the attractive interaction between β-H of the propagating chain and *ortho*-F.[1]

The author thus carried out research into the synthesis of alkylated living Ti-FI precatalysts, particularly having methyl group(s) as alkyls, which is straightforward as a model of MAO-activating species. Now this chapter will discuss the successful synthesis of $[C_6F_5N=CH(2\text{-}O\text{-}C_6H_3\text{-}3\text{-}R)]_2TiMeX$ (R: ^{t}Bu; X: Br (**52**), R: ^{t}Bu; X: Me (**51**), R:H; X: Me (**54**)) by taking a new synthetic approach, i.e., synthesis of $Me_{2-n}TiX_{2+n}$ (*n* = 1, X = Br (**55**) or *n* = 0, X = Cl (**56**)) followed by complexation with sodium salt of phenoxy-imine ligands. Subsequently, activation and (*in situ*) polymerization of ethylene and propylene with these alkyl complexes will also be reported.

Results and Discussion

Synthesis of alkyl Ti-FI complexes

Titanium precursor **55** was prepared in 70% yield according to a modified procedure in the literature. The reaction of **55** and 2 equiv. of $[C_6F_5N=CH(2\text{-}O\text{-}C_6H_3\text{-}3\text{-}^t\text{Bu})]Na$ in toluene at –78 °C afforded complex **52** as a reddish brown powder (71 %, **Scheme 2**). The ^{1}H NMR spectrum of **55** exhibited two sets of ligand signals, indicating collapse of C_2 symmetry seen for **31**, as well as a titanium bound methyl group signal at 1.97 ppm (**Figure 1**).

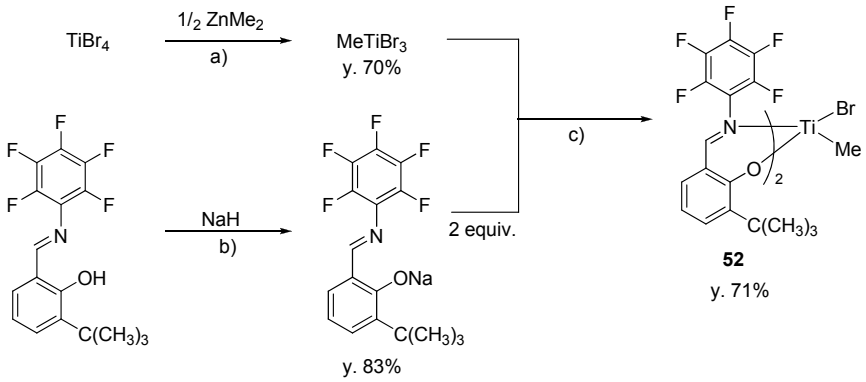

Scheme 2. Synthesis of complex **52**: a) In pentane at –78 °C; b) In Et_2O at –78 °C to room temperature; c) In toluene at –78 °C to room temperature.

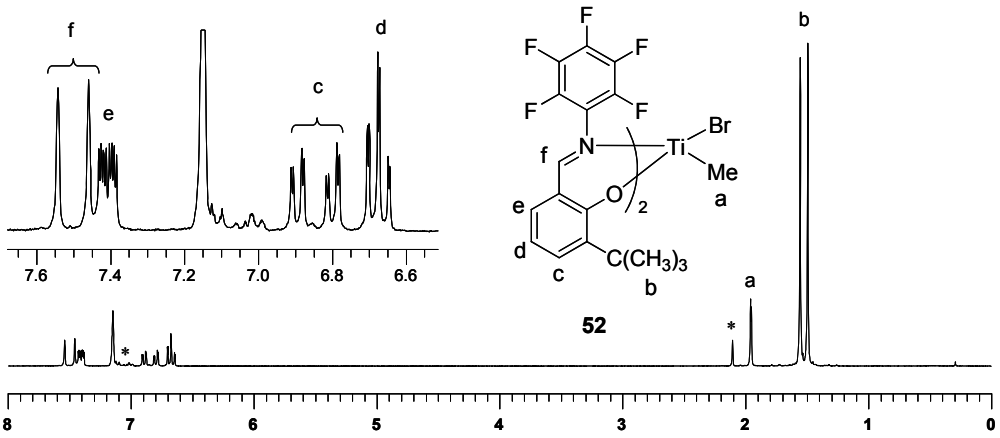

Figure 1. ^{1}H NMR spectrum of complex **52** in benzene-d_6 (FT, 270 MHz). Signals with asterisk are toluene as an impurity.

Dimethyltitanium dichloride (**56**) was generated *in situ* by the reaction of 1,2-dimethoxyethane (DME) adduct of $TiCl_4$ ($TiCl_4$·DME) and 2 equiv. of MeLi in diethyl ether at –30 °C and used without isolation in subsequent reactions with sodium salts. After removal of inorganic salts by filtration, complex **51** was precipitated from pentane solution as a dark red crystallite (**Scheme 3**).

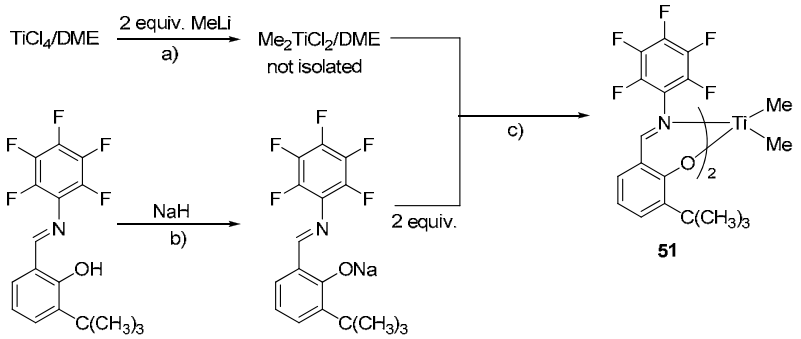

Scheme 3. Synthesis of complex **51**: a) In Et_2O at 0 °C; b) In Et_2O at –78 °C to room temperature; c) In toluene at –78 °C to room temperature.

The ^{1}H NMR spectrum of **51** exhibits 6H for two methyl groups bound to the Ti metal center at 1.65 ppm in addition to a single set of ligand signals similar to that of C_2-symmetric dichloride complex **31**.

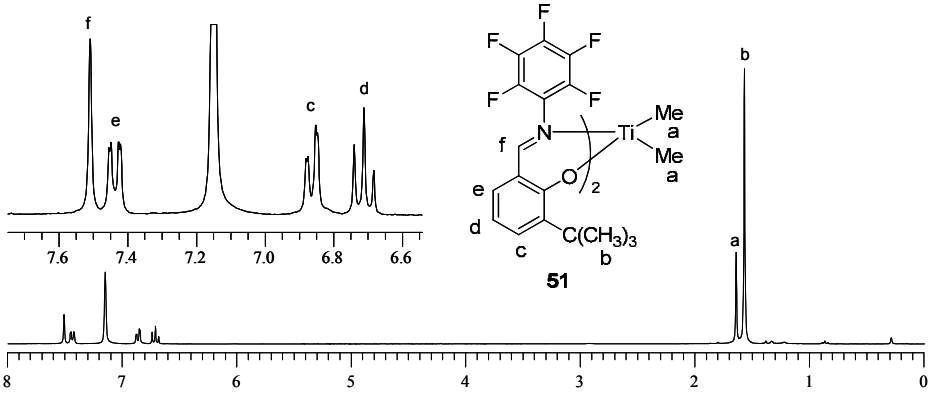

Figure 2. ^{1}H NMR spectrum of complex **51** in benzene-d_6 (FT, 270 MHz).

A single crystal suitable for X-ray crystallography was obtained by slow diffusion of pentane into a toluene solution of **51**. The molecular structure of **51** shown in **Figure 3** adopts a distorted octahedral structure having a *trans*-O/*cis*-N/*cis*-Me disposition as is commonly observed for FI dichloride complexes and is consistent with the observed NMR spectra above. To my knowledge, this represents the first structurally characterized alkyl complex bearing bis(phenoxy–imine) ligands. Dimethyl complex $[C_6F_5N{=}CH(2\text{-}O\text{-}C_6H_4)]_2TiMe_2$ (**54**) was prepared by a similar manner to complex **51** and obtained as an analytically pure compound.

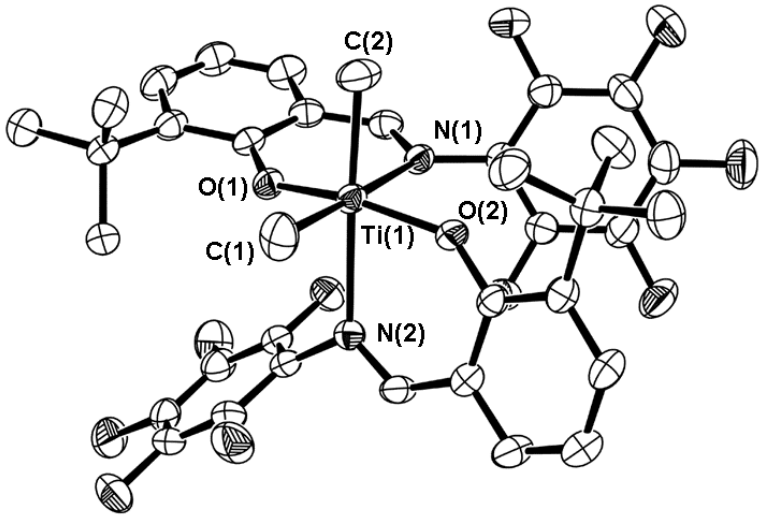

Figure 3. Molecular structure of a Ti-FI dimethyl complex, $[C_6F_5N{=}CH(2\text{-}O\text{-}C_6H_3\text{-}3\text{-}^tBu)]_2TiMe_2$ (**51**). Selected bond lengths (Å) and bond angles (deg): Ti–O(1) 1.869(2); Ti–O(2) 1.872(2); Ti–N(1) 2.345(3); Ti–N(2) 2.371(3); Ti–C(1) 2.111(4); Ti–C(1) 2.102(4); O(1)–Ti–O(2) 160.3(1); N(1)–Ti–N(2) 93.9(1); C(1)–Ti–C(2) 93.9(2).

Activation of alkyl Ti-FI complexes

Activation of complex **52** was attempted with $NaB(C_6F_5)_4$, based on equation 3.

$$(L^{FI})_2TiMe(Br) + NaB(C_6F_5)_4 \longrightarrow [(L^{FI})_2TiMe]^+[B(C_6F_5)_4]^- + NaBr \qquad (3)$$

The ^1H NMR spectra of complex **52** activated with $NaB(C_6F_5)_4$ indicated a set of ligand signals as a main component (**52***), showing a symmetric structure on an NMR time scale. However, the signals of **52*** are significantly upfield shifted (0.56 ppm for HC=N) relative to the MAO activated species.[11]

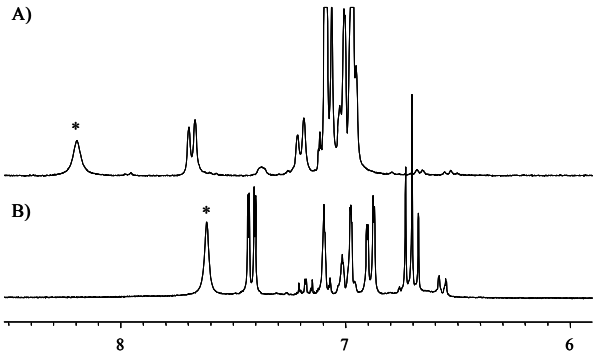

Figure 4. Aromatic region of ^{1}H NMR spectra for species A) **31**/DMAO,[11] and B) **52**/NaB(C_6F_5)$_4$ (FT 270 MHz, in toluene-d_8). The imine protons are marked with asterisks.

On the other hand, activation of **51** with the trityl salt caused immediate precipitation of a dark red oily product (**51***) indicative of a species with strong ionic character. The reaction in bromobenzene-d_5 resulted in a homogeneous solution of **51***, whose ^{1}H NMR exhibited a set of ligand signals and methyl groups of Ph_3CMe and Me–Ti at 1.88 and 1.77 ppm, respectively, and the significantly downfield shifted imine protons similar to the MAO activated species, all of which corroborate the formation of $[(L^{FI})_2Ti–Me]^+[B(C_6F_5)_4]^–$. Activation of **51** with $B(C_6F_5)_3$, which usually affords more soluble and more stable inner sphere ion pairs with metallocene dialkyls,[1,12,13] also resulted in oily precipitation in toluene at 8.1mM [Ti], implying significant cation–anion separation of this species (**51****). The methyl group bound to borate appeared at 0.826 ppm, indicating formation of $[(L^{FI})_2Ti–Me]^+[MeB(C_6F_5)_3]^–$ and the spectra of **51*** and **51**** are nearly identical despite the difference in their counteranions (**Figure 5**).

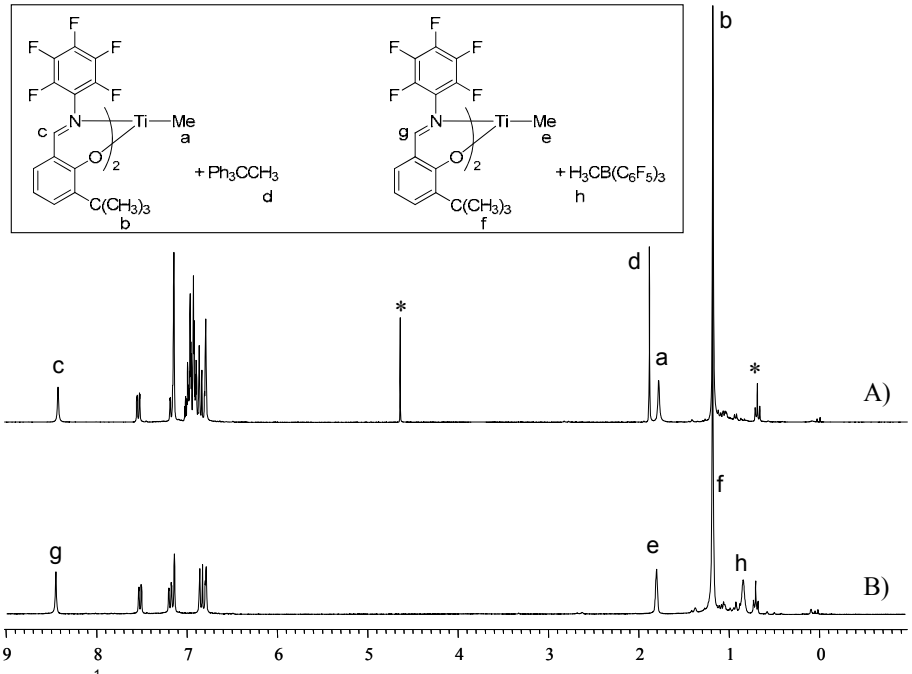

Figure 5. ^{1}H NMR spectra for the species derived from complex **51** with A) $[Ph_3C][B(C_6F_5)_4]$, and B) $B(C_6F_5)_3$ (FT 270 MHz, in BrC_6D_5). Impurities (CH_2Cl_2, pentane) are marked with asterisks.

Sterically much less encumbered complex **54** bearing no substituents adjacent to the phenolic oxygen (R^2 substituent) also gave an oily species (**54***) with $B(C_6F_5)_3$ in toluene-d_8 (13.3mM [Ti]), thus the origin of the ion separation is not primarily a steric reason from the *tert*-butyl group. The ^{1}H NMR spectra of **54*** verify the formation of a cationic methyl species with some minor species (**54'**) that is not observed for **51***. The identity of the minor species is unknown at this moment but could be a Me-bridged dinuclear species due to reduced steric bulk of **54***. The ^{1}H NMR chemical shifts of $MeB(C_6F_5)_3^-$ for **54*** as a measure of ionic character[14] are ca. 0.7–0.8 ppm in both toluene ([Ti] = 3.6 mM) and bromobenzene ([Ti] = 12.8 mM) that is almost identical to $LiMeB(C_6F_5)_3$. We attribute this enhanced ion separation to the formation of sterically more relaxed five-coordinated trigonal bipyramidal or square pyramidal cationic species that can compensate for the energy gain due to the charge separation.

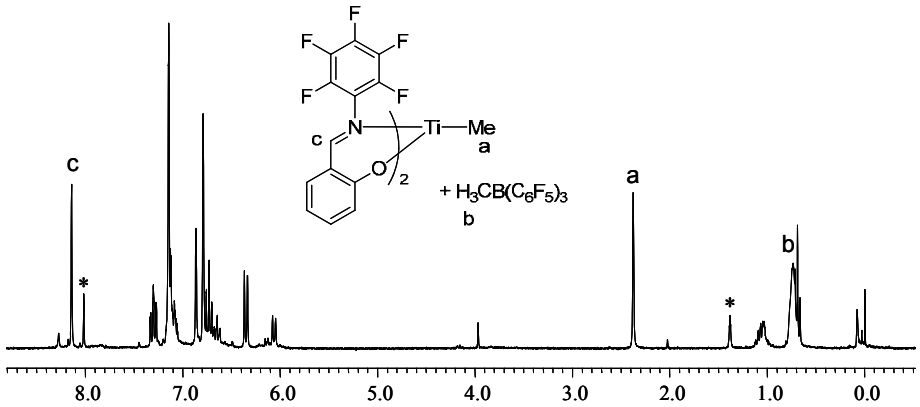

Figure 6. ^{1}H NMR spectra for the species derived from complex **54** with $B(C_6F_5)_3$ (FT 270 MHz, in BrC_6D_5). Unidentified species (**54'**) are marked with asterisks.

Table 1. Chemical shifts of key signals in ^{1}H NMR of Ti-FI complexes having methyl group(s)

	51*	**51****	**52***	**54***	**54***	**31a**	**31**	**51**	**52**	**54**
solvent	BrC_6D_5	BrC_6D_5	C_7D_8	BrC_6D_5	C_7D_8	C_7D_8	C_7D_8	C_6D_6	C_6D_6	C_7D_8
charge	cationic	cationic	cationic	cationic	cationic	cationic	neutral	neutral	neutral	neutral
N=C*H*	8.41	8.46	7.62	8.14	7.72	8.20	7.55	7.52	7.55	7.38
Ti–CH_3	1.77	1.79	1.86	2.37	2.26	1.97	–	1.65	1.97	1.67
Ph_3CCH_3	1.88	–	–	–	–	–	–	–	–	–
B–CH_3	–	0.83	–	0.73	0.75	–	–	–	–	–

Polymerization of ethylene and propylene with alkyl Ti-FI complexes

To further confirm the formation of monomethyl cationic complexes as a catalytically active species, these species were examined in ethylene and propylene polymerization. Species generated by a reaction with **52** and $NaB(C_6F_5)_4$ exhibited lower ethylene polymerization activity than MAO activation under similar conditions and was practically inactive for propylene polymerization (**Table 2**). Complex **51** upon activation with $Ph_3CB(C_6F_5)_4$ displayed comparable activities with MAO for ethylene and propylene polymerization,

whose NMR spectra were also similar to each other, showing significantly downfield shifted imine protons. These data conclude that the species, **31a**, **51***, and **51**** are the highly cationic monomethyl species having different counteranions but similar to each other in reactivity.

Therefore, the lower polymerization activities of **52*** are attributable to the less cationic character, which was demonstrated by the upfield shifted imine protons in ^{1}H NMR. We hypothesized that due to the relatively low solubility of $NaB(C_6F_5)_4$, a generated cationic methyl species can be immediately trapped by the neutral methyl bromide (**52**), forming a Br-bridged dinuclear monocationic complex, $[\{(L^{FI})_2Ti–Me\}_2(\mu\text{-}Br)]^+[B(C_6F_5)_4]^-$ (Eq. 4).

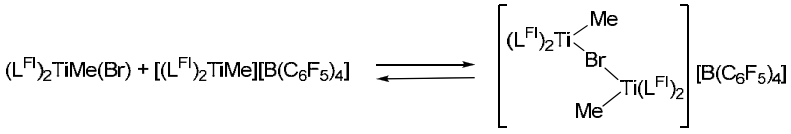

(4)

Table 2. Polymerization of alkyl Ti-FI complexes with various cocatalysts[a]

Complex	[Ti] (μmol)	Cocatalyst	[B] (μmol)	Monomer	T_p (°C)	Time (min)	Yield (g)	Activity[b]
51[c]	2.5	$Ph_3CB(C_6F_5)_4$	4.7	ethylene	25	1.5	0.293	23,400
51[c]	10	$Ph_3CB(C_6F_5)_4$	13.2	propylene	0	300	0.064	1.3
52[c]	0.50	$NaB(C_6F_5)_4$	0.50	ethylene	25	3	0.142	5,700
52[c]	18	$NaB(C_6F_5)_4$	18	propylene	0	420	0	0
31[d]	0.5	DMAO	n.a.	ethylene	25	1	0.283	34,000
31[e]	10	DMAO	n.a.	propylene	0	300	0.144	2.9

[a]Polymerization conditions: in toluene (250 mL); ethylene or propylene (continuous flow at 100 L/h). [b]In g-polymer/mmol-Ti h atm. [c]MAD (MeAl(O-2,6-^{t}Bu$_2$-4-Me-C_6H_2)$_2$) was added as a scavenger (1.25 mmol). [d]See ref. 15. [e]See ref. 16.

This situation can be created by a reaction of cationic species **51*** and neutral complex **52**, whose ^{1}H NMR spectra are shown in **Figure 7**. By adding an equimolar amount of **52** to **51*** generated from **51**/$Ph_3CB(C_6F_5)_4$ in BrC_6D_5, a considerable upfield shift of the imine proton was observed (**Figure 7C** to **7B**). Solvent substitution of the reaction mixture from BrC_6D_5 to C_7D_8 resulted in a further upfield shift and the spectrum became similar to **52*** (**Figure 7A** and **Figure 4B**).

Similar experiments were carried out by varying the molar ratios of dimethyl complex (**51**) and $Ph_3CB(C_6F_5)_4$ (**Figure 8**).[17] By adding $Ph_3CB(C_6F_5)_4$ incrementally (increasing the B/Ti ratio), the imine protons shifted downfield and when the ratio reached one (**Figure 8E**), the spectrum became almost identical to that of **51*** (**Figure 5A**). The species in **Figures 7** and **8** exhibited only one set of ligand signals at ambient temperature, implying the equilibrium shown in Eqs. 4 and 5.

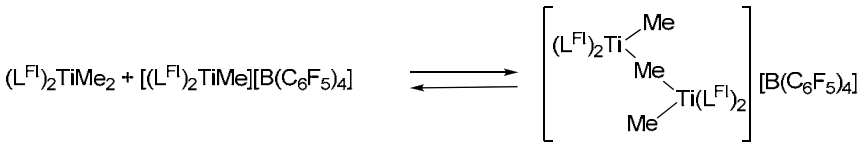

(5)

These bridged dinuclear complexes will serve as an inactive dormant species, and therefore lower the polymerization activity via reversible activation and deactivation.

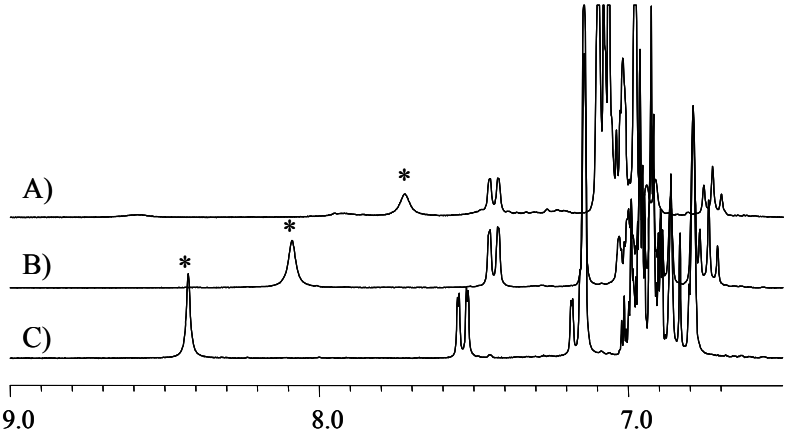

Figure 7. ^{1}H NMR spectra for the species derived from a 1 : 1 mixture of **51*** (Spectrum C) and **52** in A) C_7D_8, and B) BrC_6D_5. (FT 270 MHz, in BrC_6D_5). The imine protons are marked with asterisks.

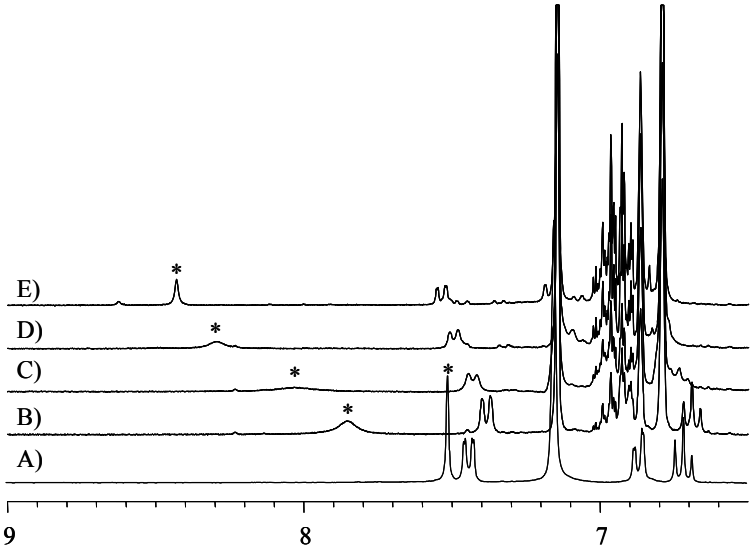

Figure 8. ^{1}H NMR spectra for the species derived from **51** (Spectrum A, solvent benzene-d_6) and $Ph_3CB(C_6F_5)_4$ at molar ratios (B/Ti) of B) 0.25; C) 0.49; D) 0.72; and E) 1.01. (FT 270 MHz, in BrC_6D_5). The imine protons are marked with asterisks.

Finally, *in situ* observation of a living propagating species was attempted. Upon addition of ethylene (ca. 5 equiv. to [Ti]) to **54*** in bromobenzene-d_5, peak intensity of species **54*** decreases along with the appearance of new signals as shown in **Figure 9**. Particularly notable are the signals at 2.88 and 1.45 ppm that are assignable to the diastereotopic α-methylene protons of the propagating "living" species (**57**). The minor species (**54'**) is virtually inactive to ethylene polymerization and there is no double bond formation indicative of chain transfers. It should be noted that NMR experiments were conducted at room temperature and that after 9 h, species **57** remained almost unchanged though **54*** slightly decreased in intensity. The same experiment for **51*** also exhibits a living propagating species (4.59 and 3.15 ppm for -CH_2Ti), although

it was rather difficult to control the reaction due to the high activity of this species under the conditions currently applied. Because two separated signals are observed for the diastereotopic methylene group, the assumed Δ/Λ site-inversion is slow under the conditions examined.

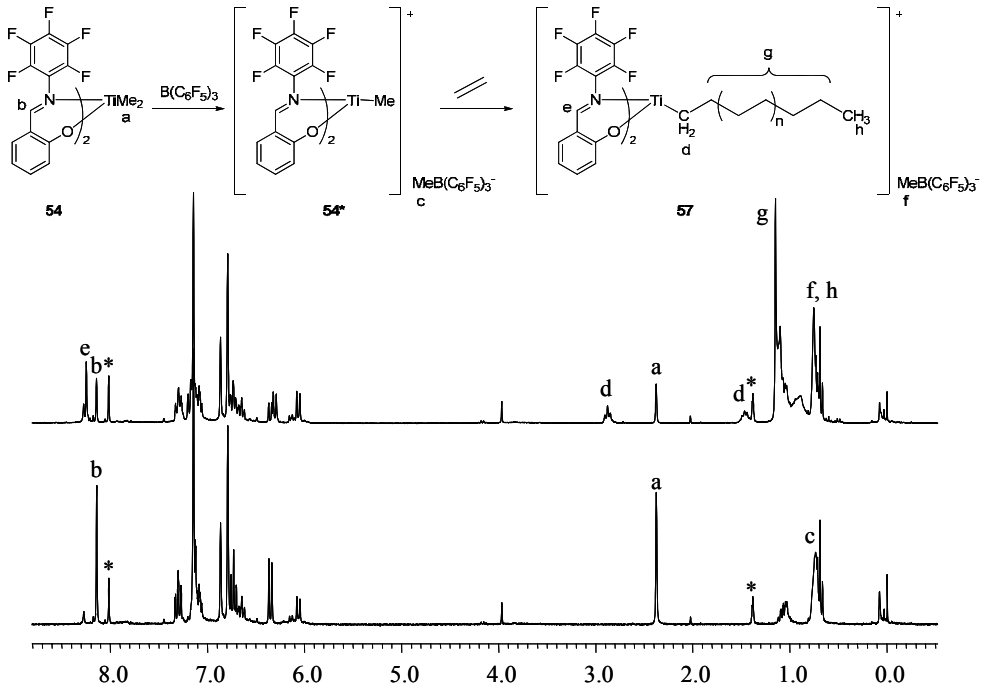

Figure 9. ^{1}H NMR spectra for the species of A) **54*** and B) **57**, which was obtained by adding 5 equiv. of ethylene to **54***. (FT 270 MHz, in BrC_6D_5). Unidentified species (**54'**) are marked with asterisks.

Conclusion

In this study, the author has shown that monomethyl and dimethyl Ti-FI catalysts with perfluorinated N-aryl groups are accessible. These complexes can be activated by common boron cocatalysts without the use of alkylaluminums and thus without reduction of the imine and Ti or without the ligand transfer to alkylaluminums. The species obtained are similar to MAO derived species in character and prove the extraordinary robust livingness of this species. The living propagating species including the Ti-bound methylene protons can be observed even at room temperature.

Experimentals

Materials and Methods.

All manipulations of air-sensitive materials were performed with the rigorous exclusion of oxygen and moisture in flamed Schlenk-type glassware on a dual-manifold Schlenk line or in a nitrogen-filled glove box with a high capacity recirculator (< 1 ppm O_2). Diethyl ether was purified by passing through activated molecular sieves and alumina columns. Dehydrated grade of hydrocarbon solvents were purchased from Wako Pure Chemical Industries, Ltd., and stored over activated molecular sieves in Tefron-valve sealed bulbs. Deuterated solvents were obtained from Cambridge Isotope Laboratories (all ≥ 99 atom %D),

freeze-pump-thaw degassed, dried over activated molecular sieves, and stored in resealable flasks.

Synthesis of $MeTiBr_3$ (**55**)

To a pentane slurry of $TiBr_4$ (6.959 g, 18.94 mmol, 19 mL), a hexane solution of MeLi (1.0 M, 9.0 mL) was added dropwise at –78 ºC. The reaction mixture was allowed to warm to room temperature for 3 h. The resulting yellow orange slurry was filtered through celite, rinsed with pentane, and the orange filtrate was concentrated to approximately two thirds volume under reduced pressure at –78 ºC to yield a dark violet crystalline compound. The supernatant was removed, from which the second crop was recovered. (The combined yield: 3.83 g, 70 %). ^{1}H NMR (270 MHz, benzene-d_6) δ 1.86 (s).

Synthesis of [C_6F_5N=CH(2-O-C_6H_3-3-^{t}Bu)]Na

Using a published method, C_6F_5N=CH(2-OH-C_6H_3-3-^{t}Bu) was prepared. To NaH (211.5 mg, 8.81 mmol in 10 mL diethyl ether), diethyl ether solution of C_6F_5N=CH(2-OH-C_6H_3-3-^{t}Bu) (2.9892 g, 8.71 mmol in 5 mL solvent) was added via cannula at –78 °C and allowed to warm overnight. The reaction mixture was filtered and washed with diethyl ether. The resulting filtrate was concentrated to afford a yellow slurry, to which toluene and pentane were added. The yellow solid was filtered, rinsed with pentane, and dried under vacuum at 5 Pa for 10 h. (2.65 g, 83 % isolated yield). ^{1}H NMR (270 MHz, toluene-d_8) δ 8.05 (s, 1H, HC=N), 7.36 (dd, *J* = 7.3, 2.0 Hz, 1H, ArH), 6.88 (dd, *J* = 7.9, 2.0 Hz, 1H, ArH), 6.46 (t, *J* = 7.6 Hz, 1H, ArH), 1.41 (s, 9H, ^{t}Bu).

Synthesis of [C_6F_5N=CH(2-O-C_6H_3-3-^{t}Bu)]$_2$TiMeBr (**52**)

To a solution of $MeTiBr_3$ (360.0 mg, 1.19 mmol) in 3 mL of anhydrous toluene, [C_6F_5N=CH(2-O-C_6H_3-3-^{t}Bu)]Na (877.5 mg, 2.40 mmol) in 10 mL toluene was added at –78 °C. After 2 h, the reaction mixture was allowed to warm to ambient temperature, filtered, and washed with 5 mL of toluene. The filtrate was concentrated and pentane was added at –78 °C to afford a deep purple crystalline compound (702 mg, the isolated yield 71 %). ^{1}H NMR (270 MHz, benzene-d_6) δ 7.55 (s, 1H, HC=N), 7.47 (s, 1H, HC=N), 7.44 (dd, J = 3.6, 1.7 Hz, 1H, ArH), 7.41 (dd, J = 3.6, 1.7 Hz, 1H, ArH), 6.91 (dd, J = 7.9, 1.7 Hz, 1H, ArH), 6.81 (dd, J = 7.9, 1.7 Hz, 1H, ArH), 6.69 (dt, J = 7.6, 1.7 Hz, 2H, ArH), 1.97 (d, J = 2.0 Hz, 3H, CH_3–Ti), 1.57 (s, 9H, ^{t}Bu), 1.51 (s, 9H, ^{t}Bu); ^{13}C NMR (67.5 MHz, benzene-d_6) δ 174.7, 174.0, 163.7, 162.9, 140.2, 139.2, 136.2, 135.1, 134.6, 134.1, 124.6, 123.7, 121.0, 86.3, 35.5, 29.8−29.3; Anal. Found: C, 51.16; H, 2.86; N, 3.44 %. Calc for $C_{28}H_{16}F_{10}N_2O_2Ti$: C, 50.81; H, 3.53; N, 3.39 %. The discrepancy in elemental analyses is due to instability of the complex.

Synthesis of [C_6F_5N=CH(2-O-C_6H_3-3-^{t}Bu)]$_2$TiMe$_2$ (**51**)

To a light yellow slurry of $TiCl_4$/(1,2-dimethoxyethane) (183.7 mg, 0.66 mmol) in 6.5 mL of anhydrous diethyl ether, 1.29 mL of MeLi (1.0 M in diethyl ether) was added at 0 °C. The dark red reaction mixture was held at

the temperature for 30 min and then cooled to –78 °C. After removing the volatiles by vacuum, [C_6F_5N=CH(2-O-C_6H_3-3-^{t}Bu)]Na (475 mg, 1.30 mmol) in 10 mL toluene was added at –78 °C. After 1 h, the reaction mixture was allowed to warm to ambient temperature. Pentane was added, filtered, and washed with pentane. The filtrate was concentrated and kept at –78 °C to afford a dark brown compound. Deep purple crystalline was obtained by slow diffusion of pentane into a toluene solution. ^{1}H NMR (270 MHz, benzene-d_6) δ 7.52 (s, 2H, HC=N), 7.45 (dd, J = 7.6, 1.7 Hz, 2H, ArH), 6.88 (dd, J = 7.6, 1.7 Hz, 2H, ArH), 6.72 (t, J = 7.7 Hz, 2H, ArH), 1.65 (s, 6H, CH_3-Ti), 1.58 (s, 18H, ^{t}Bu); ^{19}F NMR (471 MHz, benzene-d_6) δ –149.3 (d, o-F), –160.3 (t, p-F), –164.2 (m, m-F); Anal. Found: C, 56.12; H, 3.07; N, 3.60 %. Calc for $C_{36}H_{32}F_{10}N_2O_2Ti$: C, 56.71; H, 4.23; N, 3.67 %. The discrepancy in elemental analyses is due to instability of the complex.

Synthesis of [C_6F_5N=CH(2-O-C_6H_4)]$_2$TiMe$_2$ (**54**)

This complex was prepared by a similar manner to complex **51**. ^{1}H NMR (270 MHz, toluene-d_8) δ 7.38 (s, 2H, HC=N), 7.11–7.05 (m, 2H, ArH), 6.81–6.77 (m, 4H, ArH), 6.59 (dt, J = 7.6, 1.0 Hz, 2H, ArH), 1.67 (s, 6H, CH_3-Ti); ^{19}F NMR (471 MHz, benzene-d_6) δ –147.0, –149.5 (br, o-F), –160.9 (t, p-F), –163.3, –164.6 (br, m-F); Anal. Found: C, 50.69; H, 1.33; N, 4.22 %. Calc for $C_{28}H_{16}F_{10}N_2O_2Ti$: C, 51.72; H, 2.48; N, 4.31 %. The discrepancy in elemental analyses is due to instability of the complex.

References and Notes

(1) Makio, H.; Terao, H.; Iwashita, A.; Fujita, T. *Chem. Rev.* to be published in the special thematic issue on "2011 Frontiers in Transition Metal Catalyzed Reactions".

(2) Floriani, C.; Solari, E.; Corazza, F.; Chiesi-Villa, A.; Guastini, C. *Angew. Chem., Int. Ed. Engl.* **1989**, *28*, 64–66.

(3) Solari, E.; Floriani, C.; Chiesi-Villa, A.; Rizzoli, C. *J. Chem. Soc., Dalton Trans.* **1992**, 367–371.

(4) Woodman, P. R.; Alcock, N. W.; Munslow, I. J.; Sanders, C. J.; Scott, P. *J. Chem. Soc., Dalton Trans.* **2000**, 3340–3346.

(5) Knight, P. D.; Clarke, A. J.; Kimberley, B. S.; Jackson, R. A.; Scott, P. *Chem. Commun.* **2002**, 352–353.

(6) Knight, P.D.; O'Shaughnessy, P. N.; Munslow, I. J.; Kimberley, B. S.; Scott, P. *J. Organomet. Chem.* **2003**, *683*, 103–113.

(7) Knight, P. D.; Clarkson, G.; Hammond, M. L.; Kimberley, B. S.; Scott, P. *J. Organomet. Chem.* **2005**, *690*, 5125–5144.

(8) Tjaden, E. B.; Swenson, D. C.; Jordan, R. F.; Petersen, J. L. *Organometallics* **1995**, *14*, 371–386.

(9) Cozzi, P. G.; Gallo, E.; Floriani, C.; Chiesi-Villa, A.; Rizzoli, C. *Organometallics* **1995**, *14*, 4994–4996.

(10) Bei, X.; Swenson, D. C.; Jordan, R. F. *Organometallics* **1997**, *16*, 3282–3302.

(11) See Chapter 1 of this thesis.

(12) Chen, E.-X.; Marks, T. J. *Chem. Rev.* **2000**, *100*, 1391–1434.

(13) Zuccaccia, C.; Stahl, N. G.; Macchioni, A.; Chen, M.-C.; Roberts, J. A.; Marks,T. J. *J. Am. Chem. Soc.* **2004**, *126*, 1448–1464.

(14) Beck, S.; Lieber, S.; Schaper, F.; Geyer, A.; Brintzinger, H.-H. *J. Am. Chem. Soc.* **2001**, *123*, 1483–1489.

(15) Mitani, M.; Mohri, J.-i.; Yoshida, Y.; Saito, J.; Ishii, S.; Tsuru, K.; Matsui, S.; Furuyama, R.; Nakano, T.; Tanaka, H.; Kojoh, S.-i.; Matsugi, T.; Kashiwa, N.; Fujita, T. *J. Am. Chem. Soc.* **2002**, *124*, 3327–3336.

(16) Mitani, M.; Furuyama, R.; Mohri, J.-i.; Saito, J.; Ishii, S.-i.; Terao, H.; Kashiwa, N.; Fujita, T. *J. Am. Chem. Soc.* **2002**, *124*, 7888–7889.

(17) Makio, H.; Fujita, T. *Acc. Chem. Res.* **2009**, *42*, 1532–1544.

Part II. Selectivity of FI Catalysts

Chapter 3. Isoselective propylene polymerization with FI catalysts

Abstract

Highly isospecific propylene polymerization was achieved by bis(phenoxy-imine) Zr and Hf complexes combined with $^{i}Bu_3Al/Ph_3CB(C_6F_5)_4$. Microstructural analyses of the isotactic polymers suggested that the polymerization probably proceeds via a site-control mechanism with a 1,2-insertion of propylene. Among the complexes examined, a Hf complex (**58**) produced the highest tacticity polypropylene ([*mmmm*] 96.8 %, T_m 165.1 °C) which is comparable to that made by the best heterogeneous Ziegler-Natta catalysts.

Introduction

The development of homogeneous olefin polymerization catalysts based on well-defined coordination complexes has given us opportunities to synthesize polymers with precisely controlled structures and a chance to study polymerization pathways at the molecular level. For example, new complexes have been prepared that allow highly stereospecific polymerization and a rational interpretation of the polymerization mechanisms. Although highly isospecific and syndiospecific propylene polymerizations have been achieved by explicitly designed molecular catalysts,[1,2] there is still considerable interest in the development of catalysts for the controlled polymerization of propylene due to the current importance and the great possibilities of polypropylene. In particular, high stereoregularity of polypropylene is crucial for practical applications.

Part I of this thesis proved that the active species of Ti-FI catalysts possessed C_2 symmetric *cis*-N/*trans*-O geometry with *cis*-located reaction sites when activated with MAO. However, despite the homotopic reaction sites, the Ti-FI catalysts display moderate-to-exceptionally high syndioselectivity via a chain-end control mechanism toward propylene polymerizations. Research into this unique polymerization with Ti-FI catalysts has revealed that each monomer was enchained by consecutive 2,1-insertions, and also that the syndioselectivity was in direct proportion to the sizes of the R^2 substituents, despite the apparent chain-end controlled stereoregulating mechanism, for which a Δ/Λ site inversion mechanism was proposed.[3]

On the other hand, the active species of FI catalysts generated by $^{i}Bu_3Al/Ph_3CB(C_6F_5)_4$ is assumed to be reduced at the imine function by $^{i}Bu_3Al$. The postulated species, therefore, has $-CH_2–NR^1–Al^{i}Bu_2$ instead of $-CH=NR^1$ and generally displays lower activity toward polymerization but gives higher molecular weight polyolefins than the corresponding MAO-activated FI catalysts.[3] Propylene polymerization with the reduced species follows this general trend, but marked differences in polymerization characteristics by the metal center and ligand substituents are observed just as for the MAO-activated FI catalysts but in an opposite selectivity. Ti-FI catalyst **20** yields ultra-high molecular weight atactic polypropylene with a significant amount of regioirregular units upon activation with $^{i}Bu_3Al/Ph_3CB(C_6F_5)_4$. Whereas, the corresponding Zr- and Hf-FI catalysts afford moderately isotactic polypropylenes with *mmmm* tacticity of 36 % for the Zr (**21**) and 56 % for the Hf (**59**) via a site-control mechanism. In these polymerizations, the product obtained with Ti catalyst **20** exhibits a relatively broad molecular weight distribution (M_w/M_n = 4.15), indicating multiple active species, while the Zr and the Hf catalysts demonstrate single-site polymerization characteristics (**Scheme 1**).

Thus, propylene polymerization characteristics with FI catalysts are drastically altered by metal center, cocatalyts, and substituents at strategic positions in the ligands. Herein, we describe ligand modifications where the isospecificity of the Zr- and Hf-FI catalysts was dramatically enhanced enabling the highest levels of isotacticity ever reported, even when compared to the best heterogeneous Ziegler-Natta catalysts.

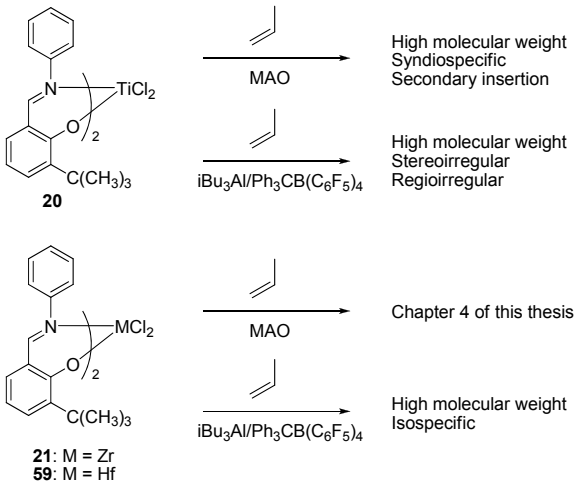

Scheme 1

Results and Discussion

Zr- and Hf-FI Catalysts **42**, **58**, **39**, **60** (**Table 1**) were synthesized using a method similar to that described in our previous papers.[4,5] Propylene polymerizations with **42**, **58**, **39**, **60** were investigated using $^{i}Bu_3Al/Ph_3CB(C_6F_5)_4$ as a cocatalyst at 25 °C under atmospheric pressure (See Experimentals). The polymerization results are summarized in **Table 1**.

Table 1. Propylene polymerization with FI catalysts using $^{i}Bu_3Al/Ph_3CB(C_6F_5)_4$ as a cocatalyst.

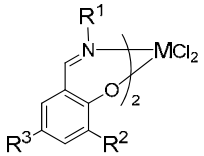

42: M = Zr, R^1 = Cyclohexyl, R^2 = Adamantyl, R^3 = Methyl
58: M = Hf, R^1 = Cyclohexyl, R^2 = Adamantyl, R^3 = Methyl
39: M = Zr, R^1 = Phenyl, R^2 = Adamantyl, R^3 = Methyl
60: M = Hf, R^1 = Phenyl, R^2 = Adamantyl, R^3 = Methyl
21: M = Zr, R^1 = Phenyl, R^2 = ^{t}Butyl, R^3 = H
59: M = Hf, R^1 = Phenyl, R^2 = ^{t}Butyl, R^3 = H

complex	Activity[a]	T_m/°C	$M_w/10^{-3}$[b]	M_w/M_n[b]
42	38	163.3	200	4.72[c]
58	62	164.8	530	14.6[c]
39	24.7	154.9	607	18.4[d]
60	638	160.1	1,453	2.99
21[e]	94	103.5	209	2.42
59[e]	76	123.8	412	2.15

Conditions: reaction time, 20 min; temperature, 25 °C; toluene, 250 mL; propylene, 0.1 MPa (100 L/h); complex, 0.005 mmol; $^{i}Bu_3Al$, 0.15 mmol; $Ph_3CB(C_6F_5)_4$, 0.01 mmol. [a]In kg/mol-M·h. [b]Measured by GPC using polystyrene calibration. [c]Bimodal distribution. [d]Multimodal distribution. [e]See reference 5.

Polypropylene obtained from FI catalysts **42**, **58**, **39**, **60** appear visually to be mixtures, which consist of sticky amorphous and crystalline polymers. The GPC elution curves of these polymers display unimodal to multimodal molecular weight distributions, which are in stark contrast to sharp unimodal peaks of polypropylene arising from FI Catalysts **21** and **59** under the same conditions.[5] In DSC studies, the polymers obtained show very high peak melting temperatures (T_m) of 154.9–164.8 °C, indicative of the

formation of highly stereoregular polymers. The multimodal behavior observed for the present catalyst systems (**Figure 1**) may be due to the incomplete reduction of the imine-functionality and/or the presence of several catalytically active species arising from the different binding geometries of the ligands.

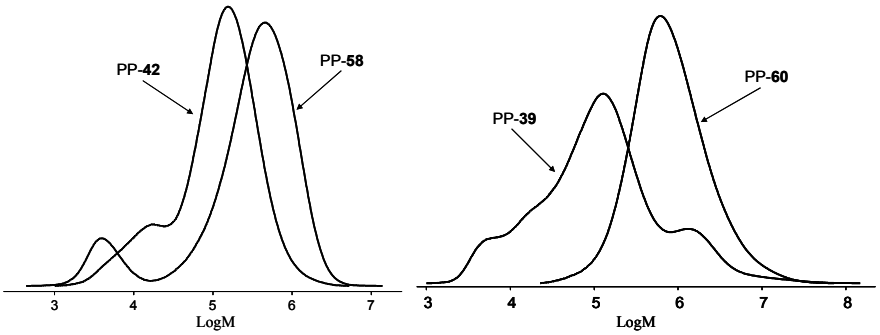

Figure 1. GPC elution curves of PP-**42**, **58**, **39**, **60** before fractionation (polystyrene calibration).

To obtain polymers in sufficient quantities for microstructural analyses, the catalyst concentration was doubled. The polypropylene obtained with complexes **42**, **58**, **39**, **60** (denoted as PP-**42**, **58**, **39**, **60**, hereafter) exhibited broad molecular weight distributions similar to those obtained with the lower catalysts concentration and can be divided into two parts by extraction with boiling hexane. The remaining crystalline polymers (hexane-insoluble parts: PP-**42**, 65 wt%; PP-**58**, 86 wt%; PP-**39**, 18 wt%; PP-**60**, 7 wt%) have relatively narrow molecular weight distributions (M_w/M_n: 2.1, M_w 172 $\times$ 10^3 for PP-**42**; 3.5, 346 $\times$ 10^3 for PP-**58**; 3.8, 1,306 $\times$ 10^3 for PP-**39**; 4.7, 2,554 $\times$ 10^3 for PP-**60**) and a T_m of 154.9–165.1 °C. The ^{13}C NMR analyses of these hexane-insoluble stereoregular polymers from PP-**42** and PP-**58** revealed that FI catalysts **58** and **39** afforded highly isotactic polypropylene whose isotacticities reached to [*mmmm*] 96.9 % for PP-**58** and 96.8 % for PP-**39** (**Figure 2**). The T_m (165.1 °C) and the isospecificity ([*mmmm*] 96.8 %) obtained with Hf-FI catalyst **39** represent some of the highest values for isotactic polypropylene ever synthesized.[1,2]

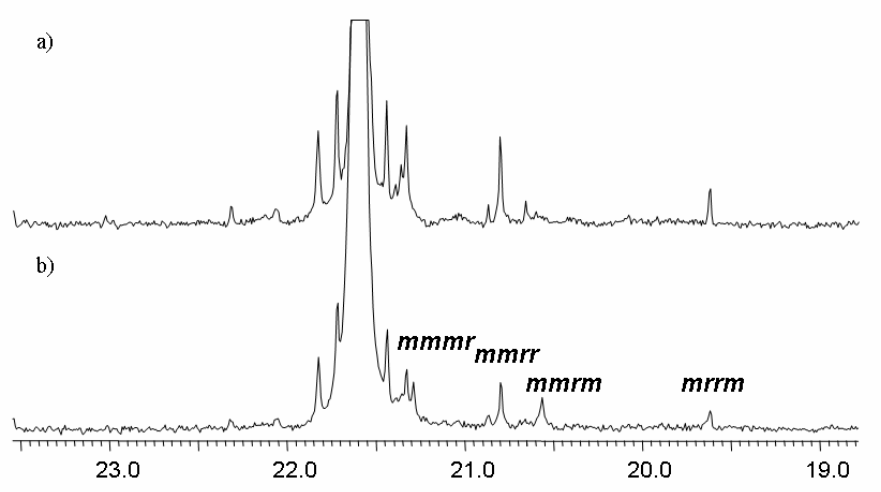

Figure 2. ^{13}C NMR spectra of the methyl pentad regions for the isotactic polypropylene: a) hexane insoluble part, PP-**42**; b) hexane insoluble part, PP-**58**.

The data in **Table 1** suggest that the higher steric congestion near the polymerization center results in the formation of higher tacticity polymers. The integration of each pentad signal indicates that a site-control mechanism would be operative as is observed for PP-**21** and PP-**59** although deviations from the expected statistics are sometimes significant because of the small quantities of stereoirregular sequences which lead to poor signal-to-noise ratio.

To investigate chain-end structures, which may provide information on regiochemistry of chain propagation, a low molecular weight polymer was synthesized with **42** using H_2 as a chain transfer agent. Interestingly, highly isotactic polymer was selectively produced in this case probably because the other less stereospecific species were deactivated or transformed to highly stereospecific species in the presence of H_2. This result may provide insight into the structure of the desired active species and mechanism for this highly stereoselective reaction. The low M_w polypropylene (M_w 17,211, M_w/M_n 1.91) formed with **42**/$^{i}Bu_3Al/Ph_3CB(C_6F_5)_4/H_2$ contains three chain-end structures (^{13}C NMR analysis), i.e., *n*-propyl (46 %), isobutyl (47 %), and *n*-butyl (6 %). Inversion structures, which were observed in the isotactic polypropylene produced in the absence of H_2 (0.1 %), could not be detected. Under the assumption that an occasional 2,1-insertion makes the subsequent monomer insertion slow and is followed exclusively by hydrogen chain transfer,[6,7] it is concluded that 1,2-enchainment is the regular monomer insertion mode resulting in *n*-propyl and isobutyl groups as initiation and termination chain ends, respectively, and *n*-butyl groups are termination chain ends resulting from occasional regioerrors, which is concentrated at the chain ends because the low reactivity of the 2,1-inserted chain end toward subsequent propylene insertion causes preferential hydrogenation at this chain end (**Scheme 2**). Since the amount of inversion units of the polypropylene produced with Hf-FI Catalyst **58** (in the absence of H_2) was below the ^{13}C NMR detection level, we could not determine the insertion mode for **58** by this method. However, we assume that the propylene polymerization with **58** proceeds via a 1,2-insertion mechanism based on the similarity between the Zr- and Hf-FI catalysts.[5]

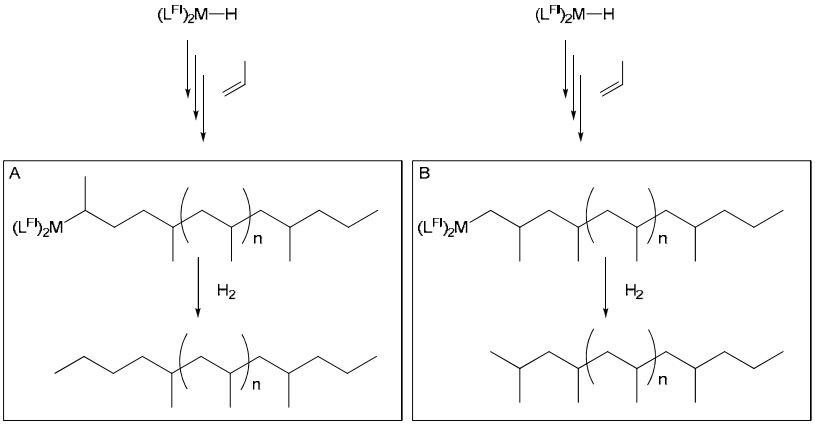

Scheme 2. A) Hydrogenation at an occasional 2,1-inserted chain end, leading to *n*-butyl chain end, B) hydrogenation at a regular 1,2-inserted chain end, leading to isobutyl chain end. The initiating chain ends are *n*-propyl group for both cases.

Conclusion

We have demonstrated that highly isotactic polypropylene with extremely high T_m (165.1 °C) can be produced by Zr- and Hf-FI catalysts upon activation with $^{i}Bu_3Al/Ph_3CB(C_6F_5)_4$. These results are remarkable in view of the tremendous technological significance of high T_m isotactic polypropylene. The isospecific polymerization presumably proceeds via a site-control mechanism with 1,2-monomer enchainment. The susceptibility of the imine-functionality towards reduction by $^{i}Bu_3Al$ (and/or its contaminant $^{i}Bu_2AlH$) seems crucial to the high yield of highly isotactic polypropylene. The results presented herein together with our previous reports[3] indicate that FI catalysts are capable of producing polypropylene architectures ranging from atactic, highly syndiotactic to highly isotactic by variation of the central metal, ligand structure and the cocatalyst.

Experimentals

Propylene Polymerization

Polymerizations were performed under atmospheric pressure using a 500-mL glass reactor equipped with a mechanical stirrer, a temperature probe, and a condenser. Toluene (250 mL) was introduced into the nitrogen-purged reactor and stirred (600 rpm). The solvent was kept at 25 °C, and then the propylene gas feed (100 L/h) was started. After 10 min, an 0.25 M solution of $^{i}Bu_3Al$ in toluene (0.2 mL, 0.05 mmol) was added into the reactor. In a Schlenk tube, an 0.001 M solution of the complex in toluene (5.0 mL, 0.005 mmol) and an 0.25 M solution of $^{i}Bu_3Al$ in toluene (0.6 mL, 0.15 mmol) were mixed and stirred for 10 min at room temperature. Polymerization was initiated by adding the Schlenk tube mixture and an 0.004 M solution of $Ph_3CB(C_6F_5)_4$ in toluene (2.5 mL, 0.01 mmol) to the reactor. After 20 min, polymerization was quenched by injection of isobutyl alcohol (10 mL). The resulting mixture was added to acidified methanol (1,000 mL containing 2 mL of concd HCl). The polymer was recovered by filtration, washed with methanol (200 mL × 2), and dried overnight in a vacuum oven at 80 °C to constant weight.

References and Notes

(1) Coates, G. W. *Chem. Rev.* **2000**, *100*, 1223–1252.

(2) Resconi, L.; Cavallo, L.; Fait, A.; Piemontesi, F. *Chem. Rev.* **2001**, *101*, 1253–1346.

(3) See General Introduction of this thesis.

(4) Furuyama, R.; Saito, J.; Ishii, S.; Mitani, M.; Matsui, S.; Tohi, Y.; Makio, H.; Matsukawa, N.; Tanaka, H.; Fujita, T. *J. Mol. Catal. A* **2003**, *200*, 31–42.

(5) Saito, J.; Onda, M.; Matsui, S.; Mitani, M.; Furuyama, R.; Tanaka, H.; Fujita, T. *Macromol. Rapid Commun.* **2002**, *23*, 1118–1123.

(6) Busico, V.; Cipullo, R.; Corradini, P. *Makromol. Chem., Rapid Commun.* **1993**, *14*, 97–103.

(7) Tsutsui, T.; Kashiwa, N.; Mizuno, A. *Makromol. Chem., Rapid Commun.* **1990**, *11*, 565–570.

Chapter 4. Stereo- and regioselectivity of zirconium and hafnium FI complexes activated with MAO

Abstract

End-group analyses of the oligo- and polypropylenes produced with bis(phenoxy–imine) Zr and Hf complexes with methylalumoxane (MAO) indicate that the polymerization is initiated by two consecutive 1,2-insertions and is terminated via a β-H transfer following a 2,1-insertion. The data indicate that chain propagation occurs with prevailing 1,2-regiochemistry but with considerable regioerrors, and with virtually no stereoselectivity.

Introduction

In α-olefin polymerization, stereo- and regioselectivities are crucial factors which influence the physical properties of the resultant polymers. Extensive research efforts have been devoted to developing new catalyst systems that can achieve better control over stereo- and regioselectivities in α-olefin polymerization, particularly in propylene polymerization due to its commercial importance.[1–3] The microstructures of the resultant polypropylenes can serve as a chronological record of the reaction mediated by a catalytically active species, i.e., information on initiation, propagation, and termination reactions is preserved in a format of monomer sequences and chain-end structures, which can be analyzed by well-established NMR techniques.[4]

As mentioned in the General Introduction and the preceded chapters of this thesis, FI catalysts have been shown to exhibit unique stereo- and regioselectivities in α-olefin polymerization. For instance, Ti-FI catalysts on activation with $^{i}Bu_3Al/Ph_3CB(C_6F_5)_4$, are capable of producing high molecular weight (M_w > 600,000) atactic poly(1-hexene)s having about 50 mol% of regioirregular units (ultra-random polymers).[5] In propylene polymerization, the same catalyst systems afforded ultra-high molecular weight (M_w > 8,000,000) atactic polypropylene with considerable regioirregular units (~9 %).[6] In contrast, the same Ti-FI catalysts with MAO produced moderately to highly syndiotactic polypropylene via a chain-end control mechanism,[7,8] and significantly, the introduction of a perfluorophenyl group on the imine-nitrogen reinforces the syndioselectivity and, moreover, induces a living polymerization to form unique polypropylene with narrow molecular weight distributions (M_w/M_n) close to one as well as very high syndiotacticity.[9,10] The syndiospecific propylene polymerization is initiated exclusively by 1,2-insertion followed by multiple 2,1-insertions as the principal mode of polymerization.[11]

These unusual observations for propylene polymerizations with Ti-FI catalysts pose intriguing questions about the propylene polymerization behavior of FI catalysts containing group 4 metal centers other than Ti. In contrast to Ti-FI catalysts/$^{i}Bu_3Al/Ph_3CB(C_6F_5)_4$ which formed ultra-high molecular weight atactic polypropylene, the corresponding Zr- and Hf-FI catalysts with $^{i}Bu_3Al/Ph_3CB(C_6F_5)_4$ provided rather isotactic polypropylene via a site-control mechanism.[12] Upon activation with MAO, the Zr- and Hf-FI catalysts with perfluorophenyl groups on the imine-nitrogens produced far higher molecular weight polyethylenes and ethylene/propylene copolymers at higher activities than the non-fluorinated counterparts,[13] which is interesting in association with the possible attractive interaction that may induce a highly controlled living polymerization with the fluorinated Ti-FI catalysts.[11,14]

Given these differences and similarities between Ti- and Zr, Hf-FI catalysts as summarized in **Scheme 1**, the author became interested in propylene polymerizations with Zr- and Hf-FI catalysts/MAO systems, focusing on stereo- and regiochemistry of these catalyst systems, which will be the subject of this chapter.

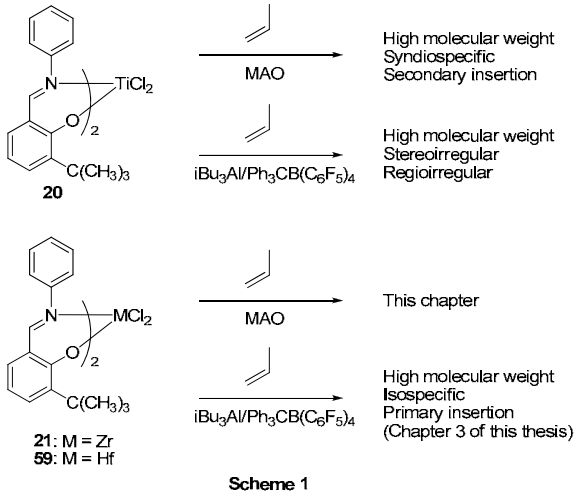

Scheme 1

Results and Discussion

The Zr- and Hf-FI Catalysts employed in this study are [2-(RN=CH)-5-^{t}Bu-$C_6H_3O]_2MCl_2$ (**21**, M = Zr, R = C_6H_5; **61**, M = Zr, R = C_6F_5; **59**, M = Hf, R = C_6H_5; **62**, M = Hf, R = C_6F_5), which were prepared according to similar procedures reported in our previous papers.[13,15]

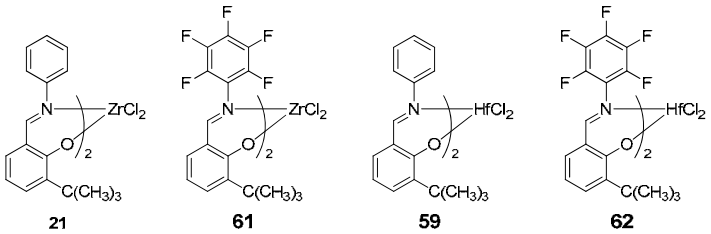

Propylene polymerization results with complexes **21**, **61**, **59**, and **62** combined with MAO are summarized in **Table 1**. Zr complex **21**/MAO displayed fairly high reactivity toward propylene and generated oligomers whose degree of polymerization (DP) is about 5. On the other hand, the corresponding fluorinated complex **61** afforded higher molecular weight oligomers (DP ~ 25) with generally enhanced activities. The oligomers produced with Zr complexes **21** and **61** possess narrow molecular weight distributions (M_w/M_n 1.31 – 2.34),[16] which are consistent with the operation of a single-site catalyst. The high molar ratio of polymer chains relative to catalyst molecules indicate that chain transfer is fast relative to propagation for the polymerizations mediated by both complexes in contrast to the living polymerization with the corresponding Ti-FI catalysts.

End group analyses of the resultant materials using ^{13}C NMR spectroscopy show the presence of practically an equal amount of saturated and unsaturated chain-end groups. The saturated chain ends were exclusively *n*-propyl groups, whereas the unsaturated chain ends were a mixture of allyl-, 1-butenyl-, *cis*-2-butenyl-, *trans*-2-butenyl-, and vinylidene groups (**Figure 1** and **Table 2**). These results indicate that virtually all chains are terminated via β-H transfers and that the first two monomer units are enchained in a 1,2-fashion.

As summarized in **Scheme 2**, each unsaturated chain-end structure represents the regiochemistry of the last two monomer insertions. A β-H transfer following two consecutive 1,2-insertions produces a vinylidene end group, whereas a β-H transfer after successive 1,2- and 2,1-insertions leads to various butenyl end groups depending on which hydrogen is transferred. Likewise, two consecutive 2,1-insertions followed by a β-H transfer results in an allyl end group.

Predominant formation of allyl and butenyl end groups among the unsaturated chain ends for both complexes clearly indicates that chain propagation becomes sluggish after a 2,1-insertion, resulting in chain release via a β-H transfer. These polymerization characteristics as well as the chain-end structures suggest that 1,2-insertion is the main propagation mode in propylene polymerization with Zr complexes/MAO systems, which is the opposite regiochemistry of the same or similar Ti counterparts/MAO systems in which 2,1-insertion is dominant for chain propagation.[9,11]

Interestingly, Zr complex **61**/MAO formed a smaller amount of the butenyl end group than **21**/MAO as an unsaturated chain end. This result demonstrates that **61**/MAO allows 1,2-insertion in part even after 2,1-insertion, which enables subsequent chain propagations to form higher molecular weight products than those obtained with **21**/MAO. This interpretation is also supported by the fact that head-to-head sequence (HH) is observed only in the products obtained with **61**/MAO.

Molecular weights of the products formed with the Zr complexes/MAO are too small to meaningfully discuss the degree of stereo- and regioselectivities. As for the **21**/MAO system, the first two monomer units are enchained in a 1,2-fashion and most of the terminations (> 80 %) occur in the sequence of 1,2- and 2,1-insertions out of 5 monomer units on average. On the other hand, the products formed from complex **61**/MAO contain significant amount of regioerrors. We could roughly estimate the molar ratios of head-to-tail (HT) and head-to-head (HH) sequences but failed to quantify tail-to-tail (TT) sequences because of the severe overlap between the signals derived from TT sequences and some chain-end groups. If one supposes that [HH] is nearly equal to [TT] in a sufficiently long polymer chain as is often seen in common propylene polymerizations, [HT] in the polypropylene produced with **61**/MAO can be estimated in 40–70 %, indicative of low regioselectivity. Thus, the following sequence of events occurs: the polymerizations with the Zr complexes/MAO are initiated exclusively by two consecutive 1,2-enchainments, propagate through prevailing 1,2-insertions with significant regioirregular enchainments, and are terminated mostly via a β-H transfer following a 2,1-insertion (> 90 %).

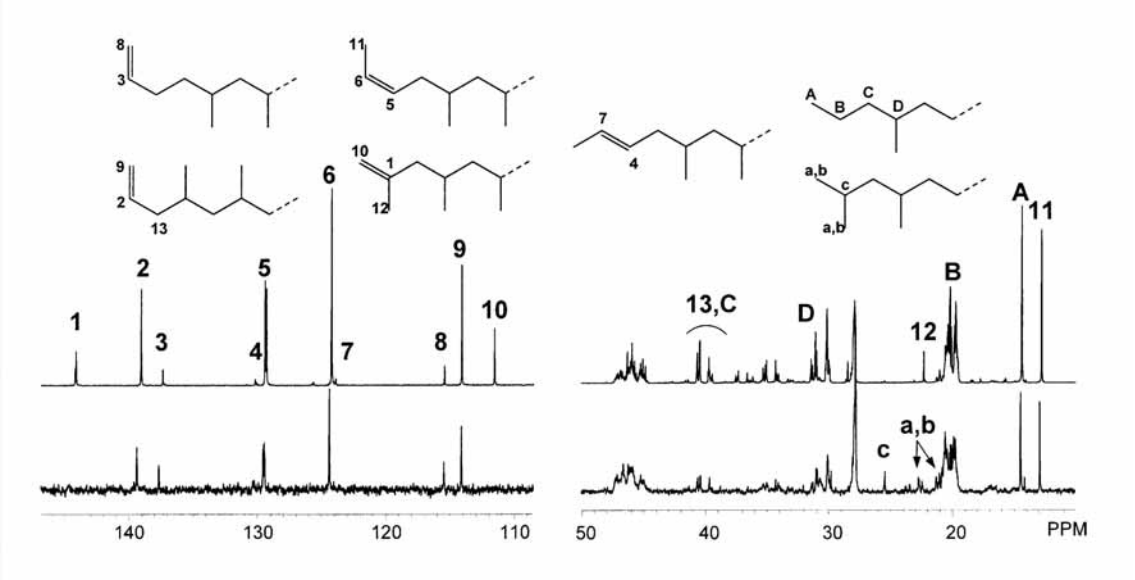

Figure 1. Representative ^{13}C NMR spectra of the propylene oligomer obtained with **21**/MAO (top, entry 1 in **Table 1** and **2**) and **59**/MAO (bottom, entry 7 in **Table 1** and **2**).

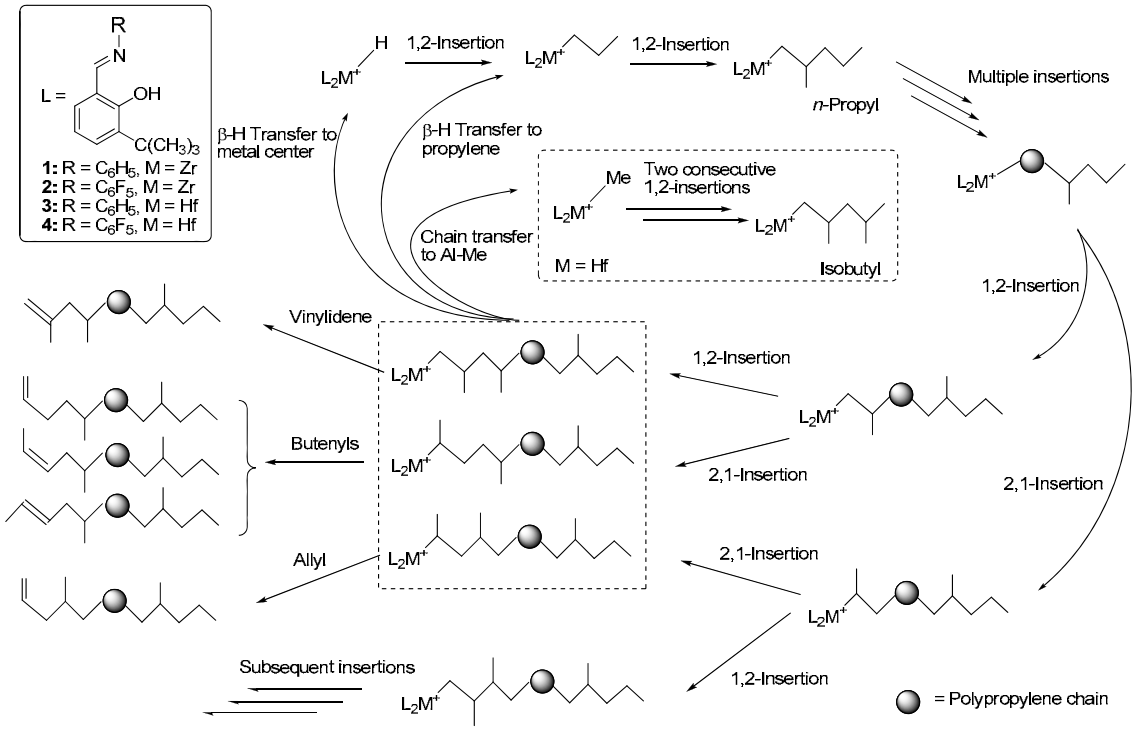

Scheme 2. Chain-end structures of polypropylene obtained with Zr- and Hf-FI catalysts activated by MAO

Table 1. Propylene polymerization with complex **21**, **61**, **59** and **62**/MAO

Entry	Complex	Cat. (μmol)	MAO (mmol)	Propylene (MPa)	Temp. (°C)	Toluene (mL)	Time (h)	Yield (g)	Activity[a]	DP[b]	M_n[c]	M_w/M_n[c]
1	**21**	5	1.25	0.1	0	250	0.5	0.77	308	5.5	210	1.31
2	**21**	5	1.25	0.1	25	250	0.5	1.72	688	5.4	150	1.55
3	**21**	5	1.25	0.1	50	250	0.5	0.21	84	5.3	n.d.[d]	n.d.[d]
4	**61**	5	1.25	0.1	0	250	0.5	0.93	372	27.3	1,460	2.22
5	**61**	5	1.25	0.1	25	250	0.5	1.07	428	22.8	1,340	2.34
6	**61**	5	1.25	0.1	50	250	0.5	0.82	328	26.9	1,340	2.23
7	**59**	10	2.50	0.1	0	500	1.5	0.37	25	n.d.[d]	450	1.70
8	**59**	10	2.50	0.1	25	500	1.5	0.89	59	n.d.[d]	370	1.62
9	**59**	10	2.50	0.1	50	500	1.5	0.09	6	n.d.[d]	n.d.[d]	n.d.[d]
10	**62**	10	2.50	0.1	0	500	1.5	5.00	333	n.d.[d]	31,890	2.29
11	**62**	10	2.50	0.1	25	500	1.5	5.71	380	n.d.[d]	9,900	2.73
12	**62**	10	2.50	0.1	50	500	1.5	1.84	123	n.d.[d]	2,220	2.65

[a]In kg-polymer/mol-cat. h. [b]Degree of polymerization calculated from ^{13}C NMR spectra. [c]Measured by GPC. [d]Not determined.

Table 2. Microstructures of polypropylene obtained with complex **21**, **61**, and **59**/MAO

Entry	Complex	Chain-end structures						Regio-structures in diad sequence		
		n-Propyl	Isobutyl	Allyl	Butenyls[a]	Vinylidene	Sat./Unsat.[b]	HT	HH	TT
1	**21**	100	0	5	26/55/2	12	1.0	n.q.[c]	n.q.[c]	none
2	**21**	100	0	7	27/54/3	9	1.0	n.q.[c]	n.q.[c]	none
3	**21**	100	0	13	31/46/5	6	1.0	n.q.[c]	n.q.[c]	none
4	**61**	100	0	41	27/21/8	3	1.0	1.5	1	n.q.[c)]
5	**61**	100	0	47	23/30/0	0	1.0	5	1	n.q.[c)]
6	**61**	100	0	50	23/18/7	3	1.0	1.3	1	n.q.[c)]
7	**59**	78	22	13	27/53/7	0	1–1.2	5	1	n.q.[c)]
8	**59**	65	35	20	23/43/5	9	1–1.4	4–5	1	n.q.[c)]
9	**59**	50	50	29	18/23/5	25	2–2.2	2–3	1	n.q.[c)]

[a]Ratio of 1-butenyl/*cis*-butenyl/*trans*-butenyl. [b]Ratio of saturated chain ends/unsaturated chain ends. [c]Detected but could not be quantified.

The polymerization characteristics of Hf complexes **59** and **62** activated with MAO were similar to those of Zr complexes **21** and **61**. Although the peaks derived from chain-end structures of the products formed with **62**/MAO were not of sufficient size to be detected by ^{13}C NMR due to the high molecular weights of the polymers, the oligomers produced with **59**/MAO (**Figure 1** and **Table 2**) were revealed by chain-end analysis using ^{13}C NMR to possess an isobutyl group in addition to the *n*-propyl group. There are two possibilities for the formation of an isobutyl group: i) chain transfer to Al-Me species followed by two successive 1,2-insertions of propylene (**Scheme 1**) or ii) β-methyl elimination followed by two consecutive 1,2-insertions of propylene. Because the molar ratio of saturated/unsaturated chain ends is larger than 1.0 for all polymer samples and Hf complexes are more susceptible to chain transfer to aluminum than Zr counterparts,[13] chain transfer to aluminum is most likely responsible for the formation of the isobutyl group.

The molecular weights of the polymers produced with **62**/MAO were significantly decreased with the increase in polymerization temperatures, which is in sharp contrast to the rather temperature-independent molecular weight behavior of the Zr complexes. These observations are also explained by chain transfer to aluminum because the molecular weight decrease is accompanied by the increase in the isobutyl/*n*-propyl and saturated/unsaturated chain-end ratios (**Table 2**). The chain-end analyses also indicate the predominant formation of allyl and butenyl groups among the unsaturated chain ends, showing that most of the terminations proceed via a 2,1-insertion followed by a β-H transfer (75–100 %). With these results, it is concluded that the polymerizations with the Hf complexes are initiated by two consecutive 1,2-insertions and are terminated mainly via a β-H transfer following a 2,1-insertion.

The polymers obtained with **62**/MAO have sufficient molecular weights to determine stereo- and regioselectivities. ^{13}C NMR indicated that the polypropylene are virtually atactic (or slightly syndiotactic-rich) and the tacticity is insensitive to polymerization temperature ([*mm*]/[*mr*]/[*rr*]: 13/50/37 (%) at 0 ºC; 9/47/44 (%) at 25 ºC; 10/48/42 (%) at 50 ºC). These polypropylenes exhibit regioselectivities ([HT]/[HH]/[TT]) as follows; 72/13/14 (%) at 0 ºC, 64/14/21 (%) at 25 ºC and 60/18/23 (%) at 50 ºC. The contents of [HT] sequences are lower than the corresponding fluorinated and non-fluorinated Ti complexes ([HT] ~ 80–90 %)[9,13,17] but are higher than those of the Zr counterpart, **61**/MAO ([HT] < 60 %). Because the polymerization characteristics and polymer microstructures of the Hf complexes are apparently similar to those of the Zr complexes except for chain transfer to aluminum, the propylene polymerizations with the Hf complexes/MAO probably proceed through 1,2-regiochemistry. The degree of regioselectivity seems higher than the corresponding Zr complexes judging from the estimated [HT] values for the Zr and Hf complexes, which is further supported by the facts that the Hf complexes produce higher molecular weight polymers than the Zr-counterparts and that the polymerization is mainly terminated via a β-H transfer following a 2,1-insertion.

Conclusion

The microstructures of the oligo- and polypropylenes together with polymerization characteristics have

revealed that propylene polymerizations with bis(phenoxy-imine) Zr and Hf complexes/MAO systems proceed via prevailing 1,2-regiochemistry with considerable regioerrors, which is opposite to the regiochemistry of the same or similar Ti counterparts.[11] The preference for 2,1-insertion decreases in the order of Ti > Zr > Hf. Since the currently proposed mechanisms for syndioselective polymerization and living polymerization displayed by bis(phenoxy-imine) Ti complexes are based on the non-bonding interaction between the ligand and a growing polymer chain, the loss of stereoselectivity as well as living characteristics of Zr and Hf complexes/MAO systems may be attributed to the difference in regiochemistry which can impair the non-bonding interaction due to a different configuration of the growing polymer chain.

Experimentals

General Procedures and Materials

All manipulations of air/moisture-sensitive compounds were performed under a dry nitrogen atmosphere using standard Schlenk techniques. Toluene (Wako Pure Chemical Industries, Ltd.) was dried over Al_2O_3. Propylene was obtained from Mitsui Chemicals, Inc. and used without further purification. Methylalumoxane (MAO) was purchased from Albemarle as a 1.2 M toluene solution, and the remaining trimethylaluminum was removed *in vacuo* prior to use.

Polymerization procedures

A representative propylene polymerization experiment was conducted as follows: To a 500 mL glass reactor equipped with a mechanical stirrer and a temperature probe, toluene (250 mL) was introduced with stirring (600 rpm) under nitrogen atmosphere. The toluene was kept at 25 °C and then the propylene gas feed (100 L/h) was initiated. After 10 min, a prescribed amount of MAO and then a complex were added as a toluene solution into the reactor to start polymerization. The polymerization was quenched after a prescribed time by adding isobutyl alcohol (10 mL). The resulting mixture was washed with water (500 mL × 2), and volatiles were removed at 100 mmHg at 40 °C and dried overnight in a vacuum oven at 40 °C.

Polymer Analyses

Molecular weights (M_n) and molecular weight distribution (M_w/M_n) values of polypropylenes were determined using a Waters Alliance GPC-2000 gel permeation chromatograph equipped with three TSKgel columns (two sets of TSKgelGMH6HT and TSKgelGMH6-HTL) at 140 °C using polystyrene calibration. ^{13}C NMR spectra of polypropylenes were recorded on a JEOL ECP500 spectrometer (125 MHz) using 1,1,2,2-tetrachloroethane-d_2 as a solvent at 100 °C with reverse gated decoupling mode.

References and Notes

(1) Coates, G. W. *Chem. Rev.* **2000**, *100*, 1223–1252.

(2) Resconi, L.; Cavallo, L.; Fait, A.; Piemontesi, F. *Chem. Rev.* **2001**, *101*, 1253–1346.

(3) Gibson, V. C.; Spitzmesser, S. K. *Chem. Rev.* **2003**, *103*, 283–316.

(4) For example, Busico, V.; Cipullo, R. *Prog. Polym. Sci.* **2001**, *26*, 443 and references therein.

(5) Saito, J.; Mitani, M.; Matsui, S.; Kashiwa, N.; Fujita, T. *Macromol. Rapid Commun.* **2000**, *21*, 1333–1336.

(6) Saito, J.; Onda, M.; Matsui, S.; Mitani, M.; Furuyama, R.; Tanaka, H.; Fujita, T. *Macromol. Rapid Commun.* **2002**, *23*, 1118–1123.

(7) Furuyama, R.; Saito, J.; Ishii, S.; Mitani, M.; Matsui, S.; Tohi, Y.; Makio, H.; Matsukawa, N.; Tanaka, H.; Fujita, T. *J. Mol. Catal. A* **2003**, *200*, 31–42.

(8) Tian, J.; Coates, G. W. *Angew. Chem., Int. Ed.* **2000**, *39*, 3626–3629.

(9) Mitani, M.; Furuyama, R.; Mohri, J.; Saito, J.; Ishii, S.; Terao, H.; Nakano, T.; Tanaka, H.; Fujita, T. *J. Am. Chem. Soc.* **2003**, *125*, 4293–4305.

(10) Tian, J.; Hustad, P. D.; Coates, G. W. *J. Am. Chem. Soc.* **2001**, *123*, 5134–5135.

(11) See General Introduction of this thesis.

(12) See Chapter 3 of this thesis and references therein.

(13) Ishii, S.; Furuyama, R.; Matsukawa, N.; Saito, J.; Mitani, M.; Tanaka, H.; Fujita, T. *Macromol. Rapid Commun.* **2003**, *24*, 452–456.

(14) See Part I of this thesis and references therein.

(15) Matsui, S.; Mitani, M.; Saito, J.; Tohi, Y.; Makio, H.; Matsukawa, N.; Takagi, Y.; Tsuru, K.; Nitabaru, M.; Nakano, T.; Tanaka, H.; Kashiwa, N.; Fujita, T. *J. Am. Chem. Soc.* **2001**, *123*, 6847–6856.

(16) The M_w/M_n values may be decreased from the real values by loss of some volatile low molecular weight materials during isolation of the oligomers.

(17) Saito, J.; Mitani, M.; Onda, M.; Mohri, J.-I.; Ishii, S.- I.; Yoshida, Y.; Nakano, T.; Tanaka, H.; Matsugi, T.; Kojoh, S.-I.; Kashiwa, N.; Fujita, T. *Macromol. Rapid Commun.* **2001**, *22*, 1072–1075.

Chapter 5. Substrate selective polymerization using zirconium FI catalysts

Abstract

An FI catalyst can discern ethylene from a mixture of ethylene and propylene with more than 99 % selectivity. DFT calculations have revealed a spatially confined reaction site in the transition states of the migratory insertion which is just the right size for an ethylene molecule but too small for a propylene one. The substituents adjacent to the phenoxy-oxygens are of crucial importance in developing the size/shape-selectivity.

Introduction

Improvements in transition metal catalyzed olefin polymerization performance can roughly be attributed to selectively increased or suppressed rates of specific elementary reaction(s), i.e., initiation, propagation, chain transfers, and irreversible terminations. Due to the inherent characteristics of polymerization reactions, where any errors tend to leave significant and sometimes fatal consequences in the polymer products, any selectivity involved in these elementary reactions needs to be extremely high for the synthesis of macromolecules with desired structures, while such errors will simply reduce the yield for the synthesis of small molecules. For example, ultra-high molecular weight polyethylene having molecular weights in the millions can be prepared with high efficiency, which means that the propagation reaction is about 99.999 % selective relative to any possible side reactions that can interrupt its chain growth. In another example, stereospecific propagation of α-olefins achieves ~99.9 % enantioselectivity to give either isotactic or syndiotactic polypropylene with extremely high melting temperatures (T_m), which are readily degraded with only the slightest microstructural errors.

However, in the field of olefin copolymerization catalysis, the selectivity among the monomers has not been considered important, or rather the research efforts have been directed toward widening the scope of comonomer variety and increasing comonomer uptake (which of course have yielded an incredibly rich variety of polyolefin products) and toward a less selective direction. This trend has been accelerated by the advent of well-defined single-site catalysts,[1] because they surpass, based on the rational understanding of polymerization mechanisms and molecular design, the limited performance attainable with the classical heterogeneous Ziegler-Natta catalysts regarding comonomer incorporation. Thus, olefin copolymerizations have rarely been perceived as a selective catalysis and have not been directed toward the other end of the spectrum, that is, a substrate selective catalysis to enchain a particular monomer from among a mixture of more than two monomers. Such selectivity among small molecules has been known to exist in catalysis by zeolites, in which the molecules are discerned by uniform pore size and topologies.[2] To the best of our knowledge, in transition metal catalyzed olefin polymerizations or any transition metal catalyzed organic reactions, there are few examples that exhibit a high selectivity based on the size or shape of the substrates in a similar way that zeolites or related catalysts do for simple alkanes or alkenes,[3,4] which have no directing functional groups to aid the selective reactions through complementary non-covalent interactions as seen in enzymatic catalysis.

Our continuing research into bis(phenoxy–imine) group 4 transition metal catalysts (FI catalysts) has revealed that the appropriate choice and design of phenoxy–imine ligands, metal, cocatalysts, and polymerization conditions make FI catalysts very selective in almost all aspects of polymerization and polymer structures. FI catalysts are 1) extraordinarily active for ethylene polymerization (TOF 64,900 s^{-1} atm^{-1}),[5,6] and 2) very selective about chain propagation to yield UHMWPE,[5,6] ultra-high molecular weight ethylene/α-olefin copolymers (> 10,000,000 Da)[5,6] and atactic polypropylenes (8,300,000 Da),[7] and also various living olefin polymers, which represent ultimate selectivity in propagation over any termination

reactions that do not exist.[8,9] FI catalysts can be 3) highly iso- and syndiospecific for both propylene[9,10] and styrene[11] polymerizations, and 4) can be selective in chain end structures to produce exclusively vinyl-[12] or R_2Al-terminated[13] olefin polymers (R: alkyl).

Here we would like to report on another unique selectivity pertaining to FI catalysts, namely, the substrate-selectivity in ethylene/propylene copolymerizations. FI complexes **63**, **64**, **21**, and **65** were examined in comparison with a typical metallocene and a linked Cp–amido complex (constrained geometry catalyst, CGC). In ethylene/propylene copolymerization with **65**/DMAO, only ethylene is enchained into polymers out of ethylene/propylene mixtures at > 99 % selectivity with high efficiency.

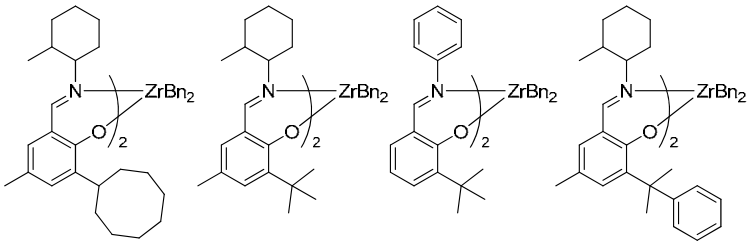

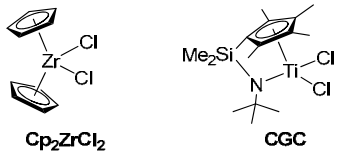

Cp_2ZrCl_2 **CGC**

Results and Discussion

The selectivity between ethylene and propylene in copolymerizations can be quantitatively estimated by monomer reactivity ratios (MRR). In this study, we assume the first-order Markov chain, where the reactivity of the propagating species depends on the last-inserted monomer unit (terminal model).[14] On this assumption, there are four propagating reactions as shown in **Scheme 1**, and the MRR (r_1, r_2) are defined as the ratios of the propagation rate constants, $r_1 = k_{11}/k_{12}$, $r_2 = k_{22}/k_{21}$ (M_1: ethylene; M_2: propylene).

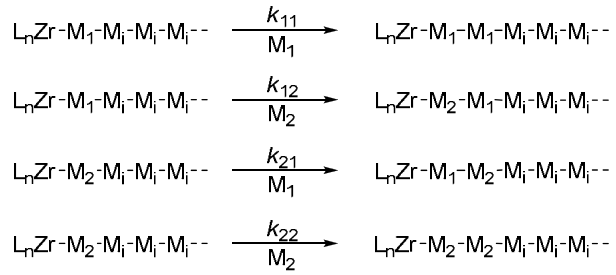

Scheme 1. Propagation reactions in the first order Markov chain (L: ancillary ligand; i = 1 or 2).

A prototypical metallocene, Cp_2ZrCl_2, and a constrained geometry catalyst, $Me_2Si(Me_4C_5)(N^tBu)TiCl_2$ (CGC), were examined in ethylene/propylene copolymerization as a benchmark. Comonomer uptake of Cp_2ZrCl_2 is modest or relatively low, while CGC is known as one of the most efficient catalysts for

incorporating higher α-olefins in ethylene/α-olefin copolymerization.[15] The MRR were evaluated using the Fineman-Ross method, and the conversions of propylene were kept below 10 % for almost all runs to minimize the change from the initial monomer compositions (See Experimentals). However, comonomer incorporation ability of the CGC was so high that the monomer conversions easily exceeded this limit. Therefore, the MRR for the CGC could not be accurately evaluated under the conditions examined. Nevertheless, the monomer compositions in feed and in the copolymer are very close to each other (**Table 1**), which suggests an even smaller r_1 value than the r_1 (= 4) estimated previously for ethylene/1-octene copolymerization using the same complex.[15] The r_1 of Cp_2ZrCl_2 was estimated at 13; meaning that the ethylene last-inserted species ($Cp_2Zr–CH_2CH_2–$polymer) is 13 times more reactive toward ethylene relative to propylene.

Table 1. Monomer reactivity ratios in ethylene/propylene copolymerizations[a]

Catalyst	Propylene in feed (mol%)[b]	Propylene conversion (%)	Propylene in polymer (mol%)[c]	r_1
Cp_2ZrCl_2	32.25	11.4	2.87	13
Cp_2ZrCl_2	58.84	6.1	4.63	
CGC[d]	36.69	16.6	31.77	–
63	32.25	8.6	2.39	
63	58.84	3.1	3.52	16
63	72.70	8.3	5.12	
64	58.84	7.7	1.79	
64	72.70	2.0	2.48	69
64	85.40	3.3	5.23	
21	58.84	7.6	2.59	
21	72.70	6.0	3.84	45
21	85.40	3.9	5.12	
65	58.84	0.42	0.88	
65	72.70	3.2	1.95	152
65	85.40	6.2	3.02	

[a]General conditions: 5.0 mL of hexane, Al(DMAO)/Zr = 300, 100 ºC, 10 min, 7.0 atm gauge pressure maintained by continuous ethylene supply. [b]Calculated initial monomer composition. [c]Determined either by IR or ^{13}C NMR. [d]5.0 mL of toluene, $^{i}Bu_3Al/Ph_3CB(C_6F_5)_4$/CGC = 300/2/1, 100 ºC, 5 min, 7.0 atm gauge pressure maintained by ethylene supply.

FI catalysts **64** ,**21**, **65** are substantially more ethylene-selective than Cp_2ZrCl_2 or CGC. In particular, FI catalyst **65** that has cumyl groups adjacent to the phenoxy-oxygen (R^2 substituents), exhibited more than 150 times higher reactivity toward ethylene than propylene, i.e., a remarkable selectivity of > 99 %, despite the difference of only one carbon in the substrates. On the other hand, the fact that **63** (R^2 = cyclooctyl group) showed the lowest selectivity demonstrates that the R^2 plays a vital role in determining the selectivity of ethylene monomers from a mixture of ethylene and propylene and that the steric bulk of R^2 near the α-carbon (to the phenoxy ring) is more important rather than the bulk of the entire R^2.

The r_1 values of **64** and **21** (R^2 = ^{t}Bu), which are similar to each other and in between those of **63** and

65, indicate that the substituents on the imine-nitrogen (R^1 substituents) have a smaller effect on monomer selectivity,[16] although considerable differences in polymer molecular weights are observed for these catalysts (See Experimentals), showing that polymer molecular weight and the substrate selectivity are determined independently as previously suggested.[5] These observations are qualitatively consistent with an assumed octahedral *cis*-N, *trans*-O, *cis*-X (the reaction site) configuration of these FI catalysts, where the R^2 is located above and below the reaction site, while the R^1 is positioned at the slightly skewed backside of the reaction site, and thus does not directly interact with a coordinating monomer.

The DFT calculations further reinforce the argument described above. **Figure 1** compares the computed transition state structures for the migratory insertions of ethylene and propylene to the alkyl propagating species derived from **63** and **65**, where the alkyl chain is represented by an *n*-propyl group, (hereafter, TS(**63**, E) and TS(**63**, P) denote the transition states of ethylene and propylene insertion to the cationic propyl derivative of **63**, respectively). The bond lengths and geometry of the four-membered metallacycles are very similar to each other for these complexes (See Experimentals). However, the environments around these metallacycles are significantly different due to the R^2 that is situated close to the reaction site. The cyclooctyl groups of **63** can ease steric tension by directing the smallest hydrogen on the α-carbon (to the phenoxy ring) toward the metallacycles (**Figure 1a,b**). Considering that the van der Waals radius of hydrogen is 1.20 Å, TS(**63** , E) and TS(**63** , P) have no significant constraint between R^2 substituents and the reaction site. On the other hand, one of the methyl groups in the cumyl group of **65** needs to protrude into the reaction sphere, and besides, the conformation of the cumyl group is much more rigid than the cyclooctyl group because of the high rotational barrier around the two C(quaternary)–C(ipso carbons in phenyl and phenoxy groups) bonds. This geometry and rigidity of the cumyl group considerably confine the space around the reaction site as can be clearly seen in the shortest distances between R^2 and the reaction site (**Figure 1c,d**). The structure of TS(**65**, E) demonstrates that even the ethylene molecule seems to be close-fitting in the confined space formed by the cumyl groups. With regard to TS(**65**, P), the spatial constraints between the cumyl groups and the transition state metallacycle seem to be critically large, apparently verified by the very short H–H distances (**Figure 1d**). From the calculated rate constants (k_{11}, k_{12}), the r_1 values were estimated at 125.5 and 57.5 for **65** and **63**, respectively, and are in appreciably good agreement with the experiments.

Kretschmer, Kempe and their coworkers reported a similar ethylene selective polymerization using zirconium complexes bearing aminopyridinato ligands.[3] Under the given conditions in their report, the selectivity seems to roughly correspond to the level of **64** (propylene mole fraction in the reaction media: 43.5 %; propylene content in polymer: < 1 mol%) at 80 °C (vs. 100 °C for our experiments), which implies that the ethylene selectivity of **65** will exceed that of their catalysts under comparable conditions. In addition, despite the significant steric difference in their ligands, the ethylene selectivity did not vary for their two complexes, from which they concluded that this selectivity is electronic in nature. This is in sharp contrast to the FI catalysts that exhibit a clear structure–selectivity relationship where the origin of the selectivity is

primarily steric in nature and thus tunable.

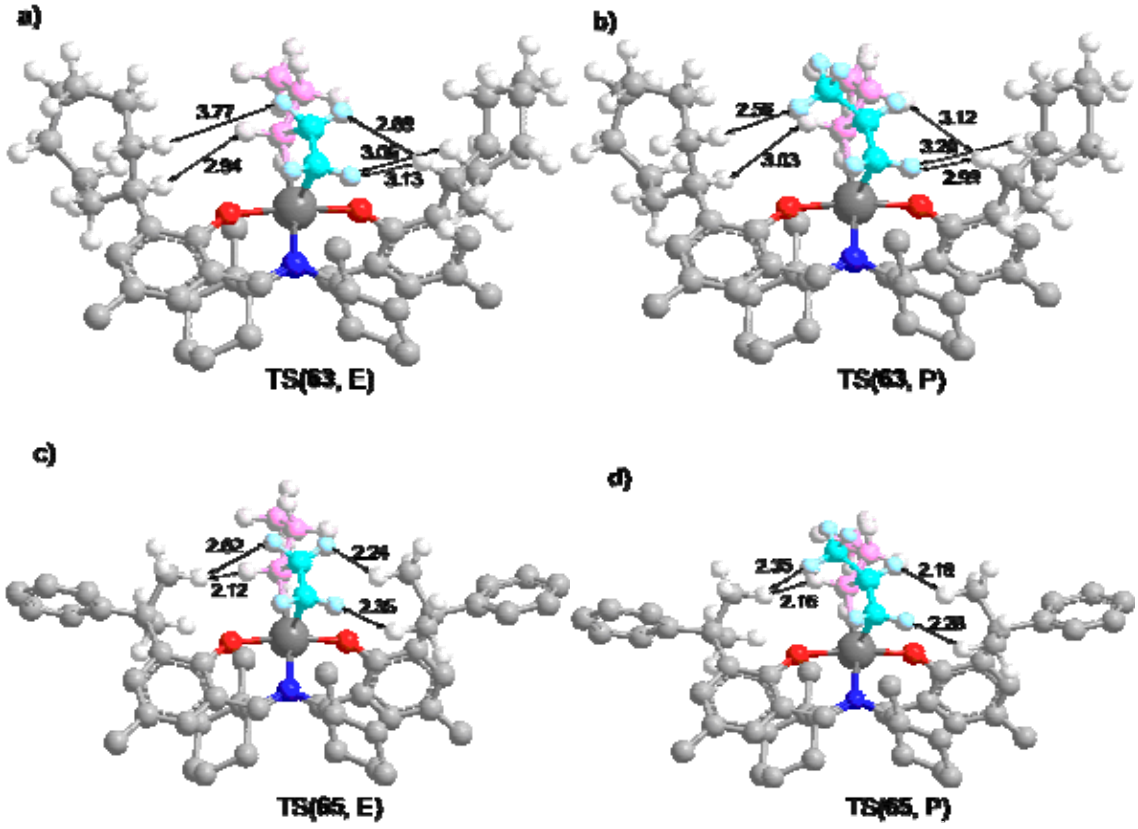

Figure 1. Calculated transition states of olefin insertion into Zr–propyl species of FI catalysts: a) TS(**63**, E); b) TS(**63**, P); c) TS(**65**, E); d) TS(**65**, P). The important distances are given in Å. The atoms highlighted in red and blue are oxygens and nitrogens, and the light blue and pink represent inserting monomers and propyl chains, respectively. Some hydrogen atoms are omitted for clarity.

This remarkably high ethylene-selectivity of the FI catalysts has resulted in applications that have not been possible using catalysts with ordinary selectivity. One of the consequences of the unique ethylene-selectivity is that FI catalysts can produce a completely linear polyethylene free from any short or long chain branches. Commercially available high density polyethylenes (HDPE) have methyl branches (0.2–0.6Me/1000C) or longer branches that are not derived from α-olefin comonomers,[17] but presumably from chain-end isomerization (**Scheme 2a**) or reinsertion of *in situ* generated vinyl macromers (**Scheme 2b**). For example, a heterogeneous Ziegler catalyst yielded polyethylene with 0.3 and 0.6 methyl branches per 1000 carbons in ethylene homopolymerizations, while polyethylenes prepared by complex **64** under comparable conditions are truly linear and have virtually no branches (under detection limit, < 0.1 branch/1000C).[17] Since the highly ethylene-selective FI catalysts possess such a confined reaction site, the isomerization, which will generate a sterically demanding secondary α-carbon or the reinsertion of large macromers, is virtually impossible. The defect free, completely linear polyethylene is expected to show higher crystallinity, stronger intermolecular forces, and thus greater tensile strength. These features are most suitable for UHMWPE having > 10^6 molecular weights, whose applications range from lithium ion

battery separators to bulletproof vests. In fact, complex **65** produces such UHMWPE under industrially relevant conditions (**Table 2**).

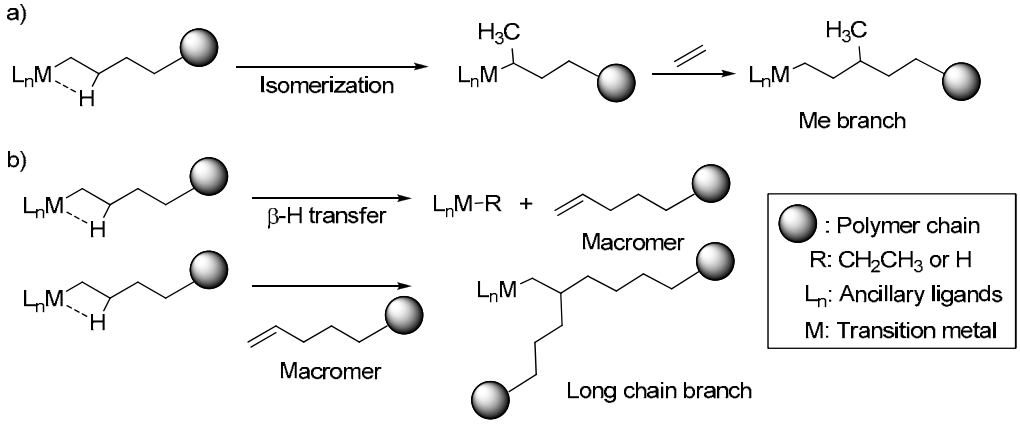

Scheme 2. Probable pathways for the formation of a) methyl, and b) long chain branches

Table 2. Ethylene homopolymerization with **65**/DMAO[a]

T_p (°C)	Efficiency (kg-PE/mmol-Zr h)	$M_v/10^{6b}$
50	1,014	2.2
75	1,514	2.1
90[c]	1,694	1.7

[a]In 500 mL of heptane, [**65**] = 0.04 μmol/L, [Al(DMAO)] = 2.50 mmol/L, 8 bar ethylene gauge pressure, 15 min. [b]Calculated from the intrinsic-viscosity numbers [η] (dL/g), using the equation, $[\eta] = 6.2 \times 10^{-4} M_v^{0.7}$. [c]Due to tangled polymer in the stirring propeller, mixing was impossible after 5 min.

Scientists at The Dow Chemical Company have recently revealed that the high ethylene-selectivity of FI catalysts can also be applied to make an olefin block copolymer in a continuous process.[18] The process includes two catalysts, one of which is a highly ethylene-selective FI catalyst (closely related to complex **64** in this work) that provides the block copolymers with crystalline segments with low comonomer contents and high melting temperatures (T_m). The hard crystalline segments produced with the FI catalyst form physical cross-linking points connecting the very elastic soft segments, which were simultaneously produced with the other catalyst, generating an infinite network and serving as a thermoplastic elastomer. The strength of the cross-linking points is directly related to the crystallinity of the hard segments, which in turn is attributed to the excellent ethylene-selectivity of the FI catalysts over 1-octene.

Conclusion

We have developed highly ethylene-selective FI catalysts based on the size/shape-recognition in the substrates. An FI catalyst can polymerize only ethylene monomers from mixtures of ethylene and propylene at > 99 % selectivity, the highest selectivity ever reported. Zeolites are known to be highly selective in size and shape of substrates or products in the reactions of small molecules based on the size and topology of

uniform pores. Similarly, the molecular size/shape-selectivity of FI catalysts stems from the confined reaction site consisting of the metal center and the appropriate substituents on the phenoxy-imine ligands, which is just right for ethylene but too small for propylene, allowing FI catalysts therefore to function as a molecular zeolite. As such, we envisage that the FI ligand framework, which is relatively rigid as an organometallic compound but significantly more flexible than inorganic zeolites, might be applicable for other reactions which require high selectivity at the molecular level.

Experimentals

Materials and methods

All manipulations of air and moisture sensitive compounds were carried out under an atmosphere of N_2 using standard Schlenk techniques or by using a nitrogen-filled glove box with a high capacity circulator (< 1 ppm O_2). Toluene and hexane were dried by passing through a column filled with commercially available Q-5 reactant and activated alumina. Ethylene (Sumitomo Seika Co.) and propylene (Mitsui Chemicals, Inc.) were used without further purification. Methylalumoxane (MAO) was purchased from Albemarle as a 1.2 M toluene solution, and the remaining trimethylaluminum was removed *in vacuo* prior to use (DMAO). The CGC was prepared following the published procedures,[19] and Cp_2ZrCl_2, $^iBu_3Al$, $Zr(CH_2Ph)_4$, and $Ph_3CB(C_6F_5)_4$ were obtained from Wako Pure Chemical Industries, Ltd., Tosoh Finechem Corp., MCAT GmbH, and Asahi Glass Co., respectively, and used without further purification.

Ligand synthesis

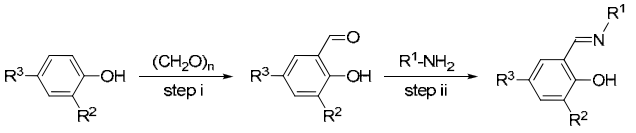

63L, R^1 = 2-Me-cyclohexyl, R^2 = cyclooctyl, R^3 = Me
64L, R^1 = 2-Me-cyclohexyl, R^2 = *t*Bu, R^3 = Me
21L, R^1 = Ph, R^2 = *t*Bu, R^3 = H
65L, R^1 = 2-Me-cyclohexyl, R^2 = cumyl, R^3 = Me

*1) Ligands **64L, 65L***

Synthesis of the respective salicylaldehydes for **64L** and **65L** have been described elsewhere.[20] Subsequent condensation of the salicylaldehydes with 2-methylcyclohexylamine (purchased from Tokyo Chemical Industry Co., Ltd. *cis/trans* = 30/70) were carried out in ethanol and **64L** and **65L** were obtained as yellow crystalline compounds by recrystallization from ethanol in 66 % and 98 % yields (step ii), respectively.

64L: ^{1}H NMR ($CDCl_3$) : δ13.94 (s, 1H, minor OH), 13.91 (s, 1H, major OH), 8.27 (s, 1H, minor CH=N), 8.24 (s, 1H, major CH=N), 7.09 (d, 1H, *J* = 1.9 Hz, aromatic-H), 6.90 (d, *J* = 1.9 Hz, minor aromatic-H), 6.88 (d, *J* = 1.9 Hz, major aromatic-H), 3.24–3.31 (multi, minor CH-N), 2.66 (dt, 1H, *J* = 4.0 Hz, *J* = 10.2 Hz, major N=CH), 2.26 (s, 3H, aromatic-Me), 0.93–1.87 (multi, 9H, cyclohexyl-H), 1.41 (s, 9H, ^{t}Bu), 0.80 (d, 3H, *J* = 6.9 Hz, major cyclohexyl-Me) 0.79 (d, 3H, *J* = 6.9 Hz, minor cyclohexyl-Me). FD-MS: 287 (M).

65L: ^{1}H NMR ($CDCl_3$) : δ13.33 (broad s, 1H, OH), 8.22 (s, minor CH=N), 8.19 (s, major CH=N) 7.04–7.28 (multi, 6H, aromatic-H), 6.90–6.97 (multi, 1H, aromatic-H), 3.15–3.26 (multi, minor CH–N), 2.58 (dt, 1H, *J* = 10.2 Hz, *J* = 4.3 Hz, major N=CH), 2.32 (s, major aromatic-Me), 2.31 (s, major aromatic-Me), 1.70–1.77 (multi, 6H, Ph–CMe_2), 0.83–1.77 (multi, 9H, cyclohexyl-H), 0.71 (d, *J* = 6.9 Hz, minor cyclohexyl-Me), 0.70 (d, *J* = 6.9 Hz, major cyclohexyl-Me). FD-MS: 349 (M).

*2) Ligand **63L***

2-cyclooctyl-4-methylphenol

The corresponding phenol for **63L** was prepared from *p*-cresol and cyclooctene in CH_2Cl_2 in the presence of concd H_2SO_4. After flush column purification using silica gel, 2-cyclooctyl-4-methylphenol was obtained as a yellow viscous liquid in 11 % yield. ^{1}H NMR ($CDCl_3$) : δ 6.96 (d, 1H, *J* = 2.0 Hz, aromatic-H), 6.79–6.85 (multi, 1H, aromatic-H), 6.64 (d, 1H, *J* = 8.2 Hz, aromatic-H), 4.45 (s, 1H, OH), 2.92–3.07 (multi, 1H, CH–Ph), 2.26 (s, 3H, aromatic-Me), 1.52–1.86 (mutli, 14H, cyclooctyl-H).

3-cyclooctyl-2-hydroxy-5-methylbenzaldehyde

A formylation reaction of the phenol was carried out using a standard technique described in the published work[20] and 3-cyclooctyl-2-hydroxy-5-methylbenzaldehyde was obtained in 78 % yield. ^{1}H NMR ($CDCl_3$) : δ11.16 (s, 1H, OH), 9.80 (s, 1H, CH=O), 7.23 (d, 1H, *J* = 2.0 Hz, aromatic-H), 7.12 (d, 1H, *J* = 2.0 Hz, aromatic-H), 3.12–3.30 (broad s, 1H, CH–Ph), 2.30 (s, 3H, aromatic-Me), 1.50–1.85 (multi, 14H, cyclooctyl-H).

*2-cyclooctyl-4-methyl-6-((2-methylcyclohexylimino)methyl)phenol (**63L**)*

The salicylaldehyde was condensed with 2-methylcyclohexylamine (purchased from Tokyo Chemical Industry Co., Ltd. *cis/trans* = 30/70) to afford **63L** in 90 % yield. ^{1}H NMR ($CDCl_3$) : δ 13.71 (broad s, 1H, OH), 8.26 (s, major CH=N), 8.24 (s, minor CH=N), 7.00–7.07 (multi, 1H, Aromatic-H), 6.83–6.90 (multi, 1H, aromatic-H), 3.19-3.37 (multi, 1H, CH–Ph), 2.67 (dt, major CH–N), 2.27 (s, 3H, aromatic-Me), 0.89–1.98 (multi, 23H, cyclooctyl-H, cyclohexyl-H), 0.81 (d, 3H, *J* = 6.6 Hz, major cyclohexyl-Me), 0.79 (d, 3H, *J* = 6.6 Hz , minor cyclohecyl-Me). FD-MS: 341 (M).

Ethylene/propylene copolymerization

Copolymerizations were carried out in a parallel, multi-reactor (Endeavor Catalyst Screening System®, Biotage AB) equipped with the reagent addition ports and automated system of gas delivery, heating and mixing control, and the entire system was placed in a nitrogen-filled glove box. Into thoroughly dried reactors, hexane (5 mL) was added via a gas-tight syringe through the reagent addition ports and saturated with propylene gas at 25 °C under vigorous stirring. In a separate vessel, a catalyst solution was prepared by mixing an FI ligand and $Zr(CH_2Ph)_4$ in 2 : 1 molar ratio in toluene. Propylene was introduced until the

reactor pressure reached the predetermined value and the reactors were closed. The reactor temperature was raised to 100 °C and ethylene gas was applied so that the total gauge pressure of the reactors was maintained at 7 bar all the time. Through the reagent addition ports, a prescribed amount of DMAO in toluene, and then the catalyst solution were added to initiate the polymerization. After 10 min, the polymerization was quenched by adding isobutyl alcohol. After removal of volatiles, the obtained polymer was dried *in vacuo* at 100 °C for 12 h.

Ethylene homopolymerization to prepare UHMWPE

Ethylene polymerization was carried out in a 1 L stainless steel jacketed autoclave equipped with a thermocouple, a propeller stirrer, a gas inlet, and a reagent addition port. The polymerization conditions and results are compiled in **Table 2**.

Calculation of MRR

The initial monomer compositions under the given conditions were calculated by using Aspen Plus® (Aspen Technology, Inc.) and the copolymer compositions were measured either by IR or ^{13}C NMR (**Table 3**). According to the Fineman-Ross equation (Eq. 1), where F is initial molar ratios of ethylene/propylene in reaction media and f is copolymer compositions (ethylene/propylene) in the obtained polymers, F(f-1)/f was plotted against F^2/f and linear approximation of the plots (mean square correlation coefficient, R^2 = 0.96–0.99) gave the r_1 as a slope of a line and the r_2 as a Y-intercept (**Table 1**, **Figure 2**).

$$F(f-1)/f = F^2r_1/f - r_2 \qquad (1)$$

Since the propylene contents in the copolymers were quite low for all the data points, the r_2 values (relative reactivity toward the propylene-inserted propagating species) can be less accurate.

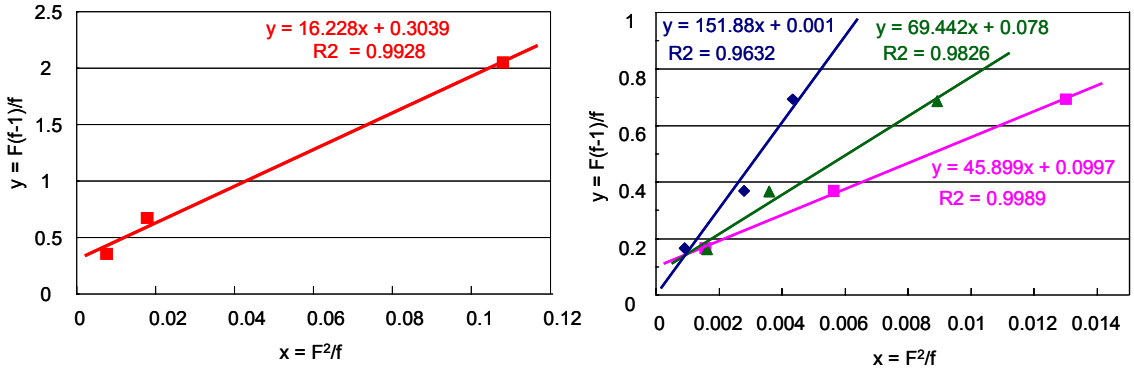

Figure 2. Fineman-Ross plots for the copolymerization of ethylene and propylene with FI catalysts **63**, **64**, **21**, **65**.

Table 3. The results of ethylene/propylene copolymerizations[a]

Catalyst	Propylene in feed (mol%)[b]	Amount of catalyst (μmol)	Activity[c]	$M_n/10^3$[d]	r_1
Cp_2ZrCl_2	32.25	0.20	2.77	nd	13
Cp_2ZrCl_2	58.84	0.20	2.16	nd	
CGC[e]	36.69	0.025	5.14	nd	–
63	32.25	0.20	2.52	7.2	
63	58.84	0.20	1.44	4.6	16
63	72.70	0.30	2.60	6.5	
64	58.84	0.15	9.38	25.2	
64	72.70	0.15	2.52	11.8	69
64	85.40	0.15	2.80	10.5	
21	58.84	0.15	6.40	6.6	
21	72.70	0.15	5.01	5.1	45
21	85.40	0.30	1.70	2.8	
65	58.84	0.10	1.54	111	
65	72.70	0.15	5.11	55.6	152
65	85.40	0.15	9.17	71.5	

[a]General conditions: 5.0 mL of hexane, Al(DMAO)/Zr = 300, 100 °C, 10 min, 7.0 atm gauge pressure maintained by continuous ethylene supply. [b]Calculated initial monomer composition. [c]In kg-polymer/mmol-catalyst h. [d]Determined by GPC (polystyrene calibration). [e]5.0 mL of toluene, ^{i}Bu$_3$Al/Ph$_3$CB(C$_6$F$_5$)$_4$/CGC = 300/2/1, 100 °C, 5 min, 7.0 atm gauge pressure maintained by ethylene supply.

DFT calculations

Geometries and energies of the reactant, intermediates, transition states, and products for complexes **63** and **65** were calculated using Becke's three-parameter hybrid functionals, B3LYP method[21–23] as implemented in the Gaussian 03 programs.[24] The standard valence-double-ζ LANL2DZ basis set[25–27] with the corresponding effective core potential (for Zr atom) was used, and the polarization functions were augmented on the C atoms of the reaction center for all calculations. The transition states were verified by means of the normal-mode analysis.

Table 4. Distances and angles of the four-membered ring in the insertion transition states.

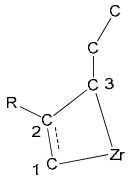

R: H or CH_3

Distances (Å) and angles (°)	TS(**63**, E)	TS(**63**, P)	TS(**65**, E)	TS(**65**, P)
$Zr–C_1$	2.370	2.316	2.373	2.319
$Zr–C_3$	2.362	2.392	2.356	2.393
$C_1–C_2$	1.415	1.438	1.414	1.438
$C_2–C_3$	2.152	2.106	2.165	2.110
O–Zr–O	170.1	169.2	171.1	170.3
N–Zr–N	89.4	88.9	88.1	87.9
C–Zr–C	82.6	81.4	83.0	81.3

Table 5. Comparison of experimental and calculated MRR

Cat	$\Delta E^{‡}_{11}$	$\Delta E^{‡}_{12}$ 1,2-inertion	$\Delta E^{‡}_{12}$ 2,1-inertion	$\Delta E^{‡}_{12} - \Delta E^{‡}_{11}$	k_{11}[a]	k_{12}[a]	r_1 (calc)[b]	r_1 (exp)
63	41.4	54.0	65.4	12.6	1.58E-06	2.75E-08	57.5	16
65	36.1	51.1	62.1	15.0	8.90E-06	7.09E-08	125.5	152

[a] k_{11} and k_{12} are estimated from $exp(-\Delta E^{‡}/RT)$ at 378 K. [b] Since MRR are the ratios of the rate constants, the entropy terms are assumed to be cancelled.

References and Notes

(1) Fujita, T.; Makio, H. in *Comprehensive Organometallic Chemistry III*, Vol. 11 (Eds: Crabtree, R. H.; Mingos, D. M. P., Volume Ed: Hiyama, T.: Elsevier, Amsterdam, 2007, pp 691-734.

(2) As a textbook, Chen, N. Y.; Garwood, W. E.; Dwyer, F. G. *Shape Selective Catalysis in Industrial Applications*, Marcel Dekker Inc., New York, 1989.

(3) Kretschmer, W. P.; Hessen, B.; Noor, A.; Scott, N. M.; Kempe, R. *J. Organomet. Chem.* **2007**, *692*, 4569–4579.

(4) Kinetic resolution of racemic α-olefins was investigated, where the selectivity stems from chirality. Byers, J. A.; Bercaw, J. E. *Proc. Natl. Acad. Sci. U S A.* **2006**, *103*, 15303–15308, and references therein.

(5) Makio, H.; Kashiwa, N.; Fujita, T. *Adv. Synth. Catal.* **2002**, *344*, 477–493.

(6) Makio, H.; Fujita, T. *Acc. Chem. Res.* **2009**, *42*, 1532–1544.

(7) Saito, J.; Onda, M.; Matsui, S.; Mitani, M.; Furuyama, R.; Tanaka, H.; Fujita, T. *Macromol. Rapid Commun.* **2002**, *23*, 1118–1123.

(8) Mitani, M.; Mohri, J.-i.; Yoshida, Y.; Saito, J.; Ishii, S.; Tsuru, K.; Matsui, S.; Furuyama, R.; Nakano, T.; Tanaka, H.; Kojoh, S.-i.; Matsugi, T.; Kashiwa, N.; Fujita, T. *J. Am. Chem. Soc.* **2002**, *124*, 3327–3336.

(9) Mitani, M.; Furuyama, R.; Mohri, J.; Saito, J.; Ishii, S.; Terao, H.; Nakano, T.; Tanaka, H.; Fujita, T. *J. Am. Chem. Soc.* **2003**, *125*, 4293 –4305.

(10) See Chapter 3 of this thesis and references therein.

(11) Michiue, K.; Onda, M.; Tanaka, H.; Makio, H.; Mitani, M.; Fujita, T. *Macromolecules* **2008**, *41*, 6289–6291.

(12) Terao, H.; Ishii, S.; Saito, J.; Matsuura, S.; Mitani, M.; Nagai, N.; Tanaka, H.; Fujita, T. *Macromolecules* **2006**, *39*, 8584–8593.

(13) Saito, J.; Tohi, Y.; Matsukawa, N.; Mitani, M.; Fujita, T. *Macromolecules* **2005**, *38*, 4955–4957.

(14) Odian, G. in *Principles of Polymerization, 4th Edition*, John Wiley & Sons, Inc., Hoboken, 2004, pp. 464-480.

(15) McKnight, A. L.; Waymouth, R. M. *Chem. Rev.* **1998**, *98*, 2587–2598.

(16) It is possible that the bulkier 2-methylcyclohexyl group makes **64** slightly more ethylene-selective than **21**.

(17) Takahashi, M.; Kasai, T.; Otsuzuki, S.; Matsumoto, T.; Tsutsui, T.; Saito, J.; Matsukawa, N. K.; Tsuru, K.; Mitani, M.; Fujita, T. (Mitsui Chemicals, Inc.) WO00/078828, 2000.

(18) Arriola, D. J.; Carnahan, E. M.; Hustad, P. D.; Kuhlman, R. L.; Wenzel, T. T. *Science* **2006**, *312*, 714–719.

(19) McKnight, A. L.; Waymouth, R. M. *Macromolecules* **1999**, *32*, 2816–2825.

(20) Matsui, S.; Mitani, M.; Saito, J.; Tohi, Y.; Makio, H.; Matsukawa, N.; Takagi, Y.; Tsuru, K.; Nitabaru, M.; Nakano, T.; Tanaka, H.; Kashiwa, N.; Fujita, T. *J. Am. Chem. Soc.* **2001**, *123*, 6847–6856.

(21) Becke, A. D. *Phys. Rev. A* **1988**, *38*, 3098–3100.

(22) Lee, C.; Yang, W.; Parr, R. G. *Phys. Rev. B* **1988**, *37*, 785–789.

(23) Becke, A. D. *J. Chem. Phys.* **1993**, *98*, 5648–5652.

(24) Frisch, M. J.; Trucks, G. W.; Schlegel, H. B.; Scuseria, G. E.; Robb, M. A.; Cheeseman, J. R.; Montgomery, Jr., J. A.; Vreven, T.; Kudin, K. N.; Burant, J. C.; Millam, J. M.; Iyengar, S. S.; Tomasi, J.; Barone, V.; Mennucci, B.; Cossi, M.; Scalmani, G.; Rega, N.; Petersson, G. A.; Nakatsuji, H.; Hada, M.; Ehara, M.; Toyota, K.; Fukuda, R.; Hasegawa, J.; Ishida, M.; Nakajima, T.; Honda, Y.; Kitao, O.; Nakai, H.; Klene, M.; Li, X.; Knox, J. E.; Hratchian, H. P.; Cross, J. B.; Adamo, C.; Jaramillo, J.; Gomperts, R.; Stratmann, R. E.; Yazyev, O.; Austin, A. J.; Cammi, R.; Pomelli, C.; Ochterski, J. W.; Ayala, P. Y.;

Morokuma, K.; Voth, G. A.; Salvador, P.; Dannenberg, J. J.; Zakrzewski, V. G.; Dapprich, S.; Daniels, A. D.; Strain, M. C.; Farkas, O.; Malick, D. K.; Rabuck, A. D.; Raghavachari, K.; Foresman, J. B.; Ortiz, J. V.; Cui, Q.; Baboul, A. G.; Clifford, S.; Cioslowski, J.; Stefanov, B. B.; Liu, G.; Liashenko, A.; Piskorz, P.; Komaromi, I.; Martin, R. L.; Fox, D. J.; Keith, T.; Al-Laham, M. A.; Peng, C. Y.; Nanayakkara, A.; Challacombe, M.; Gill, P. M. W.; Johnson, B.; Chen, W.; Wong, M. W.; Gonzalez, C.; and Pople, J. A. Gaussian 03, Revision C.02, Gaussian: Wallingford CT, 2004.

(25) Hay, P. J.; Wadt, W. R. *J. Chem. Phys.* **1985**, *82*, 270–283.

(26) Wadt, W. R.; Hay, P. J. *J. Chem. Phys.* **1985**, *82*, 284–298.

(27) Hay, P. J.; Wadt, W. R. J. Chem. Phys. **1985**, *82*, 299–310.

Part III. Synthesis of Chain-End Functionalized Polyolefins

Chapter 6. Chain-end functionalized polyolefins using a living titanium FI catalyst

Abstract

Polyethylenes and highly syndiotactic polypropylenes possessing chain-end hydroxyl groups were synthesized by living polymerizations using $(L^{FI})_2TiCl_2$ (**31**, L^{FI}: C_6F_5N=CH(2-O-C_6H_3-3-^{t}Bu)) in conjunction with MAO and ω-functionalized α-olefins, H_2C=$CH(CH_2)_n$–Y (**66**; Y = $OAlMe_2$, *n* = 4 (**66a**); Y = $OSiMe_3$, *n* = 9 (**66b**)). Because the primary insertion of **66** to a cationic species $(L^{FI})_2Ti^+$-Me (**31a**) derived from **31**/MAO is much faster than the successive secondary insertion of **66**, addition of an equimolar amount of **66** to **31a** resulted in the quantitative formation of $(L^{FI})_2Ti^+$–CH_2–CH(Me)–$(CH_2)_n$–Y (**67**; Y = $OAlMe_2$, *n* = 4 (**67a**); Y = $OSiMe_3$, *n* = 9 (**67b**)). These cationic species **67** served as functionalized initiators for the living polymerization of both ethylene and propylene and afforded polyolefins having extremely narrow molecular weight distributions and a hydroxyl group at the initiating chain end. The terminating chain end of the syndiotactic polypropylenes was also functionalized by adding an excess amount of **66b** as a chain-end capping agent to the living L_2Ti–polymeryl species. Due to much slower insertion of the second molecule of **66b** relative to the first one, the obtained polymers were end capped quantitatively by a single molecule of **66b**. Telechelic syndiotactic polypropylenes were successfully synthesized through a living polymerization initiated by **67b** and an end capping using **66b**.

Introduction

Chain-end functionalized polymers including telechelic polymers display unique material properties, and in addition, they can be used as precursors for a variety of polymeric materials. Telechelic polymers are macromolecules possessing two well-defined reactive functional groups situated at the chain termini and serve as versatile building blocks to afford higher molecular weight block polymers and polymer networks with well-defined multiple block sequences and topologies.[1] One of the most convenient approaches to telechelic polymers is a living polymerization using a functional initiator and a chain capping functional reagent. There are plenty of examples of the synthesis of telechelic polymers in many well-established and well-behaved living polymerization systems, including anionic,[2,3] cationic[4] and radical[5–7] polymerizations. However, examples of the synthesis of telechelic polymers from simple olefins such as ethylene and propylene are rather limited, and include non-living methods (thermal[8–10] or metathesis[11] chain scissions of high molecular weight polymers and bifunctional chain transfer agents[12]) and living polymerization methods with α-diimine Pd catalysts developed by Brookhart and coworkers,[13] and with a bifunctional vanadium initiator by Murata et al.[14] The lack of examples is mostly attributed to lack of a well-behaved living olefin polymerization catalyst and to general incompatibility of transition metal catalysts and polar functional groups.

As mentioned in the General Introduction, we have developed a series of titanium complexes bearing two phenoxy-imine ligands (Ti-FI catalysts) that exhibit an extremely robust living nature for the polymerization of both ethylene and propylene.[15–17] The author revealed in Part I of this thesis that the living Ti-FI catalysts generated a well-defined living monomethyl cationic species and in Chapter 5 of this thesis that R^2 substituents was a key to determine substrate selectivity. Moreover, a recent study demonstrated the generally enhanced functional tolerance of the Ti-FI catalysts relative to other olefin polymerization catalysts based on early metals.[18] To further prove the value of the (living) FI catalysts and to broaden the scope of their applications based on rational understanding of structures and reactivity of the active species, we herein describe the synthesis of chain-end functionalized polyolefins, including telechelic polyolefins, by means of living polymerizations mediated by $(L^{FI})_2TiCl_2$ (**31**, L^{FI}: C_6F_5N=CH(2-O-C_6H_3-3-^{t}Bu)) activated with methylalumoxane (MAO).

Results and Discussion

Functional Initiators

The introduction of a reactive functional group at an initiating chain end of a polymer is achieved by use of a functional initiator which bears desired functional groups at its incipient polymer chain-end group. Although we recently reported on the successful synthesis of mono and dimethyl derivatives of precatalyst **31**,[19] preparation of dialkyl complexes that have functional groups on their alkyl groups is one of the most difficult synthetic challenges. Therefore, we implemented the *in situ* generation of functional initiators using functionalized α-olefin compounds of the type, H_2C=CH$(CH_2)_n$-Y (**66**; Y = $OAlMe_2$, n = 4 (**66a**); $OSiMe_3$, n =

9 (**66b**)). A cationic monomethyl species, $(L^{FI})_2Ti^+$–Me, (**31a**) was spectroscopically identified as the initiating species in olefin polymerizations by precatalyst **31** activated with MAO,[20] which was confirmed in a well defined manner by the reaction of the dimethyl complex, $(L^{FI})_2TiMe_2$, and the boron cocatalysts, $B(C_6F_5)_3$ or $Ph_3C^+B(C_6F_5)_4^-$.[19] Regiochemistry of the first propylene insertion to $(L^{FI})_2Ti^+$–Me (**31a**) was also determined to be almost exclusively of a primary fashion.[21–23] As depicted in **Scheme 1**, a one-to-one reaction of **66** and **31a** may lead to $(L^{FI})_2Ti^+$–CH_2-CH(Me)-$(CH_2)_n$-Y (**67**: Y = $OAlMe_2$, *n* = 4 (**67a**); $OSiMe_3$, *n* = 9 (**67b**)), which can serve as functional initiators. For the quantitative formation of **67** from an equimolar mixture of **66** and **31a** without generating multiple insertion products (**67'**), the insertion of **66** to **31a** needs to be much faster than the insertion of **66** to **67** (**Scheme 1**, $k_1 > k_2$). Fortunately, this is generally true for this particular catalyst because species **31a** has excellent living polymerization characteristics and can form polyolefins with extremely narrow molecular weight distributions (M_w/M_n < 1.2), which means k_i (rate of first monomer insertion) >> k_p (rate of second monomer insertion ≈ propagation rate). In addition, the polymerization rate with this catalyst is sensitive to the steric bulk of monomers. For example, the polymerization rate of propylene is slower than that of ethylene by a factor of $1/10^4$. Multiple insertions of bulkier α-olefins will probably be even more decelerated or practically impossible.[24]

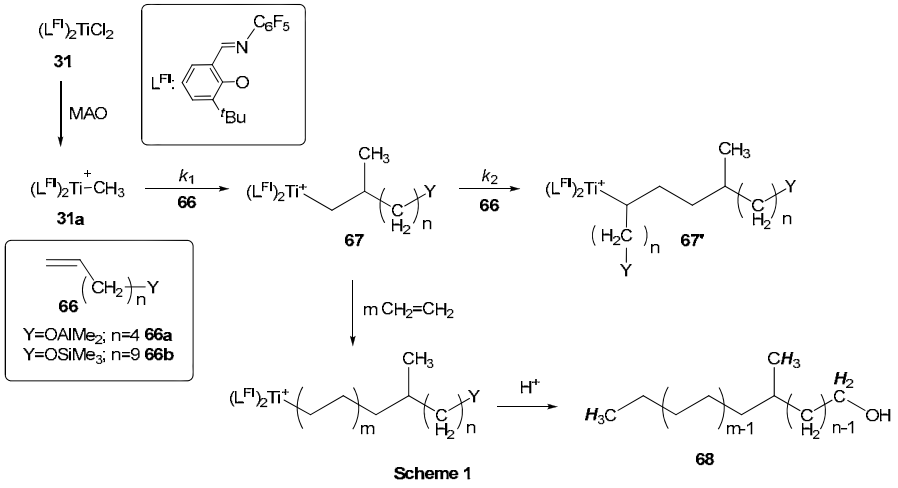

Scheme 1

Ethylene polymerization using a functional initiator was first examined because chain-end structures of polyethylene are simpler and easier to be characterized than those of polypropylene. The reaction of **66a** and **31**/MAO (**66a**: 0.135 mmol; **31**: 0.101 mmol; Al/Ti: 150, see Experimentals) followed by ethylene polymerization (0 °C × 5 min; ethylene: 5 L/h; N_2: 50 L/h) yielded 0.2655 g of polymer (**Table 1**, Run 1). The ^{1}H NMR spectrum of the polymer exhibits two characteristic signals related to chain-end structures (**Figure 1A**). The triplet at 3.64 ppm (*J* = 6.6 Hz) is easily assigned to the methylene group adjacent to the OH group and the signals around 0.90 ppm are two overlapped methyl groups at the initiating (CH–C*H*$_3$) and terminating (CH_2–C*H*$_3$) chain-end groups (See the inset of **Figure 1**). These three signals appeared in ^{13}C NMR at 63.3, 20.0, 14.2 ppm respectively, in addition to all other signals (37.5, 37.3, 33.7, 33.3, 32.2, 30.5,

30.0, 29.6, 27.4, 23.7, 22.9 ppm, the chemical shift of consecutive –CH_2– groups was set at 30.0 ppm as a reference) and are attributed to the structure in **Figure 1A**. Other possible structures derived from e.g., multiple insertion of **66a** at the initiating chain end or incorporation of **66a** in the middle of the main chain via copolymerization were below the detection limits. The integral ratio of CH_2OH/CH_3 is 2/6.4 indicating that a 94 % polymer chain has an OH group. The narrow molecular weight distribution clearly shows that the polymer was obtained through a living polymerization (M_w 11,900; M_n 10,400; M_w/M_n 1.14) and the melting temperature of the polymer (133.8 °C) is comparable to the one for high density polyethylene, which also supports the proposal that no significant amount of **66a** was incorporated in the main chain by copolymerization. All these data demonstrate that formation of a functional initiator **67a** is nearly quantitative and this species can initiate a living polymerization of ethylene to form polyethylenes with narrow molecular weight distribution and well-defined chain-end functional groups at only one end (**Scheme 1**, **68**).

Table 1. Syntheses of chain-end functionalized polyolefins via a living polymerization mediated by **31**/MAO[a]

Run	Olefins			Yield	Activity[b]	T_m	GPC			NMR
	Initiation	Propagation	Termination	g		°C	M_w	M_n	M_w/M_n	M_n
1	**66a**	Ethylene	None	0.2655	30.9	133.8	11,900	10,400	1.14	12,300
2	**66a**	Propylene	None	0.3182	2.84	144.8	8,800	8,300	1.06	8,200
3	**66b**	Propylene	None	0.2988	2.88	142.0	9,300	8,700	1.06	7,700
4	None	Propylene	**66b** (5 eq)	0.3406	2.90	142.4	9,000	8,300	1.09	9,700[c]
5	**66b**	Propylene	**66b** (2 eq)	0.3972	2.30	n.d.[d]	10,100	9,400	1.07	6,300[c]
6	**66b**	Propylene	**66b** (5 eq)	0.3165	2.65	143.0	10,300	9,600	1.08	5,200[c]

[a]See Experimentals for polymerization conditions. [b]In g-polymer/mmol-Ti h [c]Due to the signal around 3.7 ppm (Figure 2b), the integration may be less accurate. [d]Not determined.

The functional initiator **67a** was then extended to a polymerization of propylene. The propylene polymerization was carried out at 0 ºC for 105 min, following the *in situ* generation of **67a** (**Table 1**, Run 2; **66a**: 0.076 mmol; **31**: 0.064 mmol; Al/Ti: 150). The obtained polymer possessed a narrow molecular weight distribution (M_w 8,800; M_n 8,300; M_w/M_n 1.06) and high peak melting temperature (144.8 ºC) as expected for this highly syndioselective living propylene polymerization catalyst.[25] The triplet signal identical to the one observed for the chain-end hydroxylated polyethylene appeared at 3.64 ppm in the ^{1}H NMR spectrum, confirming the incorporation of the OH group. However, two additional signals were also observed at 3.89 (multiplet) and 3.46 (singlet) ppm (**Figure 1B**). Interestingly, these two signals did appear even without the addition of **66** and the intensity of the signals increases roughly in inverse proportion to molecular weights of the polymers. These observations imply that these signals are derived from a terminating chain end, into which some unidentified functional groups may be incorporated upon quenching with methanol. Because the formation of **67a** was almost quantitative, it would be safe to assume that all polymer chains have one OH group at the initiating chain end. In fact, the number-average molecular weight calculated from ^{1}H NMR (M_n (NMR) 8,200, assuming every polymer chain has the triplet (2H) at a chain end) is close to the GPC-based number-average molecular weight (M_n (GPC) 8,300).

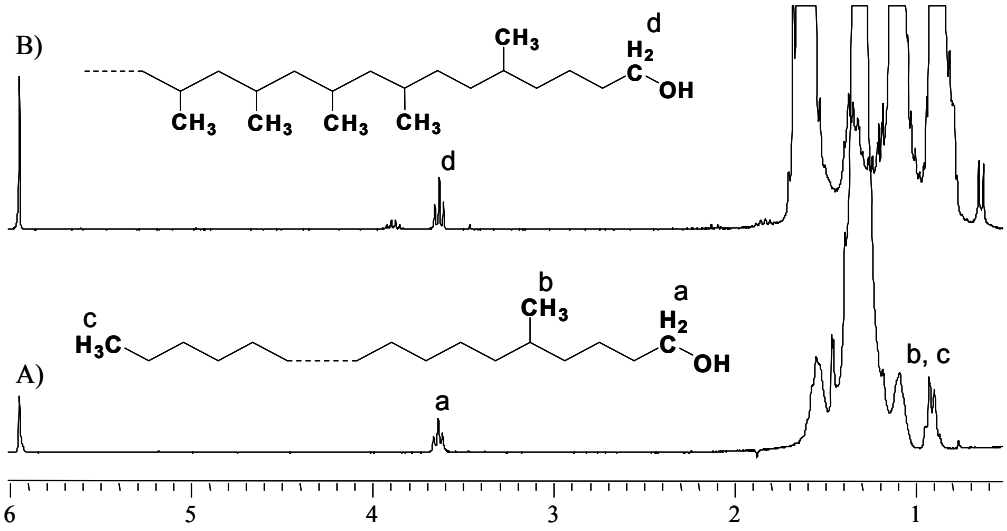

Figure 1. ^{1}H NMR spectra of a chain-end functionalized A) polyethylene (**Table 1**, Run 1) and B) polypropylene (**Table 1**, Run 2). The insets are structures and assignments of the key signals of the polymers. The chemical shifts of the signals a and d are identical.

Functional initiator **67b** was generated in an identical manner to **67a**. GC/MS analysis of **67b** after hydrolysis demonstrated the formation of no multiple insertion products even in the presence of an excess amount of **66b**, further confirming that the second monomer insertion is very slow. A propylene polymerization using **67b** (**66b**: 0.066 mmol; **31**: 0.059 mmol; Al/Ti: 150) afforded a highly syndiotactic polypropylene with a molecular weight distribution close to one (**Table 1**, Run 3). The triplet at 3.64 ppm appeared as expected together with the unassigned two signals that were mentioned above (**Figure 2a**). The M_n (NMR) was calculated to be 7,700, which is in agreement with the GPC result (the M_n (GPC) = 8,700) within experimental error.

Chain-End Capping of Terminating Chain End

The very slow consecutive insertions of **66** prompted us to employ functionalized olefins **66** as a chain-end capping agent. The olefin **66b** bearing a trimethylsilyl group is suitable as a capping agent especially when it is used in excess with a catalyst because a number of deactivating pathways of the catalyst caused by alkylaluminums were reported (e.g., reduction of Ti(IV) to low valent species, formation of a Al-Ti heterobinuclear complex, ligand transfer to aluminum,[20] etc.). Under the conditions examined, the reaction of **66b** with a living propagating species bearing a polyethylene chain (**66b**/Ti = 8) was not quantitative probably because polymer precipitation causes low reaction efficiency. Due to slow crystallization rate, reaction mixtures of syndioselective propylene polymerization remain as a homogeneous clear solution, so that we focused our attention on propylene polymerizations.

A propylene polymerization was started without addition of **66**. After the prescribed reaction time, dissolved monomer was displaced by nitrogen flow and five equivalent of **66b** to **31** was applied (**Table 1**, Run 4, also see Experimentals). The ^{1}H NMR of the obtained polymer exhibited the triplet at 3.64 ppm assignable to a methylene group next to the OH. The M_n (NMR) and the M_n (GPC) are close (9,700 and

8,300, respectively), indicating one OH group per chain. Quite interestingly, the strange signals observed at 3.89 and 3.46 ppm disappeared and a new broad signal appeared around 3.7 ppm (**Figure 2b**). This observation validates the assumption that the two signals were derived from the termination chain ends. The signal around 3.7 ppm would probably also be related to terminating chain-end structures involving monomer unit **66b**.

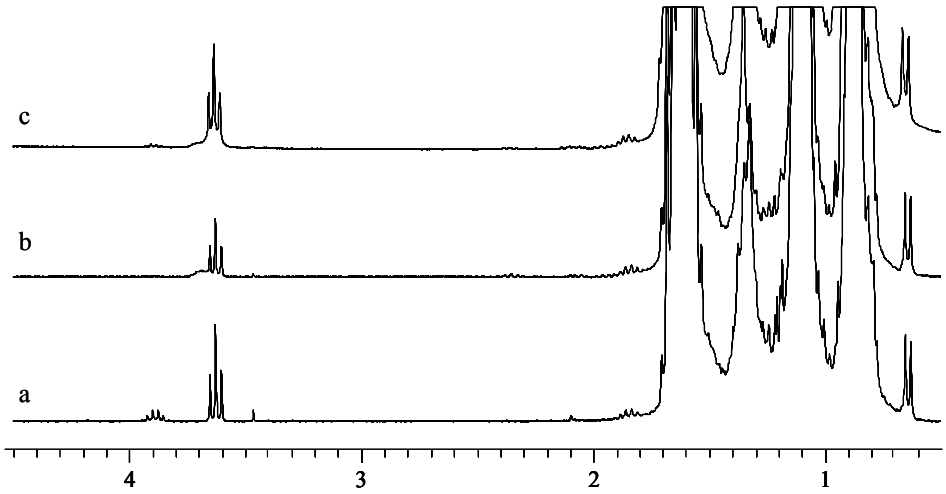

Figure 2. ^{1}H NMR spectra of polypropylene functionalized a) at the initiating chain end (**Table 1**, Run 3); b) at the terminating chain end (**Table 1**, Run 4) and c) at both chain ends (telechelic, **Table 1**, Run 6).

Finally, attempts to prepare a telechelic polyolefin were made by the combination of a functional initiator **67b** and a chain-end capping agent **66b** (**Scheme 2** and **Table 1**, Runs 5 and 6). Highly syndiotactic polypropylenes with narrow molecular weight distributions close to one were obtained as expected. Judging from the NMR-based M_n, two equivalents of **66b** as a chain-capping agent were not sufficient to functionalize all the polymer chain ends (Run 5). If one assumes that the initiating chain end was quantitatively functionalized, functionality of the terminating chain end of this polymer was estimated to be about 50 % from the ratio of M_n (GPC)/M_n (NMR) which was about 1.5 (= 9,400/6,300). (Note that M_n (NMR) was calculated as a unifunctional polymer). When five equivalents of **66b** were added to precatalyst **31** (Run 6), the value of M_n (GPC)/M_n (NMR) became close to 2 (9,600/5,200), indicative of the successful preparation of a telechelic polymer. Chain-end structures of the syndiotactic polypropylenes formed with **31**/MAO were reported to be isopentyl and isobutyl groups as initiating chain ends and *n*-propyl and isobutyl groups as terminating chain ends.[21] None of the peaks originating from these chain ends were observed for this telechelic polypropylene in ^{13}C NMR spectrum except for a trace amount of peaks possibly derived from the isopentyl group. The telechelic polymer has a very narrow molecular weight distribution of 1.08, high syndioregularity (T_m = 143.0 °C) and two well defined hydroxyl groups at both chain ends.

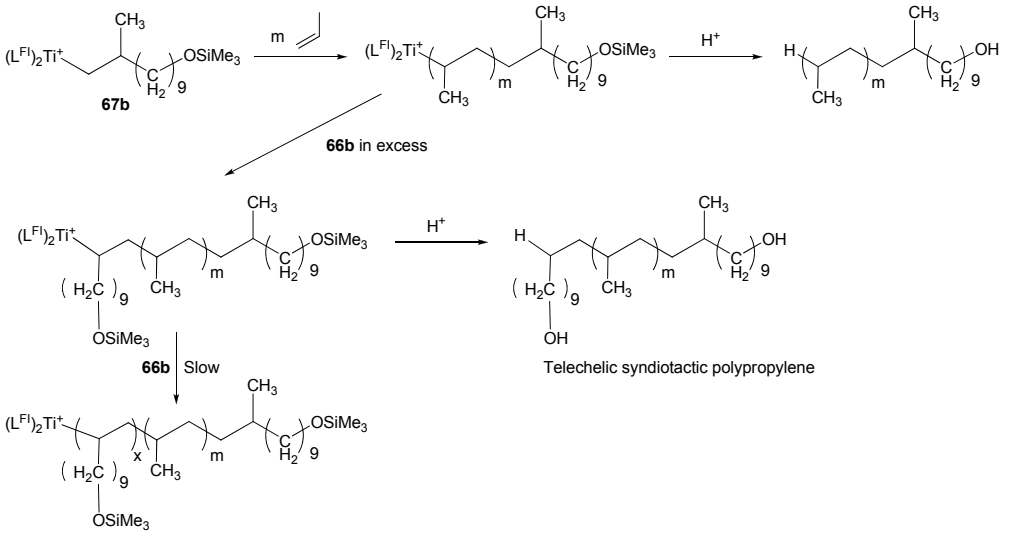

Scheme 2

Conclusion

In conclusion, a simple and widely applicable method for the preparation of polyolefins incorporating well-defined functional groups at their chain termini was developed, which is based on the large rate difference in the first and the second monomer insertions of functionalized α-olefins to an initiating or a propagating species, both of which possess highly active and robust living polymerization characteristics. This method is extendable to other functional groups having appropriate protecting groups and heterotelechelic polyolefins can be synthesized if one applies different functionalized α-olefins at the initiation and termination stages.

Experimentals

General Procedures and Materials

All manipulations of air/moisture-sensitive compounds were performed under a dry nitrogen atmosphere using standard Schlenk techniques. Toluene (Wako Pure Chemical Industries, Ltd.) was dried over Al_2O_3. Ethylene (Sumitomo Seika Co.) and propylene (Mitsui Chemicals, Inc.) were used without further purification. Methylalumoxane (MAO) was purchased from Albemarle as a 1.2 M toluene solution, and the remaining trimethylaluminum was removed *in vacuo* prior to use. Precatalyst $(L^{FI})_2TiCl_2$ (**31**, L^{FI}: C_6F_5N=CH(2-O-C_6H_3-3-^{t}Bu)) was prepared following the published procedures.[26]

*Synthesis of H_2C=CH$(CH_2)_4$-OAlMe_2 (**66a**)*

To a toluene solution of trimethylaluminum (~14 mmol) at –45 °C was added 5-hexen-1-ol (1.028 g, 10.3 mmol) via a syringe and the reaction mixture was kept at the temperature for 90 min and then at room temperature for 15 min. All volatiles were removed under vacuum at 0 °C and the crude product obtained was used without further purification. ^{1}H NMR (270 MHz, benzene-d_6) δ 5.58–5.75 (m, 1H, vinyl), 4.95–5.02

(m, 2H, vinyl), 3.43 (t, J = 6.6 Hz, 2H, CH_2O), 1.83 (m, 2H, $CH_2CH{=}CH_2$), 1.37 (m, 2H, CH_2CH_2O), 1.16 (m, 2H, $CH_2CH_2CH_2O$), −0.45 (s, 6H, $(CH_3)_2Al$). Several minor signals appeared probably due to the equilibrium between a monomer and a dimer.

*Synthesis of $H_2C{=}CH(CH_2)_9$-$OSiMe_3$ (**66b**)*

Triethylamine (~5 mL) was added to a solution of 10-undecen-1-ol (6.0 mL, 30 mmol) and trimethylsilyl chloride (Ca. 17 mL) in toluene. A white solid immediately formed and was filtered and the filtrate was concentrated to a constant weight. Yield 5.87 g (80 %); ^{1}H NMR (270 MHz, toluene-d_8) δ 5.69–5.84 (m, 1H, vinyl), 4.95–5.05 (m, 2H, vinyl), 3.53 (t, J = 6.6 Hz, 2H, CH_2O), 1.97 (m, 2H, $CH_2CH{=}CH_2$), 1.52 (m, 2H, CH_2CH_2O), 1.15–1.40 (br, 12H, $(CH_2)_6$), 0.12 (s, 9H, $(CH_2)_3Si$).

Polymerization Procedures Using Functional Initiators

Into a 500 mL dried glass reactor equipped with a mechanical stirrer and a thermocouple probe, toluene (250 mL) was charged under a nitrogen atmosphere. The toluene was equilibrated at a prescribed temperature under stirring (600 rpm) and a measured amount of MAO, a functionalized α-olefin (**66a** or **66b**), and then precatalyst **31** were added in this order as a toluene solution and allowed to react (0–25 °C, 15–30 min). Ethylene or propylene was fed from the bottom of the reactor to initiate polymerization and the polymerization was quenched after a prescribed time by adding methanol (~5 mL). The product was precipitated in acidified methanol (1.5 L), collected by filtration, and dried under vacuum at 80 °C for 10 h.

Chain-End Capping with Functionalized α-Olefins

Before quenching polymerization, monomer gas feed was halted and dry nitrogen was bubbled through the reaction mixture to remove dissolved monomers. After 20 min, a prescribed amount of a functionalized α-olefin (**66b**) was added. The reactions were carried out at 25 °C for > 1 h, and the products were isolated as described above.

Polymer Analyses

Molecular weights and molecular weight distributions (M_w/M_n) of polymers were determined using a Waters Alliance GPC-2000 gel permeation chromatograph equipped with three TSKgel columns (two sets of TSKgelGMH6HT and TSKgelGMH6-HTL) at 140 °C using either polyethylene or polypropylene calibration. ^{1}H and ^{13}C NMR spectra of the polymers were recorded on a JEOL GSX 270 spectrometer (FT, 270 MHz, ^{1}H, 67.5 MHz, ^{13}C) using 1,1,2,2-tetrachloroethane-d_2 as a solvent at 120 °C. Thermal analyses of the polymers were carried out on a Shimadzu DSC 60 and recorded upon a second heating cycle at a heating rate of 10 °C/min.

References and Notes

(1) Goethals, E. J. *Telechelic Polymers: Synthesis and Applications*, CRC Press: Boca Raton, 1989, and references therein.

(2) Kamigaito, M.; Ando, T.; Sawamoto, M. *Chem. Rev.* **2001**, *101*, 3689–3746.

(3) Hawker, C. J.; Bosman, A. W.; Harth, E. *Chem. Rev.* **2001**, *101*, 3661–3688.

(4) Gridnev, A. A.; Ittel, S. D. *Chem. Rev.* **2001**, *101*, 3611–3660.

(5) Young, R. N.; Quirk, R. P.; Fetters, L. J. *Adv. Polym. Sci.* **1984**, *56*, 1–90.

(6) Matyjaszewski, K. *Cationic Polymerizations: Mechanisms, Synthesis, and Applications* (Plastics Engineering 35), Marcel Dekker, 1996.

(7) Szwarc, M. *Ionic Polymerization Fundamentals*, Hanser Gardner Pubns., 1996.

(8) Sawaguchi, T.; Suzuki, Y.; Sakaki, A.; Saito, H.; Yano, S.; Seno, M. *Polym. Int.* **2000**, *49*, 921–925.

(9) Sawaguchi, T.; Ikemura, T.; Seno, M. *Macromolecules* **1995**, *28*, 7973–7978.

(10) Shiono, T.; Naga, N.; Soga, K. *Macromol. Chem. Rapid Commun. 1993*, *14*, 323–327.

(11) Ishihara, T.; Shiono, T. *Macromolecules* **2003**, *36*, 9675–9677.

(12) Shiono, T.; Kurosawa, H.; Soga, K. *Macromolecules* **1995**, *28*, 437–443.

(13) Gottfried, A. C.; Brookhart, M. *Macromolecules* **2003**, *36*, 3085–3100.

(14) Murata, M.; Fukui, Y.; Soga, K. *Macromol. Rapid Commun.* **1998**, *19*, 267–270.

(15) Makio, H.; Kashiwa, N.; Fujita, T. *Adv. Synth. Catal.* **2002**, *344*, 477–493.

(16) Mitani, M.; Nakano, T.; Fujita, T. *Chem. –Eur. J.* **2003**, *9*, 2396–2403.

(17) Furuyama, R.; Saito, J.; Ishii, S.; Makio, H.; Mitani, M.; Tanaka, H.; Fujita, T. *J. Organomet. Chem.* **2005**, *690*, 4398–4413.

(18) Terao, H.; Ishii, S.; Mitani, M.; Tanaka, H.; Fujita, T. *J. Am. Chem. Soc.* **2008**, *130*, 17636 –17637.

(19) See Chapter 2 of this thesis and references therein.

(20) See Chapter 1 of this thesis and references therein.

(21) Saito, J.; Mitani, M.; Onda, M.; Mohri, J.-I.; Ishii, S.- I.; Yoshida, Y.; Nakano, T.; Tanaka, H.; Matsugi, T.; Kojoh, S.-I.; Kashiwa, N.; Fujita, T. *Macromol. Rapid Commun.* **2001**, *22*, 1072–1075.

(22) Lamberti, M.; Pappalardo, D.; Zambelli, A.; Pellecchia, C. *Macromolecules* **2002**, *35*, 658 –663.

(23) Hustad, P. D.; Tian, J.; Coates, G. W. *J. Am. Chem. Soc.* **2002**, *124*, 3614–3621.

(24) See Chapter 5 of this thesis.

(25) Under the conditions (T_p = 0 °C), peak melting temperatures of the syndiotactic polypropylenes prepared by this catalyst are in the range of 143–146 °C. Mitani, M.; Furuyama, R.; Mohri, J.; Saito, J.; Ishii, S.; Terao, H.; Nakano, T.; Tanaka, H.; Fujita, T. *J. Am. Chem. Soc.* **2003**, *125*, 4293–4305.

(26) Mitani, M.; Mohri, J.-i.; Yoshida, Y.; Saito, J.; Ishii, S.; Tsuru, K.; Matsui, S.; Furuyama, R.; Nakano, T.; Tanaka, H.; Kojoh, S.-i.; Matsugi, T.; Kashiwa, N.; Fujita, T. *J. Am. Chem. Soc.* **2002**, *124*, 3327–3336.

Chapter 7. Silanolytic chain transfer for end-functionalization of polyolefins

Abstract

Silanolytic chain transfer processes have been shown to be applicable to supported single-site Ziegler-Natta olefin polymerization catalysts. Primary silanes (*n*-hexylSiH_3, $PhSiH_3$) are effective chain transfer agents in SiO_2/MAO/Cp_2ZrCl_2-mediated ethylene homopolymerizations and in ethylene + α-olefin copolymerizations. The microstructures of the polymers produced in the SiO_2/MAO/Cp_2ZrCl_2-mediated processes have been characterized in detail (^1H, ^{13}C, ^{29}Si NMR; IR) and reveal two kinds of chain ends, silyl-capped chain ends ($RSiH_2$-polymer; R = *n*-hexyl, Ph) with a selectivity as high as 62 %, and non-capped saturated chain ends (CH_3-polymer). Analysis of low molecular weight by-products indicates that chain transfer by H_2, produced in concomitant dehydrogenative silane coupling, competes with the silanolytic chain transfer process, resulting in non-capped, saturated CH_3-chain ends. In contrast to these results and those in solution, supported organotitanium complexes do not effectively mediate silanolytic chain transfer.

Introduction

The introduction of versatile functional groups into non-polar polyolefin macromolecules offers an attractive approach[1–4] for modifying interfacial properties via surface segregation of the polar functional groups. In addition to surface modifying characteristics, robust, linking functional groups, especially at chain ends, offer a means to construct a variety of polymer architectures such as block and graft copolymers. In the previous Chapter, chain-end functionalities were introduced at initiating and terminating chain ends, taking advantage of the robust and versatile living polymerizations with Ti-FI catalysts.

Chain transfer processes to organometalloids[5] such as silanes,[6–10] borane,[11,12] and main group metal alkyls[13–20] offer another excellent means to achieve the introduction of functional groups because they introduce organometalloid functionality at chain termini via an *in situ* catalytic cycle that simultaneously achieves molecular weight control. Silanes are promising candidates for organometalloid chain transfer processes because of their efficiency as chain transfer agents, structural diversity and tunability, environmental stability as building block linkers, and versatility in subsequent functional group transformations.[6–10] By using single-site homogeneous organotitanium and organolanthanide catalysts, efficient "drop-in" silanolytic chain transfer processes for α-olefin polymerization has been demonstrated (**Scheme 1**).[6–10] These results raise intriguing questions about catalyst and monomer generality, especially in regard to catalysts suitable for slurry and gas-phase polymerization processes, and chain transfer to ethylene homopolymers, which is not efficient for homogeneous group 4 systems.[7,8] In this chapter, we report on initial observations extending the scope of silanolytic chain transfer processes to heterogeneous single-site Ziegler-Natta catalysts, which are currently of considerable scientific and technological interest.[21–23]

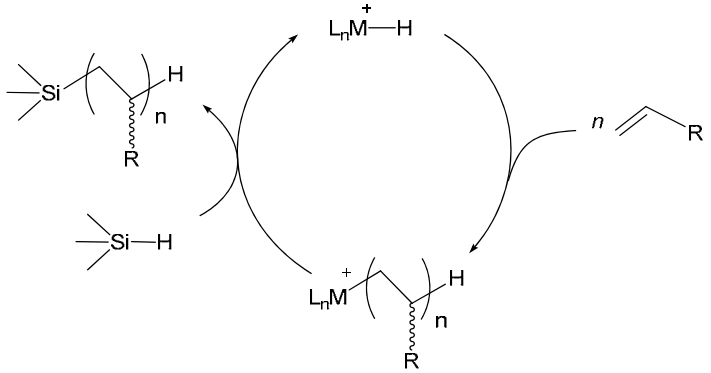

Scheme 1. Proposed catalytic cycle for silanolytic chain transfer coupled to single-site olefin polymerization.

Results and Discussion

Supported catalysts were prepared with rigorous exclusion of air and moisture via the following two-fold procedure.[21–23] 1) Preparation of SiO_2/MAO: Calcined silica (Davison Grade 62, specific surface area, ~250 m^2/g, dried at 320 – 380 °C for 14 h under high vacuum) was stirred with an MAO solution (Aldrich, 10 wt% in toluene) at 90 °C for 4 h. The solid was then collected by filtration under inert atmosphere and washed thoroughly with toluene. The anchored MAO coverage on the silica was ~3

mmol-Al/g-solid. 2) Metallocene or quasi-metallocene chemisorption: Solutions of the single-site catalyst precursors, Cp_2ZrCl_2 (**69**), *rac*-[CH_2CH_2(indenyl)$_2$]$ZrCl_2$ (**70**), [$Me_2Si(Me_4C_5)(^tBuN)$]$TiMe_2$ (**71**), and (Me_5C_5)$TiMe_3$ (**72**), were stirred with SiO_2/MAO slurries (Al/Zr, Al/Ti ≈ 90 – 130) in toluene at 80 °C for 2 h (**69**, **70**), and at 45 °C for 1 h for (**71**, **72**) to yield yellow to dark-red, fine powders. Non-chemisorbed catalyst components in the supernatants were removed by filtration and several washings with hot toluene. The supported catalysts were then dried under high vacuum.

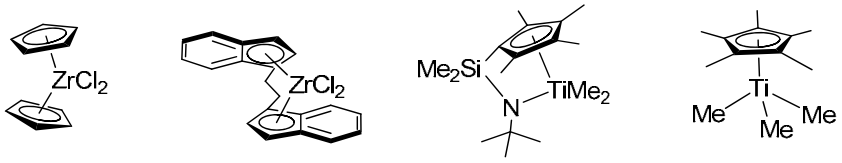

69 **70** **71** **72**

Polymerizations were carried out in toluene slurries under rigorously anhydrous/anaerobic high-vacuum line conditions.[7] A weighed portion of a completely dried solid catalyst was charged into a 100 mL flame-dried flask equipped with a large stirring bar in a nitrogen-filled Vacuum Atmospheres glovebox (< 1 ppm O_2). Measured quantities of toluene and silane in pseudo zero-order stoichiometric excess were then vacuum-transferred into the flask on a high-vacuum (10^{-5} Torr) line, and monomer gas was introduced at 25 °C with rapid stirring. After a measured time interval, polymerizations were terminated by injecting 2 mL of methanol, and the reaction mixtures were then poured into a large quantity of methanol. The products were collected by filtration, washed with methanol and acetone, and dried on a high-vacuum line. In order to completely remove the catalyst residue,[24,25] the white solid products were slurried in *o*-xylene at 120 – 140 °C with silica gel and slowly cooled to ambient temperature, which caused the dissolved polymers to deposit on the silica gel in the form of thin layers. The slurries were next packed into a column and the deposited polymers eluted with *o*-xylene which was slowly increased in temperature to 100 – 140 °C. The eluted polymers were then reprecipitated with methanol. The precipitated polymers were collected by filtration, washed with methanol and acetone, and dried under high vacuum at room temperature. The recovery of product polymers averaged ~74 % (~85 % excluding entries 6, 12, and 15 in **Table 1**, which appear to have very high molecular weights) by this method, whereas negligible quantities could be extracted from the catalyst residues by conventional Soxhlet techniques. Control NMR-scale experiments indicate negligible reaction between Et_2SiH_2 and SiO_2 over 5 h at 140 °C, arguing that reaction of the polymer silyl end groups with the SiO_2 of the column is negligible.

Polymerization data are summarized in **Table 1**. Catalyst SiO_2/MAO/**69** exhibits reasonable activity in the absence of silane, 3.44 g polyethylene/g catalyst·atm·h, which is comparable to literature results without additional alkylaluminum as the cocatalyst.[21–23] The molecular weight of the product is significantly higher than that produced by comparable homogeneous systems,[21–23] and the PDI (M_w/M_n) is slightly larger than 2.0; both are common observations in supported organometallic olefin polymerization systems.[21–23]

Table 1. Ethylene and propylene polymerization with heterogeneous Ziegler-Natta catalysts in the presence of various silanes

Entry	Catalyst precursor[a]	Catalyst (mg)	Monomer	Silane	Toluene (mL)	Silane (M)	Rxn time (min)	Polymer yield (mg)	Activity[b]	M_w[c] x 10^{-3}	M_w/M_n[c]	MeOH soluble fraction (mg)
1.	**69**	401	ethylene	-	30	0	10	230	3.44	374	3.99	n.d.
2.	**69**	405	ethylene	*n*-HexylSiH$_3$	30	0.093	45	230	0.74	26	2.95	0
3.	**69**	400	ethylene	*n*-HexylSiH$_3$	30	0.200	45	280	0.93	39	3.98	130
4.	**69**	401	ethylene	*n*-HexylSiH$_3$	30	0.682	60	370	0.92	7	1.57	180
5.	**69**	510	ethylene	*n*-HexylSiH$_3$	30	1.436	90	550	0.72	6	1.44	460
6.	**69**	388	ethylene	PhSiH$_3$	22	0.111	390	180	0.07	n.d.	n.d.	100
7.	**69**	400	ethylene	Et$_2$SiH$_2$	22	0.168	15	220	2.20	57	3.61	n.d.
8.	**69**	260	ethylene	Et$_2$SiH$_2$	30	1.074	60	260	1.00	30	3.20	40
9.	**69**	404	ethylene	Et$_2$SiH$_2$	30	2.410	120	440	0.54	18	2.74	50
10.	**69**[d]	8.7	ethylene	*n*-HexylSiH$_3$	30	0.413	60	850	28.56[e]	10	1.80	40
11.	**70**	418	ethylene	*n*-HexylSiH$_3$	30	0.337	20	390	2.81	n.d.	n.d.	360
12.	**70**	404	propylene	*n*-HexylSiH$_3$	30	0.511	1320	820	0.09	14	1.95	760
13.	**71**	252	ethylene	-	15	0	15	250	3.97	n.d.	n.d.	n.d.
14.	**71**	308	ethylene	PhSiH$_3$	15	0.081	150	400	0.52	216	5.10	100
15.	**72**	474	ethylene	*n*-HexylSiH$_3$	30	0.748	60	130	0.27	n.d.	n.d.	140

[a]Supported on SiO_2/MAO [b]g polymer/g catalyst·atm·h. [c]By GPC in 1,2,4-trichlorobenzene vs polystyrene standards unless otherwise indicated. [d]Homogeneous reaction as a control. Al/Zr = 150. [e]g-polymer/mmol-Zr atm h.

Polymerization activity was decreased to < 0.3x and the product molecular weights were also depressed as the *n*-hexylSiH$_3$ concentration was increased (entries 1 – 5; run to approximately constant conversion). A small portion of polymer exhibits GPC elution characteristics indistinguishable from those of the polymer produced without *n*-hexylsilane (entries 2 and 3). This non-uniformity of reaction products likely reflects variations in active site structures and *n*-hexylSiH$_3$ local concentrations within the solid catalyst. Such effects have ample precedent.[21–23] The decreased activity as silane concentration is increased is reasonably ascribed to the Lewis basicity of this reagent.[6–10] Microstructural analysis of the polymeric product reveals *n*-hexylSiH$_2$-capped polyethylene (^{1}H NMR in $C_2D_2Cl_4$, at 120 °C: δ 3.72 (*SiH$_2$*); ^{13}C NMR in $C_2D_2Cl_4$, at 120 °C: δ 9.09 (*CH$_2$*SiH$_2$); ^{29}Si NMR in $C_2D_2Cl_4$, at 120 °C: δ –29.8 (*SiH$_2$*); IR in a KBr pellet: 2020 cm^{-1} (ν_{Si-H})), which compares favorably with an authentic capped polyethylene sample produced using *n*-hexylSiH$_3$ and an effective homogeneous polymerization/chain transfer catalyst, [Me$_2$Si(Me$_4$C$_5$)$_2$]SmCH(SiMe$_3$)$_2$ (**Figure 1B**).[6]

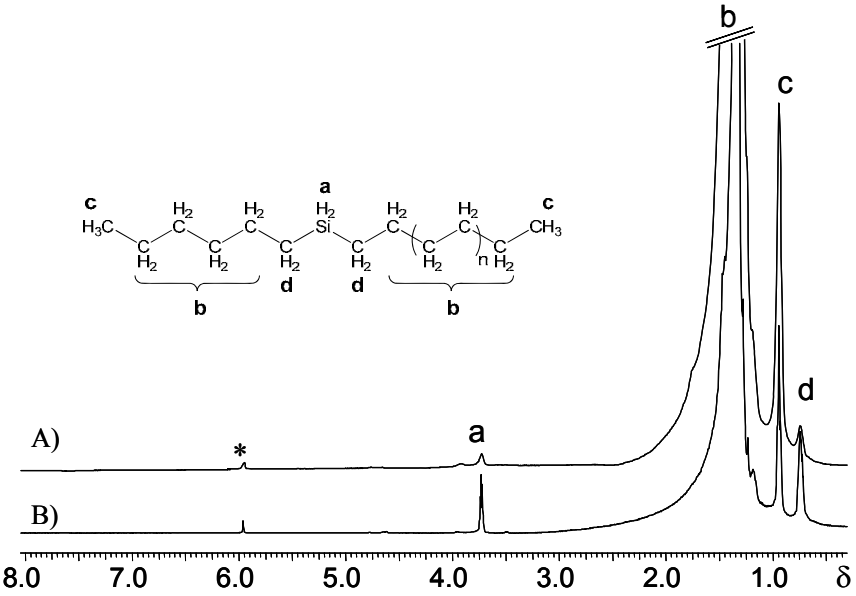

Figure 1. ^{1}H NMR Spectra of silyl-capped polyethylene prepared with A) SiO$_2$/MAO/**69** and B) [Me$_2$Si(Me$_4$C$_5$)$_2$]SmCH(SiMe$_3$)$_2$ (in $C_2D_2Cl_4$ at 120 °C).

It can be seen from the ^{1}H NMR spectrum of the polyethylene produced from SiO$_2$/MAO/**69** in the presence of *n*-hexylSiH$_3$ (**Figure 1A**) that the combined intensity of the CH$_3$ groups (peak C in Figure 1) at the saturated chain end, overlapping with the *n*-hexylsilyl CH$_3$ signal, is larger than the C*H$_3$*:C*H$_2$*Si:Si*H$_2$* intensity ratio of 6.0 : 4.0 : 2.0 expected from **Scheme 1**. These observations indicate that this polymer sample is a mixture of *n*-hexylSiH$_2$-capped polyethylene (~53 %) and uncapped polyethylene with saturated end groups (~47 %).[26] Because of overlap between the CH$_3$ and polyethylene backbone resonances, we estimate uncertainties in this assay of ±5 % and ±10 % for high and low silane concentrations, respectively.

NMR and GC/MS analysis of the methanol-soluble polymerization reaction by-products isolated from work-up reveal linear and cyclic silane coupling products[27–36] and *n*-alkanes having exclusively even carbon numbers between 14 and 26. It is well known that cationic organo-group 4 complexes catalyze

dehydrogenative silane coupling to produce polysilane oligomers (**Scheme 2**, cycle B).[27–36] It is reasonable that the H_2 by-product of this reaction functions as a chain transfer agent, resulting in saturated polyethylene chain ends (**Scheme 2**, cycle A). Various conceivable mechanistic scenarios for this coupling reaction give rates of H_2 production which scale either to first-order[27–36] or second-order in silane concentration, while the rate of chain transfer should scale linearly with [silane].[6–10] In the present study, it is found that increasing [*n*-hexylSiH_3] does not result in higher silyl group incorporation levels, and the relative ^{1}H NMR CH_2SiH_2 group : CH_3 group intensity ratio decreases with increasing *n*-hexylSiH_3 concentration,[26] while M_w generally declines (**Table 1**).

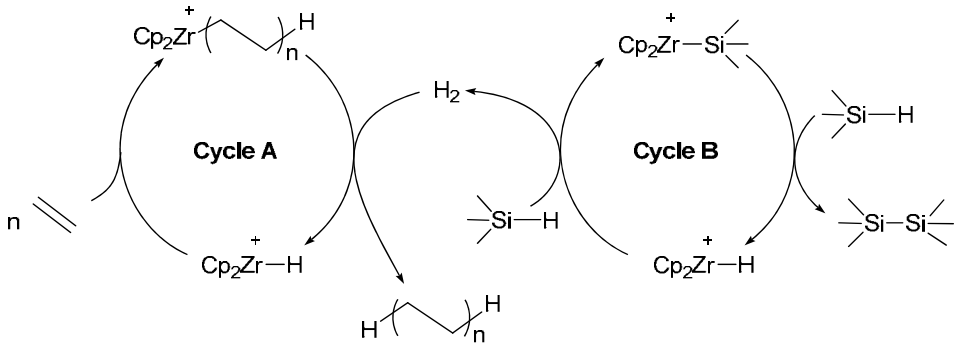

Scheme 2. Proposed cycle for catalytic olefin polymerization (cycle A), dehydrogenative silane coupling (cycle B), and formation of saturated chain-end polymeric products.

The absence of detectable unsaturated polyethylene chain ends and the presence of even carbon number *n*-alkanes in the methanol-soluble products argue that any other chain transfer pathways such as β-H elimination or Zr-CH_2CH_2(polymer)/Me-Al(MAO) transposition (Eq. 1) are not the dominant chain termination steps in this system.

$$Cp_2Zr^+\text{-}CH_2CH_2\text{-polymer} + MAO\text{-}CH_3 \longrightarrow Cp_2Zr^+\text{-}CH_3 + MAO\text{-}CH_2CH_2\text{-polymer} \qquad (1)$$

In the case of $PhSiH_3$, which is an effective chain transfer agent in homogeneous organolanthanide-[6,8,10] and organotitanium[7–9]-catalyzed olefin polymerizations, the present product polymers are a mixture of silyl-capped and uncapped saturated polyethylenes (**Figure 2**). Copolymerization of ethylene and 1-hexene with the supported catalyst system forms partially silyl-capped copolymers, in which the phenylsilyl group is incorporated adjacent to an ethylene subunit (**I**) and *not adjacent* to a 1-hexene subunit (**II**)[37] as in the case of the homogeneous organolanthanide chain transfer systems.[6,10]

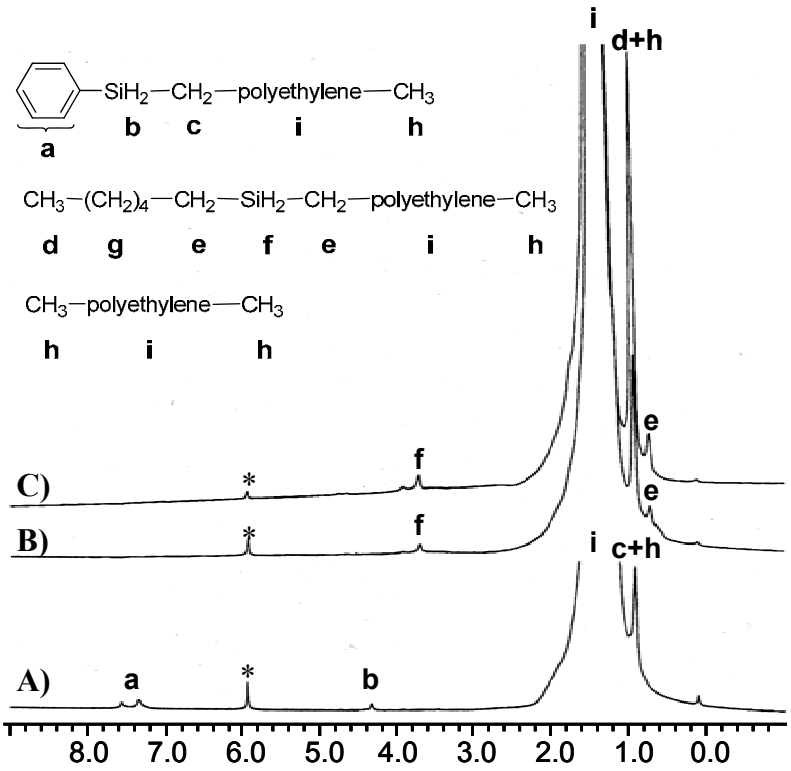

Figure 2. (A) ^{1}H NMR spectrum (400 MHz) of a $PhSiH_2$-capped polyethylene sample in $C_2D_2Cl_4$ at 120 °C. (B) ^{1}H NMR spectrum (400 MHz) of an *n*-hexylSiH_2-capped polyethylene sample in $C_2D_2Cl_4$ at 120 °C. Synthesized with [*n*-hexylSiH_3] = 0.09 M. (C) ^{1}H NMR spectrum (400 MHz) of an *n*-hexylSiH_2-capped polyethylene sample in $C_2D_2Cl_4$ at 120 °C. Synthesized with [*n*-hexylSiH_3] = 0.68 M. * denotes the solvent resonance ($Cl_2HCCDCl_2$).

Sterically more hindered secondary silanes generally exhibit lower reactivity in the present silanolytic chain transfer reactions.[6–10] For the supported SiO_2/MAO/**69** catalyst, Et_2SiH_2 decreases the product molecular weight, although there are no spectroscopically observable (IR, ^{1}H, ^{13}C, ^{29}Si NMR) silyl end groups. The even-numbered *n*-alkanes detected in the methanol-soluble fractions suggest that the secondary silane also produces H_2 through dehydrogenative silane coupling. Interestingly, the homogeneous counterpart of this catalyst, MAO/**69**, with *n*-hexylSiH_3 yields exclusively non-capped polyethylene with saturated chain ends (**Table 1**, entry 10).[38]

Polyethylene and isotactic polypropylene formation mediated by SiO_2/MAO/**70** in the presence of *n*-hexylSiH_3 does not yield silyl-capped polymers. Vinylidene chain ends (**III**) instead of silyl groups are observed in the case of polypropylene, and vinyl chain ends (**IV**) in the case of polyethylene. We additionally observe CH_3-chain ends in higher quantities than unsaturated chain-end groups, although the methanol-soluble products in these polymerizations do not include *n*-alkanes. Interestingly and in sharp contrast to the homogeneous chain transfer systems, the supported single-site organotitanium catalysts SiO_2/MAO/**71** and SiO_2/MAO/**72** do not afford silyl-capped polyethylenes. The polyethylene from SiO_2/MAO/**72** contains vinyl chain ends (**IV**) and negligible *n*-alkanes in the methanol-soluble part. In these

organotitanium systems, all product polymers have relatively high molecular weights, and chain transfer with H_2 is clearly not extensive, even though small quantities of oligosilane coupling products are detected by GC/MS. The classical heterogeneous Ziegler-Natta catalysts, $TiCl_3 \cdot 1/3AlCl_3$-Et_2AlCl and $MgCl_2/TiCl_4$/(ID)-Et_3Al-(ED) (ID = diisobutyl phthalate as an internal donor; ED = diphenyldimethoxysilane [$Ph_2Si(OMe)_2$] as an external donor), were also examined with added $PhSiH_3$ in ethylene and propylene polymerization experiments. Negligible yields of silyl-capped polyolefins are obtained from these catalyst systems.

Conclusion

These results show that the scope of silanolytic chain transfer can be extended to heterogeneous Zr olefin polymerization catalysts. While the breadth of applicability appears to be somewhat narrower than the case of homogeneous single-site catalysts,[6–10] the first group 4 systems capable of functioning in the slurry mode and of producing functionalized ethylene homopolymers have been developed. Moreover, there appear to be distinct and large differences in mechanism and regiocontrol between the homogeneous and silica-supported heterogeneous systems.

Experimentals

Materials and Methods

All manipulations of air-sensitive materials were performed with the rigorous exclusion of oxygen and moisture in flamed Schlenk-type glassware on a dual manifold Schlenk line, or interfaced to a high vacuum (10^{-5} torr) line, or in a nitrogen-filled Vacuum Atmospheres glovebox with a high-capacity recirculator(< 1 ppm O_2). Argon and ethylene (Matheson, prepurified) were purified by passage through a MnO oxygen-removal column and a Davison 4 A molecular sieve column. Toluene was distilled under nitrogen from Na/K alloy. All solvents for vacuum line manipulations were stored *in vacuo* over Na/K alloy in resealable bulbs. The comonomer 1-hexene was obtained from Aldrich, stirred over CaH_2 for 24 h, and vacuum transferred. Phenylsilane and *n*-hexylsilane were obtained commercially (Aldrich and Gelest), dried over CaH_2 for 24 h, and distilled prior to use. The organolanthanide catalyst $Me_2Si(Me_4C_5)_2SmCH(SiMe_3)_2$ was prepared by published procedures.[39]

Physical and Analytical Measurements

NMR spectra were recorded on a Varian Inova 400 (FT, 400 MHz, ^1H; 100 MHz, ^{13}C; 79.46 MHz, ^{29}Si) instrument. Chemical shifts for ^1H and ^{13}C spectra were referenced to internal solvent resonances and are reported relative to tetramethylsilane. For NMR analyses of polymer microstructures, 70-100 mg polymer samples were dissolved in 0.5 mL of $C_2D_2Cl_4$ with a heat gun in a 5 mm NMR tube, and the samples were immediately transferred to the NMR spectrometer with the probehead pre-equilibrated at 120 °C. GPC analyses of polymer samples were performed on a Waters Alliance GPCV 2000 (column: Waters Styragel

HT 6E, operation temperature: 140 °C, mobile phase: tricholorobenzene, flow rate: 1 mL/min). IR spectra (KBr pellets) were recorded using a Bio-Rad FTS-40 FT-IR spectrometer.

Preparation of Heterogeneous SiO_2/MAO/Cp_2ZrCl_2 Catalyst

Calcined silica (7.09 g, Davison Grade 62; calcined at 320 – 380 °C for 14 h under high vacuum) was treated with 38.0 mL of MAO (Aldrich, 10 wt% in toluene) in toluene at 90 °C for 4 h. The solid was filtered off and washed thoroughly with toluene and dried on the high vacuum line (yield, 8.65 g). The solid, SiO_2/MAO (3.470 g), was then reacted with 34.7 mg of Cp_2ZrCl_2 (0.12 mmol) in toluene at 80 °C for 2 h. The resulting reddish-orange solid was filtered off and washed with warm toluene (~50 °C) 3 times, and then dried on the high vacuum line at room temperature.

n-HexylSiH_2-Capped Polyethylene

Representative Experiment. In the glovebox, a 100 mL flame-dried reaction flask equipped with a large magnetic stirring bar was charged with 401 mg of the heterogeneous catalyst SiO_2/MAO/Cp_2ZrCl_2. On the high-vacuum line, toluene (30 mL) was then condensed into the flask at –78 °C. Next, 3.3 mL (20.4 mmol) of *n*-hexylSiH_3 was vacuum transferred into the flask at –78 °C. Under vacuum, the reactor was closed off from the vacuum line, rapidly warmed to 25 °C, and ethylene monomer then introduced at this temperature with rapid stirring. After a measured time interval (60 min), the reaction was quenched by the addition of 2.0 mL of methanol, and the reaction mixture was poured into a large quantity of methanol. The precipitate was collected by filtration, washed with methanol and acetone, and dried on the high-vacuum line. In order to remove the catalyst residue, the white solid product (770 mg) was slurried in 100 mL of *o*-xylene at 130 °C with 40 g of silica gel and slowly cooled to ambient temperature, which allowed the dissolved polymer to deposit on silica gel in the form of thin layers. The slurry was then packed into a chromatography column (0.75" diameter and 12" effective length) equipped with a dropping funnel filled with *o*-xylene. The entire length of the column was wrapped with heating tape and the temperature was slowly increased. In the temperature range 80 – 140 °C, the polymer was eluted with *o*-xylene, and reprecipitated in a large quantity of methanol. The precipitated polymer was filtered off, washed with methanol and acetone, and dried on the high-vacuum line at room temperature. Yield, 0.30 g; M_n = 4,220, M_w = 6,627 by GPC; ^{1}H NMR ($C_2D_2Cl_4$, 400 MHz, 120 °C, relative intensity): δ 3.72 (*SiH_2*, 0.38), 1.32 (-*CH_2CH_2*-, 187), 0.93 (-*CH_3*, 5.88 (shoulder)), 0.73 (-*CH_2*Si, 1.00 (shoulder)). ^{13}C NMR ($C_2D_2Cl_4$, 100 MHz, 120 °C): δ31.7, 29.4, 29.1, 22.4, 13.7, 9.1. ^{29}Si NMR ($Cr(acac)_3$/$C_6H_3Cl_3$/$C_2D_2Cl_4$, 79.46 MHz, 120 °C): δ –27.8 (**Figure 3**). IR (KBr pellet): 2020 cm^{-1} (ν_{Si-H}).

The filtrate from the above reaction mixture contained 180 mg of non-volatile material. ^{1}H NMR (C_6D_6, 400 MHz, 25 °C): δ 4.84, 3.72, 3.38, 1.27, 0.84, 0.71. All peaks have complex splitting patterns (**Figure 4**).

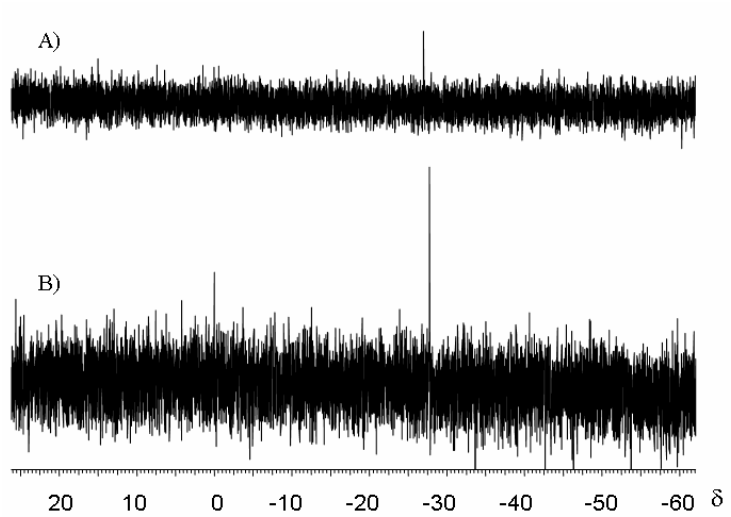

Figure 3. ^{29}Si NMR Spectra of silyl-capped polyethylene prepared with A) SiO_2/MAO/**69** and B) $[Me_2Si(Me_4C_5)_2]SmCH(SiMe_3)_2$ (in $C_2D_2Cl_4$ at 120 °C).

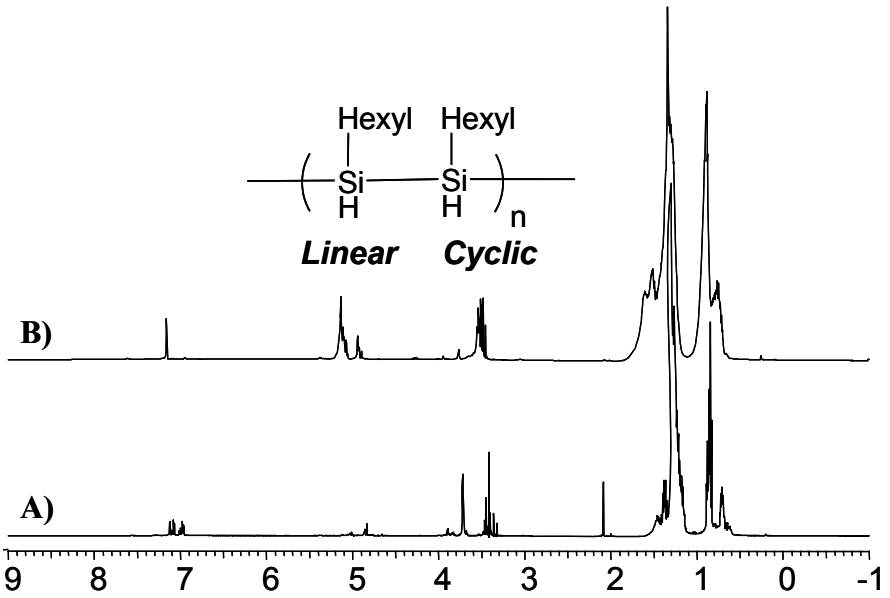

Figure 4. ^{1}H NMR spectra of methanol soluble products. A) **Table 1**, Entry 4 in benzene-d_6, and B) **Table 1**, Entry 3 in toluene-d_8. GC/MS detected *n*-alkane with even carbon numbers in addition to polysilanes and low molecular weight silyl-capped polyethylene.

References and Notes

(1) Ittel, S. D.; Johnson, L. K.; Brookhart, M. *Chem. Rev.* **2000**, *100*, 1169–1204.

(2) Boffa, L. S.; Novak, B. M. *Chem. Rev.* **2000**, *100*, 1479–1494.

(3) Functional Polymers: *Modern Synthetic Methods and Novel Structures*; Patil, A. O.; Schulz, D. N.; Novak, B. M., Eds., ACS Symposium Series 704; American Chemical Society: Washington, DC, 1998.

(4) *Desk Reference of Functional Polymers: Syntheses and Applications,* Arshady, R. Ed., American Chemical Society: Washington, DC, 1996.

(5) Amin, S. B.; Marks, T. J. *Angew. Chem. Int. Ed.* **2008**, *47*, 2006–2025

(6) Koo, K.; Fu, P.-F.; Marks, T. J. *Macromolecules* **1999**, *32*, 981–988.

(7) Koo, K.; Marks, T. J. *J. Am. Chem. Soc.* **1999**, *121*, 8791–8802.

(8) Koo, K.; Marks, T. J. *CHEMTECH, OCTOBER* **1999**, 13–19.

(9) Koo, K.; Marks, T. J. *J. Am. Chem. Soc.* **1998**, *120*, 4019–4020.

(10) Fu, P.-F.; Marks, T. J. *J. Am. Chem. Soc.* **1995**, *117*, 10747–10748.

(11) Xu, G.; Chung, T. C. *Macromolecules* **1999**, *32*, 8689–8692.

(12) Xu, G.; Chung, T. C. *J. Am. Chem. Soc.* **1999**, *121*, 6763–6764.

(13) Naga, N.; Mizunuma, K. *Polymer* **1998**, *39*, 5059–5067.

(14) Shiono, T.; Kang, K. K.; Soga, K. *Macromolecules* **1997**, *30*, 5997–6000.

(15) Kojoh, S.; Kioka, M.; Kashiwa, N.; Itoh, M.; Mizuno, A. *Polymer* **1995**, *36*, 5015–5018.

(16) Shiono, T.; Kurosawa, H.; Soga, K. *Macromolecules* **1995**, *28*, 437–443.

(17) Kurosawa, H.; Shiono, T.; Soga, K. *Macromol. Chem. Phys.* **1994**, *195*, 3303–3309.

(18) Kurosawa, H.; Shiono, T.; Soga, K. *Macromol. Chem. Phys.* **1994**, *195*, 1381–1388.

(19) Kurosawa, H.; Shiono, T.; Soga, K. *Macromol. Chem. Phys.* **1992**, *193*, 2751–2761.

(20) Mogstad, A.-L.; Waymouth, R. M. *Macromolecules* **1992**, *25*, 2282–2284.

(21) Hlatky, G. G. *Chem. Rev.* **2000**, *100*, 1347–1376.

(22) Fink, G.; Steinmetz, B.; Zechlin, J. Przybyla, C.; Tesche, B. *Chem. Rev.* **2000**, *100*, 1377–1390.

(23) Ribeiro, M. R.; Deffieux, A.; Portela, M. F. *Ind. Eng. Chem. Res.* **1997**, *36*, 1224–1237.

(24) This procedure, essentially a variant of temperature rising elution fractionation (TREF),[25] is typically used to analyze polymer microstructure distributions. Here it is applied for polymer separation in high yields.

(25) Xu, J.; Feng, L. *Eur. Polym. J.* **2000**, *36*, 867–878, and references therein.

(26) CH_3:CH_2Si integral ratios in the ^1H NMR spectra indicate that ~53 % of the polymer chains have *n*-hexylsilyl groups at the chain ends in the polymerization with [*n*-hexylSiH_3] = 0.09 M; ~62 % at 0.20 M, ~26 % at 0.68M, and ~9 % at 1.43 M silane. These values may include appreciable uncertainties because of significant overlap with a ^1H polyethylene main chain signal.

(27) Dioumaev, V. K.; Harrod, J. F. *Organometallics* **2000**, *19*, 583–589.

(28) Gauvin, F.; Harrod, J. F.; Woo, H. G. *Adv. Organometal. Chem.* **1998**, *42*, 363–405.

(29) Fu, P. -F.; Brard, L.; Li, Y.; Marks, T. J. *J. Am. Chem. Soc.* **1995**, *117*, 7157–7168.

(30) Forsyth, C. M.; Nolan, S. P.; Marks, T. J. *Organometallics* **1991**, *10*, 2543–2545.

(31) Watson, P. L.; Tebbe, F. N. U.S. Patent 4,965,386 (1990).

(32) Tilley, T. D. *Acc. Chem. Res.* **1993**, *26*, 22–29 and references therein.

(33) Corey, J. Y.; Huhmann, J. L.; Zhu, X. -H. *Organometallics* **1993**, *12*, 1121–1130 and references therein.

(34) Woo, H. G.; Walzer, J. F.; Tilley, T. D. *J. Am. Chem. Soc.* **1992**, *114*, 7047–7055.

(35) Harrod, J. F. In *Inorganic and Organometallic Polymers with Special Properties*; Laine, R. M., Ed.; Kluwer Academic Publishers: Amsterdam, 1991; Chapt. 14, and references therein.

(36) Kobayashi, T.; Sakakura, T.; Hayashi, T.; Yumura, M.; Tanaka, M. *Chem. Lett.* **1992**, 1157–1160.

(37) $PhSiH_2$-CH_2CH_2- chain ends were confirmed by ^{13}C NMR; no $PhSiH_2$-CH_2CH(*n*-butyl)- chain ends were detected.

(38) That minor peaks from *n*-alkanes having odd carbon-numbers in the GC/MS are observed implies MAO also functions as a chain transfer agent in this system.

(39) Jeske, G.; Schock, L. E.; Swepston, P. N.; Schumann, H.; Marks, T. J. *J. Am. Chem. Soc.* **1985**, *107*, 8103–8110.

List of Publications

Chapter 1 Makio, H.; Fujita, T. Observation and identification of the catalytically active species of bis(phenoxy-imine) group 4 transition metal complexes for olefin polymerization using ^{1}H NMR spectroscopy. *Macromolecular Symposia* **2004**, *213* (Stereospecific Polymerization and Stereoregular Polymers), 221–233.

Chapter 2 Makio, H.; Oshiki, T.; Takai, K.; Fujita, T. Synthesis of Bis(phenoxyimine) Ti alkyl complexes and observation of living species by ^{1}H NMR spectroscopy. *Chemistry Letters* **2005**, *34*, 1382–1383.

Chapter 3 Prasad, A. V.; Makio, H.; Saito, J.; Onda, M.; Fujita, T. Highly isospecific polymerization of propylene with bis(phenoxy-imine) Zr and Hf complexes using $^{i}Bu_3Al/Ph_3CB(C_6F_5)_4$ as a cocatalyst. *Chemistry Letters* **2004**, *33*, 250–251.

Chapter 4 Makio, H.; Tohi, Y.; Saito, J.; Onda, M.; Fujita, T. Regio- and stereochemistry in propylene polymerization catalyzed with bis(phenoxy-imine) Zr and Hf complexes/MAO systems. *Macromolecular Rapid Communications* **2003**, *24*, 894–899.

Chapter 5 Makio, H.; Ochiai, T.; Tanaka, H.; Fujita, T. FI Catalysts: A Molecular Zeolite for Olefin Polymerization. *Advanced Synthesis & Catalysis* **2010**, *352*, 1635–1640.

Chapter 6 Makio, H.; Fujita, T. Synthesis of chain-end functionalized polyolefins with a bis(phenoxy imine) titanium catalyst. *Macromolecular Rapid Communications* **2007**, *28*, 698–703.

Chapter 7 Makio, H.; Koo, K.; Marks, T. J. Silanolytic Chain Transfer in Olefin Polymerization with Supported Single-Site Ziegler-Natta Catalysts. *Macromolecules* **2001**, *34*, 4676–4679.

Publications not included in this thesis

Effect of external donor in polymerization of propylene by a magnesium chloride-supported titanium catalyst
Makio, H.; Kioka, M.; Kashiwa, N. *Macromolecular Symposia* **1994**, *84* (POLYMEX-93, International Symposium on Polymers, 1993), 1–4.

Metathesis copolymerization of norbornene with phenylacetylene and its ring-substituted derivatives catalyzed by tungsten hexachloride: 2. Reactivity of monomers
Makio, H.; Masuda, T.; Higashimura, T. *Polymer* **1993**, *34*, 2218–2223.

Metathesis copolymerization of norbornene with phenylacetylene and its ring-substituted derivatives catalysed by tungsten hexachloride. 1. Product characterization
Makio, H.; Masuda, T.; Higashimura, T. *Polymer* **1993**, *34*, 1490–1495.

Indirect Substituent Effects upon the Olefin Polymerization Reactivity of Titanium(IV) Chelating σ-Aryl

Catalysts
Tam, K.-H.; Chan, M. C. W.; Kaneyoshi, H.; Makio, H.; Zhu, N. *Organometallics* **2009**, *28*, 5877–5882.

Styrene Polymerization Behavior of Phenoxy-Imine Ligated Ti Complexes/MAO: Formation of Highly Isotactic and Syndiotactic PS
Michiue, K.; Onda, M.; Tanaka, H.; Makio, H.; Mitani, M.; Fujita, T. *Macromolecules* **2008**, *41*, 6289–6291.

Polymerization of higher α-olefins with a bis(phenoxyimine)Ti complex/i-Bu_3Al/$Ph_3CB(C_6F_5)_4$: Formation of stereo- and regioirregular high molecular weight polymers with high efficiency
Saito, J.; Suzuki, Y.; Makio, H.; Tanaka, H.; Onda, M.; Fujita, T. *Macromolecules* **2006**, *39*, 4023–4031.

Fluorinated bis(phenoxy-imine) Ti complexes with MAO: Remarkable catalysts for living ethylene and syndioselective living propylene polymerization
Furuyama, R.; Saito, J.; Ishii, S.; Makio, H.; Mitani, M.; Tanaka, H.; Fujita, T. *Journal of Organometallic Chemistry* **2005**, *690*, 4398–4413.

FI catalysts: New olefin polymerization catalysts for the creation of value-added polymers
Mitani, M.; Saito, J.; Ishii, S.; Nakayama, Y.; Makio, H.; Matsukawa, N.; Matsui, S.; Mohri, J.; Furuyama, R.; Terao, H.; Bando, H.; Tanaka, H.; Fujita, T. *Chemical Record* **2004**, *4*, 137–158.

Living copolymerization of ethylene with norbornene catalyzed by bis(pyrrolide-imine) titanium complexes with MAO
Yoshida, Y.; Mohri, J.; Ishii, S.; Mitani, M.; Saito, J.; Matsui, S.; Makio, H.; Nakano, T.; Tanaka, H.; Onda, M.; Yamamoto, Y.; Mizuno, A.; Fujita, T. *Journal of the American Chemical Society* **2004**, *126*, 12023–12032.

Polyethylenes having well-defined bimodal molecular weight distributions formed with bis(phenoxy-imine) Zr complexes
Tohi, Y.; Nakano, T.; Makio, H.; Matsui, S.; Fujita, T.; Yamaguchi, T. *Macromolecular Chemistry and Physics* **2004**, *205*, 1179–1186.

Behavior of bis(phenoxy-imine)titanium complexes in ethylene and propylene polymerization
Furuyama, R.; Saito, J.; Ishii, S.; Mitani, M.; Matsui, S.; Tohi, Y.; Makio, H.; Matsukawa, N.; Tanaka, H.; Fujita, T. *Journal of Molecular Catalysis A: Chemical* **2003**, *200*, 31–42.

Polyethylenes with Uni-, Bi-, and Trimodal Molecular Weight Distributions Produced with a Single

Bis(phenoxy-imine)zirconium Complex

Tohi, Y.; Makio, H.; Matsui, S.; Onda, M.; Fujita, T. *Macromolecules* **2003**, *36*, 523–525.

A new titanium complex having two phenoxy-imine chelate ligands for ethylene polymerization

Saito, J.; Mitani, M.; Matsui, S.; Tohi, Y.; Makio, H.; Nakano, T.; Tanaka, H.; Kashiwa, N.; Fujita, T. *Macromolecular Chemistry and Physics* **2002**, *203*, 59–65.

A Family of Zirconium Complexes Having Two Phenoxy-Imine Chelate Ligands for Olefin Polymerization

Matsui, S.; Mitani, M.; Saito, J.; Tohi, Y.; Makio, H.; Matsukawa, N.; Takagi, Y.; Tsuru, K.; Nitabaru, M.i; Nakano, T.; Tanaka, H.; Kashiwa, N.; Fujita, T. *Journal of the American Chemical Society* **2001**, *123*, 6847–6856.

Post-metallocenes: a new bis(salicylaldiminato) zirconium complex for ethylene polymerization

Matsui, S.; Mitani, M.; Saito, J.; Tohi, Y.; Makio, H.; Tanaka, H.; Fujita, T. *Chemistry Letters* **1999**, 1263–1264.

New bis(salicylaldiminato) titanium complexes for ethylene polymerization

Matsui, S.; Tohi, Y.; Mitani, M.; Saito, J.; Makio, H.; Tanaka, H.; Nitabaru, M.; Nakano, T.; Fujita, T. *Chemistry Letters* **1999**, 1065–1066.

Tacticity distribution of polypropylene prepared by $MgCl_2$-supported titanium catalyst

Kioka, M.; Makio, H.; Mizuno, A.; Kashiwa, N. *Polymer* **1994**, *35*, 580–583.

Copolymerization of phenylacetylenes with norbornene by transition metal catalysts

Higashimura, T.; Masuda, T.; Makio, H.; Ohgane, T. *Yuki Gosei Kagaku Kenkyusho Koenshu* **1993**, *7*, 14–25.

Metathesis copolymerization of cycloalkenes with substituted acetylenes

Masuda, T.; Yoshida, T.; Makio, H.; Rahman, M. Z. A.; Higashimura, T. *Journal of the Chemical Society, Chemical Communications* **1991**, *7*, 503–504.

Reviews, Book chapters

FI Catalysts for Olefin Polymerization – A Comprehensive Treatment

Makio, H. Terao, H. Iwashita, A. Fujita, T. *Chemical Reviews* to be published.

Development and Application of FI Catalysts for Olefin Polymerization: Unique Catalysis and Distinctive

Polymer Formation

Makio, H.; Fujita, T. *Accounts of Chemical Research* **2009**, *42*, 1532–1544.

Stereoselective propylene polymerization with early and late transition metal catalysts

Makio, H.; Fujita, T. "*Stereoselective Polymerization with Single-Site Catalysts*" Eds.: Baugh, L. S.; Canich, J. A. M. CRC Press LLC, Boca Raton (2008), p. 157–168.

Polymerization of Alkenes

Fujita, T.; Makio, H. "*Comprehensive Organometallic Chemistry III*" Eds.: Crabtree, R. H., Mingos, D. M. P., Volume Ed.; Hiyama, T., Elsevier, Amsterdam (2007) Vol. 11, p. 691–734.

Living polymerization of olefin

Fujita, T.; Makio, H. Mirai Zairyo **2006**, *6*, 16–25.

Propene polymerization with bis(phenoxy-imine) Group 4 transition metal complexes

Makio, H.; Fujita, T. *Bulletin of the Chemical Society of Japan* **2005**, *78*, 52–66.

FI catalysts: A new family of high performance catalysts for olefin polymerization

Makio, H.; Kashiwa, N.; Fujita, T. *Advanced Synthesis & Catalysis* **2002**, *344*, 477–493.

Coordination polymerization catalysts

Kioka, M.; Makio, H. *Petrotech* (Tokyo) **1996**, *19*, 809–810.

Patents (related to this thesis)

Method for preparation of imine-containing-alkyl transition metal complex.

Makio, Haruyuki; Fujita, Terunori. JP 2005-169673

Polyolefins having functional groups at one end.

Makio, Haruyuki; Fujita, Terunori. WO 2005021600 A1. Priority: JP 2003-302240.

Polyolefins having functional groups at each end.

Makio, Haruyuki; Fujita, Terunori. WO 2005021601 A1. Priority: JP 2003-302240.

Catalysts for olefin polymerization and manufacture of olefin polymers with sharp particle size distribution using them.

Makio, Haruyuki; Doi, Yasushi; Fujita, Terunori. JP 97-129480.

Olefin polymerization catalysts, transition metal compounds, processes for olefin polymerization, and alpha-olefin/conjugated diene copolymers.
Fujita, Terunori; Tohi, Yasushi; Mitani, Makoto; Matsui, Shigekazu; Saito, Junji; Nitabaru, Masatoshi; Sugi, Kiyoaki; Makio, Haruyuki; Tsutsui, Toshiyuki. EP 874005 A1. Priority: JP 97-109922; JP 97-111439; JP 97-132333; JP 98-50541.

Acknowledgements

This thesis presents a part of the studies which the author carried out at Northwestern University from 1999 to 2001 under the direction of Professor Tobin J. Marks, and at Research Center, Mitsui Chemicals, Inc. during the years from 2001 to 2010.

The author would like to express his deepest gratitude to Professor Mitsuo Sawamoto for his kind guidance, insightful suggestions, and continuous encouragement throughout the writing process of this thesis as well as for his support in many other occasions since my graduation from Kyoto University. The author's gratitude extends to Professors Yoshiki Chujo and Kazuo Akagi at Kyoto University for their critical comments and invaluable advice.

The author would like to thank Professor Tobin J. Marks for accepting him as a visiting scholar and letting him work on those exciting projects. The auhtor would never have been able to complete some of the later work without the days he spent at NU with Professor Marks and the colleagues in the laboratory.

The author also wish to thank Dr. Terunori Fujita at Mitsui Chemicals for his support, encouragement, and understanding to my work over the years. The author has learned so much from being a part of the post-metallocene project, which Dr. Fujita launched and have carried through since the 1990s. His insight, humor, and passion for the work are always inspiring to the author.

The author is also very much grateful to the following people who have supported him and made this work possible: Dr. Akihiro Yamaguchi, Dr. Norio Kashiwa, Dr. Noriaki Kihara, Dr. Kenji Fujiwara, Dr. Toshiyuki Tsutsui.

Dr. Michael C. W. Chan has the author's cordial gratitude for his insightful comments and suggestions to the work and his longstanding friendship with the author. The author is also equally grateful to Dr. S.-W. Lai for the same reasons. The author thanks his collaborators, many of their names can be found in the cited references of this thesis, for their helpful and fruitful discussions and technical supports. The author is also grateful to Mr. Andrew Valentine for his hard work and his generous and helpful suggestions.

The author's parents, Nobuo Makio and Tatsuko Makio, are responsible for providing him with the resilience, patience, and strength in order for him to complete this work, for which the author thanks them with his whole heart. The author would like to thank his daughter, Miyako, and his son, Riku, for making the best effort with their homework while their father spent his time on his own at home. And finally, the author would like to thank Junko Makio, his wife, for her caring, listening, understanding, and so many more.

Haruyuki Makio

Sodegaura, Chiba
February 2010